

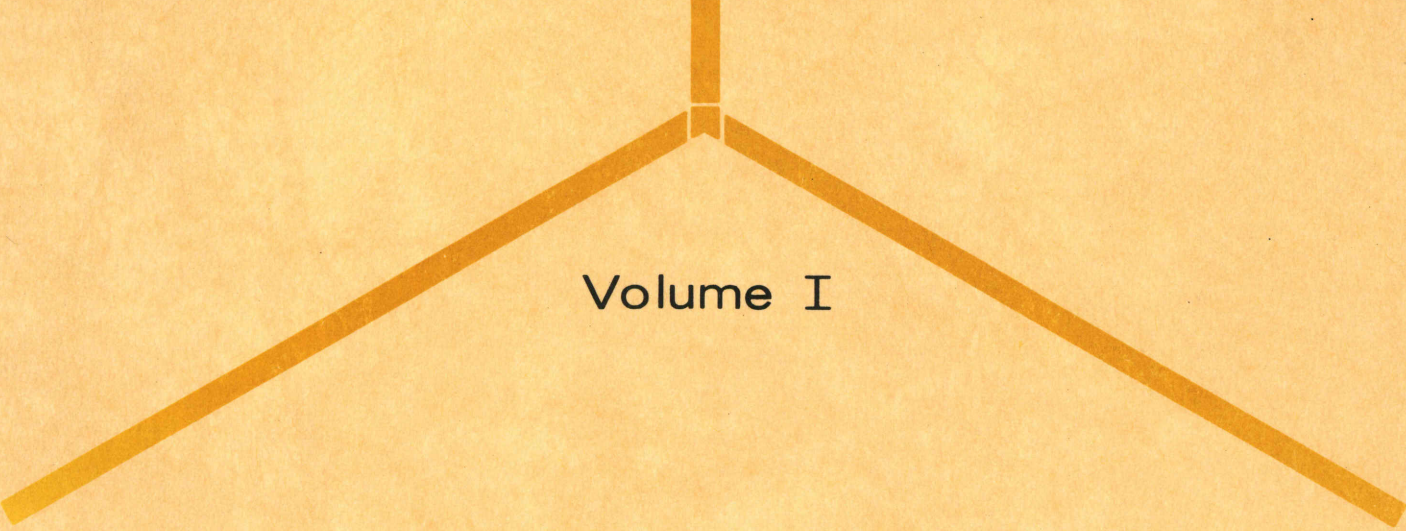
VLA LIBRARY

THE

VLA



A Proposal For  
A VERY LARGE ARRAY  
RADIO TELESCOPE



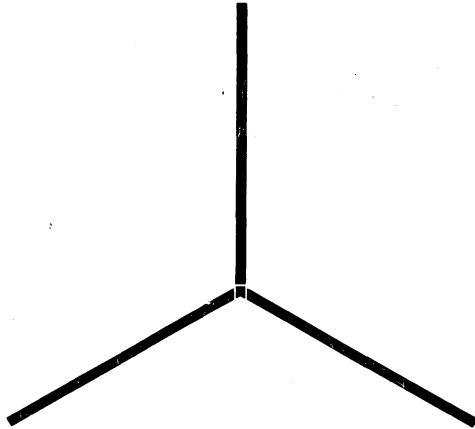
Volume I

NATIONAL RADIO ASTRONOMY OBSERVATORY

- A Proposal For -  
**A VERY LARGE ARRAY  
RADIO TELESCOPE**

Volume I

**THE VLA CONCEPT**



January, 1967

National Radio Astronomy Observatory\*  
Green Bank, West Virginia

\* OPERATED BY ASSOCIATED UNIVERSITIES, INC., UNDER CONTRACT  
WITH THE NATIONAL SCIENCE FOUNDATION.

Contents

Volume I - The VLA Concept

Chapters 1 - 10

	<u>Page</u>
Chapter 1. <u>SUMMARY</u>	1-1
A. Introduction .....	1-1
B. Historical Background .....	1-2
C. Description of the VLA .....	1-3
D. Operation of the VLA .....	1-4
E. Summary of Costs .....	1-5
Chapter 2. <u>SCIENTIFIC CONSIDERATIONS</u>	2-1
A. The Need for Higher Resolution .....	2-1
B. Performance Goals of the VLA .....	2-7
1. Angular resolving power .....	2-7
2. Sensitivity, side-lobe levels, field of view .....	2-8
3. Polarization and frequency range .....	2-9
4. Speed .....	2-9
5. Spectral-line capability .....	2-12
6. Versatility .....	2-12
C. The VLA Performance .....	2-13
1. Wavelength .....	2-13
2. Resolution .....	2-14
3. Side-lobe levels .....	2-14
4. Sensitivity .....	2-14
5. Time required for an observation .....	2-14
6. Polarization .....	2-14
7. Versatility .....	2-15
8. Hydrogen-line configuration .....	2-15
D. Some Specific Capabilities of the VLA .....	2-17
1. Array sensitivity .....	2-17
2. Structure of extragalactic sources .....	2-19

	<u>Page</u>
3. Faint sources .....	2-22
4. Galactic sources .....	2-23
5. Solar system studies .....	2-24
6. Dual frequency work .....	2-26
7. Spectral line work .....	2-26
Chapter 3. <u>POSSIBLE SYSTEMS</u>	3-1
A. Continuous, Completely Filled, Phased Arrays .....	3-1
B. Continuous Cross Type Arrays .....	3-1
C. Grating Cross Arrays .....	3-2
D. Aperture Synthesis Antennas .....	3-3
Chapter 4. <u>THE CORRELATOR ARRAY</u>	4-1
A. The Transfer Function and the Radiation Pattern .....	4-2
B. The Rectangular Sampling Grid .....	4-3
C. Separable Transfer Functions .....	4-5
D. Beamwidth and Sidelobe Levels .....	4-8
E. A Correlator Array Using Sidereal Tracking ..	4-9
Chapter 5. <u>THE FEASIBILITY OF THE CORRELATOR ARRAY</u>	5-1
A. Introduction .....	5-1
1. Stability of the mechanical structure ..	5-1
2. Phase stability of the electronic system .....	5-1
3. Delay tracking .....	5-1
4. Stability of the atmosphere .....	5-1
B. The Green Bank Interferometer .....	5-2
C. Stability of the Mechanical System .....	5-3
D. Phase Stability of the Electronic System ....	5-5
Chapter 6. <u>THE ARRAY CONFIGURATION</u>	6-1
A. The Computer Program for the Selection of an Array Configuration .....	6-1
1. The basic program .....	6-1
2. The effect of element size .....	6-2
3. The effect of bandwidth .....	6-3

	<u>Page</u>
B. The Figure of Merit of an Array Configuration .....	6-5
C. The Hollow Circle .....	6-6
D. Configurations With Three Arms .....	6-8
1. The optimum orientation of the arms .....	6-9
2. The distribution of elements along the arms .....	6-12
3. The optimum arm length .....	6-16
E. The Recommended Configuration .....	6-18
F. Appendix: The Application of the Theory of Random Arrays to the VLA .....	6-20
1. Percentage holes and side-lobes .....	6-20
2. An estimate of the percentage of holes ..	6-24
3. The effects of bandwidth .....	6-26
Chapter 7. <u>ARRAY SENSITIVITY AND REQUIRED ELEMENT SIZE</u>	7-1
A. Introduction .....	7-1
B. Assumptions .....	7-1
C. The Effective Integration Time .....	7-3
D. The Minimum Detectable Flux Density .....	7-4
E. The Minimum Detectable Brightness Temperature .....	7-5
F. Some Simplification .....	7-7
G. The Effective Area of the Array and Element Size .....	7-7
Chapter 8. <u>THE ARRAY SITE</u>	8-1
A. Introduction .....	8-1
B. The Primary Criteria .....	8-1
1. Geographic .....	8-1
2. Topographic .....	8-2
3. Cultural .....	8-2
C. The Secondary Criteria .....	8-2
1. Elevation .....	8-2
2. Proximity to urban areas .....	8-3
3. Utilities and access .....	8-3

	<u>Page</u>
4. Drainage .....	8-4
5. Land ownership .....	8-4
D. Site Search and Evaluation .....	8-4
1. Orientation .....	8-4
2. Roughness .....	8-4
3. Existing activity .....	8-5
Chapter 9. <u>MANAGEMENT AND OPERATION</u>	9-1
A. Project Management .....	9-1
B. Operation .....	9-2
Chapter 10. <u>COST ESTIMATES AND TIME SCHEDULE</u>	10-1

(Continued)

## Contents

### Volume II - The System Design

#### Chapters 11 - 21

	<u>Page</u>
Chapter 11. <u>THE ANTENNA ELEMENT</u>	11-1
A.    Introduction .....	11-1
1.    The design of the antenna elements .....	11-1
2.    Construction .....	11-1
3.    Assembly .....	11-2
B.    Preliminary Performance Specifications .....	11-3
C.    Discussion of General Factors Which Influence Performance and Cost .....	11-5
1.    Type of mount .....	11-5
2.    The wind environment .....	11-12
3.    Antenna reflector surface .....	11-15
4.    The reflector back-up structure .....	11-21
5.    The servo drive system .....	11-22
6.    The mobility system .....	11-24
D.    Recommended System .....	11-29
E.    Antenna Element Construction and Erection ....	11-33
F.    Cost Summary .....	11-34
Chapter 12. <u>SITE DEVELOPMENT</u>	12-1
A.    Introduction .....	12-1
B.    General Discussion .....	12-2
1.    General site factors .....	12-2
2.    Geology and foundation investigation ....	12-2
3.    Topography and drainage .....	12-3
4.    Railway .....	12-5
5.    Access roads .....	12-7
6.    Airstrip .....	12-7
7.    Water supply .....	12-7

	<u>Page</u>
8. Utilities .....	12-8
9. Real estate .....	12-8
10. Building complex .....	12-10
11. Sewage treatment .....	12-10
C. Facilities Considered Identical for Either Site .....	12-10
1. Building complex .....	12-10
2. Sewage treatment .....	12-16
3. Underground cable trenches .....	12-16
D. Cost Estimate .....	12-17
Chapter 13. <u>ELECTRONICS SYSTEM</u>	13-1
A. Introduction .....	13-1
B. Two Element Interferometer Theory .....	13-1
C. VLA Electronics - System Description .....	13-8
Chapter 14. <u>LOCAL OSCILLATOR SYSTEM</u>	14-1
A. Requirements .....	14-1
B. General Design Approach .....	14-2
C. The Proposed System .....	14-3
D. System Block Diagram .....	14-7
E. Appendix: Analysis of the Proposed Local Oscillator Distribution System .....	14-9
Chapter 15. <u>RECEIVER FRONT-ENDS</u>	15-1
A. Requirements .....	15-1
B. The Proposed System .....	15-2
1. Dual circular polarization feed .....	15-2
2. Paramp, Stage 1 and Stage 2 .....	15-2
3. Ferrite switch .....	15-2
4. Tunnel-diode amplifier .....	15-3
5. Mixer-preamp .....	15-3
6. LO distributor .....	15-3
7. Frequency doubler .....	15-3
8. Pump distributor .....	15-3

	<u>Page</u>
9. Noise source .....	15-3
10. Sweep oscillator .....	15-4
C. Degenerate Paramp - Double Sideband Mixer System .....	15-5
D. Front-End Physical Configuration .....	15-8
Chapter 16. <u>IF TRANSMISSION SYSTEM</u>	16-1
A. Introduction .....	16-1
B. Requirements .....	16-2
C. Possible Systems .....	16-2
D. Proposed System .....	16-4
Chapter 17. <u>DELAY LINE SYSTEM</u>	17-1
A. Introduction .....	17-1
B. Requirements and Specifications .....	17-1
1. Total delay .....	17-1
2. Bandwidth .....	17-2
3. Delay resolution .....	17-2
4. Delay stability .....	17-3
5. Loss variation .....	17-3
6. Equalization .....	17-4
7. Environmental control .....	17-4
C. Possible Designs .....	17-5
D. Proposed Design .....	17-8
Chapter 18. <u>CORRELATOR SYSTEM</u>	18-1
A. Specifications .....	18-2
B. Proposed Design .....	18-5
C. Mechanical Configuration, Signal Distribution, and ALC Loop .....	18-7
D. Cost .....	18-9
Chapter 19. <u>SYSTEM RELIABILITY AND MAINTENANCE</u>	19-1
A. Reliability .....	19-1
B. System Monitor .....	19-2
C. Test Equipment .....	19-4

	<u>Page</u>
Chapter 20. <u>THE COMPUTER SYSTEM FOR THE VLA</u>	20-1
A.    The Relation of the Computer to the VLA .....	20-1
B.    Correlator Data Processing .....	20-4
C.    Monitor and Control Function of the Computer .....	20-6
D.    Inversion and Display Function .....	20-11
E.    Total Computing Requirements .....	20-13
F.    Appendix: Fringe Reduction Computation Loads for Various Block Diagrams .....	20-16
1.    Data processing with no lobe-rotators ...	20-16
2.    Approximate lobe-rotators .....	20-18
3.    Integration in analog .....	20-20
Chapter 21. <u>SPECTRAL LINE SYSTEM</u>	21-1
A.    Introduction .....	21-1
B.    Basic Limitations and Capabilities .....	21-1
C.    Frequency Channels for Antenna Beams Trade-Off .....	21-3
D.    Spectral Analysis Method .....	21-4
E.    System Cost Estimates .....	21-5

Chapter 1

SUMMARY

## Chapter 1

## SUMMARY

A. Introduction

This is a proposal for the design, construction, and operation of a large radio telescope system for research in radio astronomy, to be undertaken by the National Radio Astronomy Observatory (NRAO) in the national interest and on behalf of the national and world community of radio astronomers. The proposed telescope system would consist of a very large array (VLA) of antennas and associated electronic equipment arranged in such a way as to yield, in 8 to 12 hours observing time, a radio "picture" of a region of sky with 1" angular resolution. The high resolution, sensitivity, and speed of the VLA will provide unique capabilities for radio astronomical research. These capabilities are one to two orders of magnitude greater than those of any other existing or planned instrument. With the VLA, it will be possible, for example, to investigate the detailed brightness and polarization characteristics of extragalactic radio sources with a resolution of 1" and negligible side-lobe effects. It will also be possible to conduct cosmological studies of objects almost to the edge of the "visible" universe and therefore almost back to the zero of cosmological time -- a possibility of tremendous import.

The work described in this report includes design of the array configuration, individual antennas, electronics system, control and data processing computer system, and the physical plant and support facilities. The design of all components of the system has been carried sufficiently far to establish realistic cost estimates. Estimates of operating staff and budgets have also been made.

Criteria for selecting the site of the VLA have been established. The principal criteria -- a large amount of flat land, low geographic latitude, and high elevation -- are imposed by the scientific and technical requirements of the array. In addition, it became apparent early in the design that the specific nature of the terrain and subsoil of the site were significant factors in the cost of the system. Two sites were, therefore, chosen as being representative of the range of

conditions that might be expected, and cost estimates were developed for each site.

The VLA consists of thirty-six 25-m diameter antennas, arranged in an equiangular Wye configuration. Each arm of the Wye is 21 km long. All of the antennas and their associated electronics are computer-controlled from a central location, to which the signals from each antenna are also returned for processing. The system provides several different modes of operation, is extremely flexible, and can be readily expanded or modified in the future if that should be desirable.

B. Historical Background

Higher resolution has always been a major goal of radio astronomy instrumental development. The need for resolution led, in the 1950's and early 1960's, to the extensive development and use of radio interferometers, particularly at the radio observatories in Cambridge and Manchester, England; Sydney, Australia; and Cal Tech in the United States. But even the sophisticated interferometers that have been developed have serious disadvantages, in that they produce high side-lobe levels or fan beams which limit their usefulness or they are very slow instruments. In 1960, and before, ideas began to develop at various places for an instrument that would map, in reasonable observing time, a region of sky with a high-resolution pencil beam. Since then, various technical developments have occurred which make feasible the achievement of such an instrument, with 1" resolution.

The general concept of the VLA as an instrument to obtain radio "pictures" with high resolution, sensitivity, and speed began developing at the NRAO in 1961, and some preliminary studies were done in 1961 and 1962. In the spring of 1963, development of a variable-baseline interferometer giving 8" resolution was begun in order to investigate and develop the techniques that would be required for the VLA. In particular, the technique of supersynthesis developed by Ryle (1962) appeared to offer the most promising means of achieving the VLA concept, and the interferometer was built to be used in that technique.

The Panel on Astronomical Facilities of the National Academy of Sciences' Committee on Science and Public Policy published its report -- Ground-Based Astronomy, A Ten-Year Program (National Academy of Sciences;

National Research Council, Washington, D. C. 1964) -- in August, 1964. The report of the Panel stated " ... that the primary need in radio astronomy is a very powerful high-resolution instrument." The Panel recommended construction, by the NRAO, of a large array that would achieve a resolution of less than 10" at centimeter wavelengths, with low side-lobe levels, and with sufficient sensitivity to detect 25 sources per square degree of sky. The Panel further recommended, as a secondary goal, that the array should if possible achieve 1' resolution at 21-cm wavelength, with extremely low side-lobe levels.

In response to these recommendations, the NRAO began detailed systems studies in the summer of 1964. Funds for design work have been provided by the National Science Foundation in Observatory budgets for Fiscal Year 1965, 1966, and 1967. The design has been carried out by the NRAO staff with the assistance of a number of radio astronomers from other institutions. Several general meetings were held during the course of the work to review progress and problems. Approximately twenty-five radio astronomers from throughout the country participated in each of these review meetings. The discussions at these meetings have had a strong influence on the final design; in particular, the resolution of the instrument has been progressively improved from 10" to 1". A preliminary progress report of the design work was issued and widely distributed in January, 1966.

#### C. Description of the VLA

The proposed VLA consists of thirty-six 25-m diameter antennas, together with their associated electronics and other equipment. The system is operated as a correlator array, utilizing the principle of aperture supersynthesis. The output of each antenna is correlated with that of every other antenna in the array. The 630 simultaneous correlator outputs, each representing one component of the complex Fourier transform of the brightness distribution of the region of sky under observation, are processed and accumulated in a computer for a period of up to 12 hours, during which time the array tracks the region of sky as the earth rotates. Some  $10^4$  independent Fourier components are obtained in 8 to 12 hours, which are then transformed into a "picture" of the source or region observed.

The individual antennas are paraboloids of revolution with solid surface permitting operation to wavelengths as short as 3 cm. They are altitude-azimuth mounted, giving full sky coverage to within 5° of the horizon. Positioning and tracking of the antennas are under control of a central computer.

The antennas are placed along the arms of an equiangular Wye configuration. Each arm of the Wye is 21 km in length. A pair of standard-gauge railroad tracks runs the full length of each arm of the Wye. The characteristics of the array -- resolution and side-lobe levels -- may be modified as needed by moving the antennas along the arms of the Wye on the track system. Three self-propelled transport systems consisting of standard railroad trucks are used to move the antennas, which are normally bolted to concrete foundations when in use. A complete change of array configuration can be accomplished in two days.

The electronic system is basically that of a conventional double sideband correlation interferometer, with some complexity introduced by the long distances and large number of elements involved. Low noise, uncooled, degenerate parametric amplifiers are employed in the front ends, giving high stability and total system noise of less than 100°K. A phase stable LO signal is provided at each antenna through use of a coaxial cable round-trip phase correcting system.

A central computer is used to perform data processing and all monitor and control functions for the antennas and electronics.

#### D. Operation of the VLA

The VLA will be operated as a national facility whose use is open to all, solely on the basis of the scientific merit of the programs proposed. A permanent staff of engineers and technicians will be at the site to operate and maintain the instrument and assist scientists in their observing programs. No permanent scientific staff will be based at the VLA site.

A variety of different operating configurations are available with the VLA, so the instrument performance can be tailored to a particular program. The four primary configurations give 1", 3", 9", and 27" resolution at 11-cm wavelength, with rms side-lobe levels less than - 30 dB, in an observing time of 8 hours. Fig. 1-1 shows the antenna pattern of the VLA for the configuration giving 1" resolution. At 1" resolution, the minimum

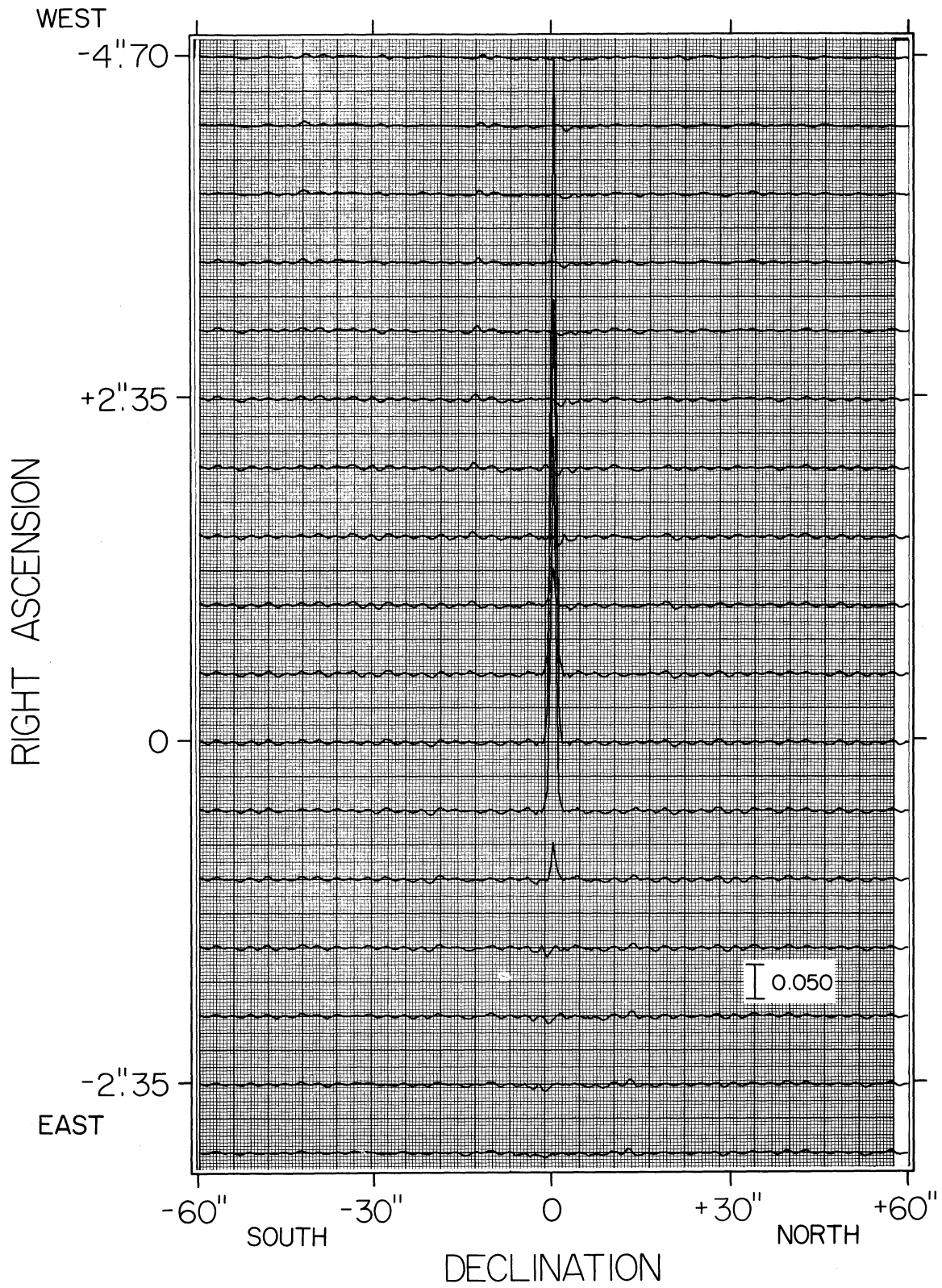


Figure 1 - 1. The antenna pattern of the VLA, with one second-of-arc resolution.

detectable flux density is about  $1.5 \times 10^{-30} \text{ W m}^{-2} \text{ Hz}^{-1}$ . The system is highly versatile: circular or linear polarization measurements can be readily made; changing operating frequency, though not a minor operation, can be accomplished with only one or two days of down time; configuration changes likewise require a few days down time; the system can, if desired, be broken up into several smaller arrays for simultaneous use on several programs not requiring all of the characteristics of the full array.

The data processing will be a major aspect of any observing program conducted with the VLA. Since the array measures a selected sample of the components of the Fourier transform of a brightness distribution and a Fourier inversion of these components is necessary to recover the brightness distribution, a number of choices are open to the observer as to how the data are processed. The array computer will produce, for each observation, a map of the brightness distribution obtained from the principal solution of the Fourier transform. In addition, the individual Fourier components, some  $10^4$  measures of phase and amplitude in a typical 8-hour observation, will be put on magnetic tape along with the  $10^4$  picture elements of the map for alternate reductions and further analysis by the observer.

Provisions for easy and reliable operation, maintenance, and repair are also major considerations of the VLA system. The entire array is operated and monitored through the central computer via a simple set of instructions. The entire system is monitored semi-continuously and diagnostic routines will quickly isolate a malfunction and output the pertinent data to the operator.

#### E. Summary of Costs

The estimated cost of the proposed basic VLA system is given in Table 1-1 in 1966 dollars. The estimates include design, fabrication, and installation of all components, engineering and inspection, administration costs and architect engineering costs. Site development and acquisition costs will depend on the particular site chosen. The figures in Table 1-1 are for the less expensive of two possible sites for which detailed estimates were made.

Table 1-1  
Construction-Cost Estimate Summary, VLA Facility

	<u>Cost (millions)</u>
Antenna System	\$ 17.1
Track System	6.7
Electronic System	5.6
Computer System	3.7
Site Development and Utilities	2.9
Site Acquisition	<u>0.1</u>
Total, VLA Facility	\$ 36.1

A 15% contingency should be added to the costs in Table 1-1, at this stage of the design. Provision for cost escalation through the procurement and construction stage should also be included. The estimated cost is \$4.6 million. Additional research equipment over that included in the basic facility is needed to bring the array to its full potential and is estimated at \$5.8 million. This includes equipment for multi-frequency and multi-polarization operation and for spectral line work. It is desirable for both scientific and economic reasons to obtain this equipment at the same time as the basic array, if at all possible. The total construction authorization requested, therefore, is \$51.9 million, as shown in Table 1-2.

Table 1-2  
Summary of Total Authorization Request

	<u>Cost (millions)</u>
VLA Facility (Table 1-1)	\$ 36.1
Contingency	5.4
Escalation	4.6
Research Equipment	<u>5.8</u>
Total Construction Authorization	\$ 51.9

The annual cost of operating the VLA system is estimated to be \$1.7 million. This includes operating and maintenance costs and general plant and research equipment but does not include any major new research equipment or facility expansion. Construction is estimated to require four years from date of authorization.

#### REFERENCE

Ryle, M. 1962, Nature 194, 517.

Chapter 2

SCIENTIFIC CONSIDERATIONS

## Chapter 2

## SCIENTIFIC CONSIDERATIONS

A. The Need for Higher Resolution

Radio observations of celestial objects are of fundamental importance to a better understanding of the universe. This has been amply demonstrated by the recent history of astronomy. But the radio "picture" of the universe attainable today is still blurred and confused by the relatively poor resolution and sensitivity of radio telescopes. The design of the VLA is based on the very great need in radio astronomy for an instrument that can produce high-resolution "pictures" of radio sources or regions of sky. High-resolution "pictures" are needed for two basic reasons: (1) to study the detailed radio structure of celestial objects, and (2) to allow the measurement of faint sources of radiation without confusion due to the blending of neighboring sources. Greater resolution has been a major, continuing goal of instrumental developments in radio astronomy for just these reasons.

While the need for much greater resolution and sensitivity is apparent in almost every branch of radio astronomy, from studies of the sun and planets to examination of the most distant galaxies, it is in the study of extragalactic radio sources that present limitations are perhaps most keenly felt. Extragalactic radio sources exhibit some of the most puzzling phenomena found in the physical world today. The nature of the phenomena suggests that they are of fundamental importance, not only to astronomy but to physics as well. Intense radio emission appears to be associated most frequently with giant elliptical galaxies, although the cause of the association is not known, and radio emission is found in other types of extragalactic objects as well. The energy involved in the processes giving rise to radio emission is estimated to be as high as  $10^{61}$  ergs in some objects -- a significant fraction of the total energy of a galaxy. The source of this energy is unknown. The radio emission arises in volumes ranging from much smaller to much larger than a galactic volume, and the regions of radio emission are often displaced from the optical galaxy by tens of thousands of parsecs. The distribution of radio emission across the emitting regions is often extremely complex.

The recently discovered quasi-stellar sources are also objects of very great interest. In general, they are much smaller in size than are radio galaxies but emit comparable -- and in some cases much more -- energy. In some of them the emission is variable with time. These characteristics suggest two interesting conclusions: the lifetimes must be very short -- a few tens of years; and the linear dimensions must be very small -- a few tens of parsecs or less. How the huge amount of energy is generated in so short a time and so small a volume is a question of fundamental physical importance.

The great interest in these extragalactic radio sources is due principally to the large energies and the very wide range of phenomena they exhibit. The large energies and complexity of the phenomena imply the occurrence of events of a physically fundamental nature, hitherto unrecognized. The large energies also permit observations of these objects at very great distances, which make them of utmost importance to cosmological studies.

In order to understand the physics of radio sources and to use them for cosmology, it is necessary to observe a large number of sources in as great detail as possible. This, in turn, requires instruments with the highest attainable sensitivity and resolution. Sensitivity to weak signals is needed to study sources at large distances. Resolution is needed both to achieve the sensitivity, by preventing the instrument from being confusion-limited at too high a flux level, and to allow study of the detailed brightness and polarization distributions within nearby sources and the general structure and dimensions of distant sources. The recent history of extragalactic research clearly illustrates these needs.

Much progress has been made in recent years in determining some of the observational characteristics of extragalactic radio sources, such as radio spectra, optical identifications, radio diameters, and gross radio form. However, relatively little progress has yet been made in understanding the physical processes involved in the radio galaxies, or even in a systematic classification or correlation of the principal observed characteristics, which is a necessary first step both to further understanding of them and to their use in cosmology.

The total number of sources that have been studied in any detail is still small -- of the order of a few hundred. The range in observed parameters -- flux density, angular size, polarization -- is also small. But the range in physical parameters -- luminosity, dimensions, radio and optical forms, etc. -- is very large. The range in radio luminosity, for example, is greater than  $10^9$ , while the observable range of flux density is only about  $10^3$ . Similarly, the range in dimensions is of the order of  $10^5$ , but the observable range of angular size is more like  $10^2$ . Thus, it is difficult to establish correlations between parameters, or to determine which features are of a general, fundamental nature and which are secondary perturbations, or to place the observed characteristics in any meaningful sequence relating to evolution or to physical nature. Detailed data on a very large number of sources are needed to overcome this problem. The observations must reach sufficiently low flux-density levels that the present great disparity between the directly observable range of a parameter, such as flux density or angular diameter, and the very large inferred physical range, such as luminosity and linear dimension, is significantly reduced. Until this can be accomplished, there may be severe selection effects in all observed data which make physical interpretations difficult.

In addition, there are two observable parameters of fundamental importance which are not now available in any quantity and which cannot be obtained with existing instruments. These are the detailed radio brightness and polarization distributions within sources and the possible variation of these quantities with time and with frequency. Instruments of the highest possible resolution, sensitivity, and speed are required to observe these parameters.

The influence of resolution on studies of the physics of extragalactic radio sources is clearly illustrated by the example shown in Fig. 2-1. This figure shows the brightness distribution of the radio source Cygnus A, as observed with 24" resolution with the Cambridge synthesis instrument (Ryle, et al., 1965) and with 8" resolution with the NRAO synthesis instrument (Wade, 1966). The difference is striking, and it is quite clear that any attempt to develop a physical theory from the lower-resolution data will be fruitless.

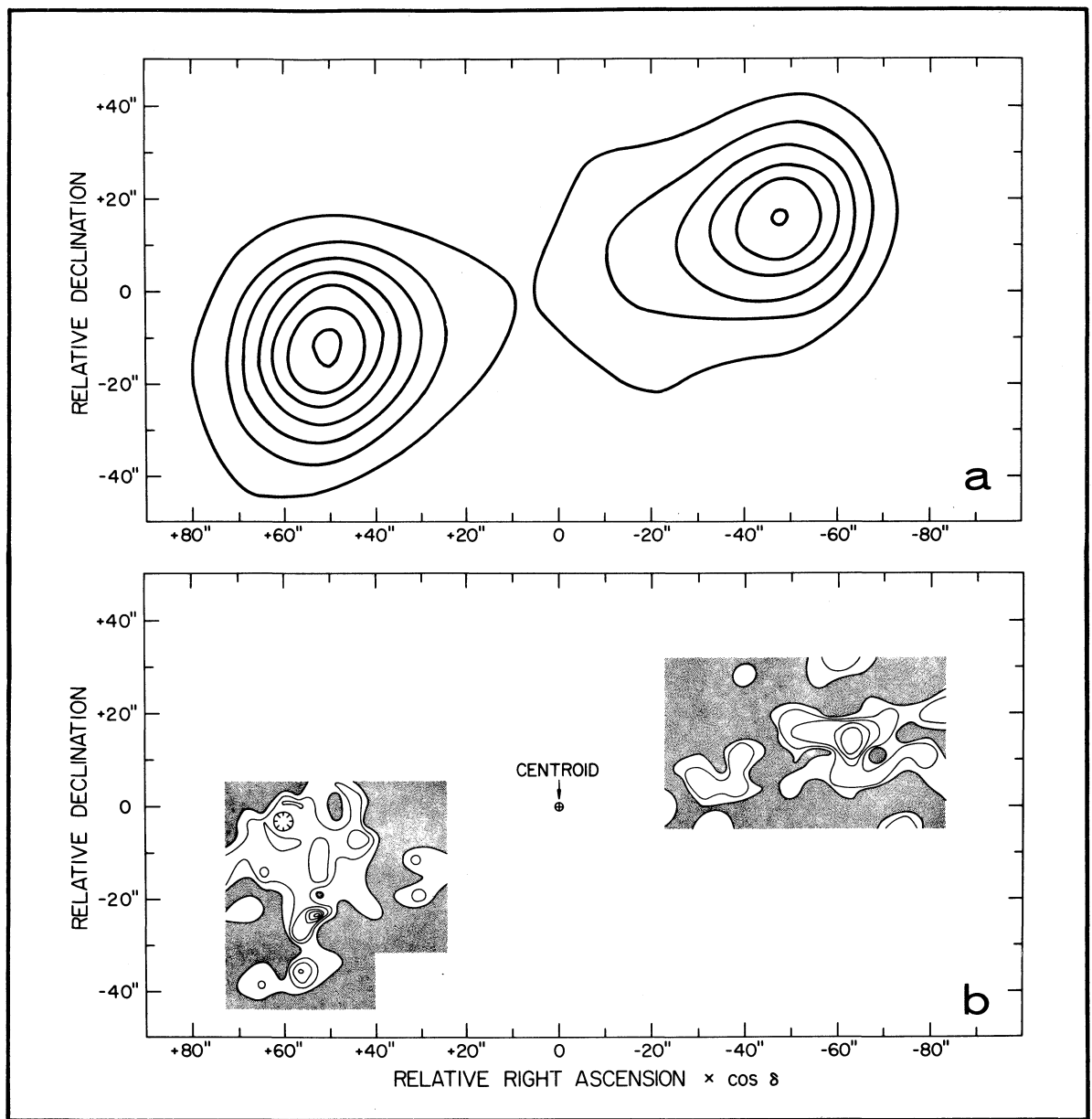


Figure 2 - 1

(a) Map of Cygnus A based on Cambridge super-synthesis observations at  $\lambda$  21.3 cm (adapted from Ryle et al. 1965). Contour interval is 52000 °K; effective synthesized half-power beamwidths are 23" (EW) by 35" (NS). The coordinates are arbitrary.

(b) Map of Cygnus A derived from NRAO interferometer observations at  $\lambda$  11.1 cm (Wade 1966). Contours are drawn at intervals of a factor of two in surface brightness; the lowest is at brightness temperature 20000 °K. Effective angular resolution ranges from 3" for the brightest features up to 8" for the faintest. The features shown here account for about 80% of the total source flux density.

Cygnus A is the brightest and best-known extragalactic radio source. It was first identified optically in 1952, it has been extensively observed at many observatories and at many frequencies during the past fifteen years, and its gross features are well established. But there has been practically no theoretical progress in understanding the source, and one major reason has almost certainly been the lack of a very high-resolution picture such as that shown in Fig. 2-1. Even here it is clear that some features of the source structure remain unresolved and that still higher resolution is needed.

Most extragalactic radio sources have angular dimensions less than  $1'$ , and recent observations, such as those shown in Fig. 2-1 and others obtained with very long-baseline interferometers, indicate that many extragalactic sources have extremely complex brightness distributions with angular scales of the order of seconds of arc or less. High-resolution, high-sensitivity observations of the brightness and polarization distributions in a large number of sources are required to make significant progress in understanding these very baffling objects.

Cosmology is another area which requires the data from high-resolution, high-sensitivity radio telescopes. A principal hope for progress in cosmology rests on the expectation that radio telescopes can examine galaxies to very great distances in the universe. Thus, the most distant galaxy ever seen optically was initially noted as a strong radio source. Cosmologists require data on many radio sources at the greatest possible distances, and for many years a major activity of radio astronomers has been the attempt to provide accurate and systematic catalogs, free from selection effects, of radio sources with the smallest possible lower limits on flux densities. The pioneer catalogs of this type were produced at Cambridge, England, and Sydney, Australia. These catalogs immediately demonstrated that the sensitivity of the radio telescope was not necessarily the limiting factor governing the number of detectable sources. Confusion, due to the blending of weak sources, is the most common limitation of the number of sources observable. Thus, antennas with smaller beam widths, as well as greater sensitivities, are needed to study sources at great distances.

There are at least two lines of attack on the cosmological problem which utilize radio observations of extragalactic sources. The first is

the investigation of the way in which the number of sources brighter than a given limiting flux density increases as the limiting flux density is decreased, the  $N(S)$  relation. In principle, this relationship can give information about the type of universe in which we live and about the evolution of radio sources and the universe. Different cosmological world models predict different  $N(S)$  relations, and these predictions can be tested if the counts of numbers of sources as a function of flux density can be pushed to sufficiently faint flux densities. However, two other factors may also affect the  $N(S)$  relationship.

First, if radio sources evolve in such a way and with such a time scale that their average characteristics vary with time, then the  $N(S)$  relationship may be altered. Looking deeper into space necessarily implies looking farther back in time, and the most distant objects are thus seen at an earlier epoch than are the nearby objects.

Second, if the universe itself is evolving, the observed  $N(S)$  relationship will also be affected. For example, if the physical state of the universe earlier in its history was such that the rate of formation of radio galaxies was different from what it is today, then in looking farther into space and farther back in time, a greater or lesser average space density of radio sources would be observed, depending on whether the rate of formation of radio sources was greater or less at earlier times. Thus, the  $N(S)$  relationship may contain information about the cosmological world model, about the evolution of radio sources, and about the evolution of the universe. If, as may be the case, there are different classes of extragalactic radio sources, with different spatial distribution, evolutionary history, or other characteristics, investigation of the  $N(S)$  relationship should give information about these parameters too, provided that the different classes of source can be separated. Quasi-stellar radio sources, for example, if their red shifts are true cosmological Doppler shifts, can also be observed at very great distances, perhaps even greater distances than the radio galaxies. However, at least some of them are apparently in a stage of very rapid evolution -- with time scales of the order of tens of years, as opposed to perhaps millions of years or tens of millions of years for the radio galaxies -- and their cosmological history and significance may be very different from that of radio galaxies.

At present, the only certain means of distinguishing between radio galaxies and quasi-stellar sources is by their optical characteristics. This information may not be available for objects at very great distances, and some means of radio identification must be found. Recent investigations of the correlation between radio spectra and diameters of sources offer some hope in this connection, but the relations need to be much more firmly established. Thus, the identification and separation of different classes of radio sources is an important problem for many lines of investigation. This again requires observations of the detailed characteristics of a large number of sources to find possible correlations between different parameters. These observations, in turn, require high sensitivity and resolution, and reasonable speed.

The second class of radio astronomical data of great potential value to cosmology is the statistics of radio source diameters or the statistics of the separations of double radio sources, the  $N(\theta)$  relationship. The same general considerations discussed above for the  $N(S)$  relationship also apply to the  $N(\theta)$  relationship. There are not yet enough data available to determine the real value of such a line of research to cosmological problems. If successful, it will provide another observational approach to finding the geometry and history of our universe. Again, large masses of high-resolution data are needed.

As already mentioned, a necessary adjunct to studies of source statistics is the investigation of individual characteristics of a large number of sources, in order to classify and correlate their properties. It is not sufficient simply to count numbers of distant sources and measure their flux densities or diameters; it is also necessary to know the principal characteristics of the sources being counted.

Recent comparisons of optical and radio features of those radio sources which have been optically identified have shown, as mentioned earlier, that extragalactic radio sources have a wide variety of characteristics. In order to make meaningful use of the statistics produced by deep sky surveys, it is essential that a realistic classification of radio galaxies be developed, including the evolutionary sequence and intrinsic luminosities. The best hope for success in this effort lies in the detailed examination of a large number of relatively nearby

galaxies. This, in turn, again requires the highest possible angular resolution, of the order of seconds-of-arc.

The highest possible resolution and sensitivity are needed in virtually all areas of radio astronomy. In addition to the areas of extragalactic research, briefly discussed above, planetary studies, galactic studies, and radio spectroscopy -- particularly investigations of the 21-cm line of hydrogen -- are also urgently in need of instruments which will yield increased resolution and sensitivity. It is clear that radio resolution comparable to that of optical resolution, at least of the order of a few seconds-of-arc, is ultimately needed for these types of studies. Our present radio "pictures" of our own galaxy, and even of the solar system, are very fuzzy. As a prime example drawn from solar system astrophysics, high-resolution radio telescopes offer the possibility of studying the atmospheres and radiation belts of Jupiter and Saturn. As longer wavelengths are used, the observed radiation originates at greater depths in the atmosphere. By obtaining high-resolution radio "pictures" of these planets at different wavelengths, we can determine the contributions from radiation belt and planet, and from the latter the temperature profile in the atmosphere. The results deriving from the latter data would have great impact on problems of planetary atmospheres.

#### B. Performance Goals of the VLA

General consideration of the problems in radio astronomy, such as those discussed briefly in the preceding section, has led to the concept of a radio analog of the 200-inch optical telescope -- a radio telescope which can produce a "picture" of a radio source or region of sky with resolution and sensitivity comparable to that achieved with optical telescopes, in reasonably short observing time. This is the basic performance goal of the VLA. No such instrument exists at present, even, except for the VLA, on the drawing board. When a radio telescope with these capabilities does exist, it will revolutionize radio astronomy.

The major specific performance goals set for the VLA design are discussed below.

##### 1. Angular resolving power

There is no particular value of resolution which can be stated as being "adequate." Better resolution always brings better results, and the

quest for higher resolution needs to be pushed until some fundamental limit is reached. In the optical case, the limit for ground-based observations is determined by atmospheric inhomogeneities and has already been reached. In the radio case, the limit is probably also set ultimately by atmospheric inhomogeneities. These inhomogeneities do not produce significant degradation of performance in any antennas constructed to date. If possible within reasonable budgetary limits, it is desirable to produce an instrument capable of the greatest resolution permitted by atmospheric limitations. Although these limitations are not yet fully established, it appears possible to achieve 1", at least, which would be comparable to the capabilities of ground-based optical telescopes. It would also be more than an order of magnitude improvement over existing radio telescope capability. Therefore, the goal for the VLA has been set at 1" resolution. The VLA system design should not preclude attainment of still higher resolution at a future date, by use of a shorter wavelength, or expansion of the dimensions of the system, or both.

## 2. Sensitivity, side-lobe levels, field of view

These three parameters are related in a complicated way to each other and to resolution, length of observing time, and distribution of sources. No absolute goals can be easily stated. Instead the design should be established on the basis of minimum requirements plus attainment of a balance between these parameters. The sensitivity of the system may be determined by system noise and collecting area, length of observing time, confusion in the main beam, confusion in side-lobes, or a combination of these factors. Thus, the design must attempt to achieve a balance between them.

The Panel on Astronomical Facilities of the National Academy of Sciences (1964) recommended a sensitivity sufficient to detect 25 sources per square degree of sky. This requires a minimum detectable flux density of about  $2 \times 10^{-2}$  flux units (one flux unit is  $10^{-26} \text{ W m}^{-2} \text{ Hz}^{-1}$ ). To measure 1% polarization in those sources, or to measure brightness distributions in them with a dynamic range of 100, would require a minimum detectable flux density of about  $2 \times 10^{-4}$  flux units. At 1" resolution, there is a fundamental limit set on sensitivity by the confusion of unresolved sources in the one-second beam. This limit is between  $10^{-3}$

and  $10^{-4}$  flux units, depending on the density of faint sources. Thus the array sensitivity should approach  $10^{-4}$  flux units as closely as proves feasible, and it should not be less than about  $10^{-3}$  flux units. It is necessary to reach the limit set by confusion in the main beam in order to fully utilize the system capability.

The above goal of  $10^{-3}$  to  $10^{-4}$  flux units for the sensitivity imposes conditions on the side-lobe levels, in order to minimize confusion due to sources outside the main beam. It requires that rms side-lobe levels be at least 30 dB below the main beam. In addition, side-lobes within the observed field of view should be below about - 20 dB, in order that they not interfere with the measurement of brightness distribution of extended sources.

The field of view to be covered in an observation must also be specified. For studies of the brightness and polarization characteristics of individual sources, it should be larger than the dimensions of most of the sources of interest. A field of view of 1' to 2' would suffice for this purpose. For statistical and cosmological investigations, the field of view should be large enough to allow a reasonable number of sources to be observed per day. This will depend on the density of faint sources and on other characteristics of the system but might be as large as 10'. Therefore, fields of view not smaller than 1' and not larger than about 10' appear to be reasonable goals.

### 3. Polarization and frequency range

Knowledge of both the spectral distribution and the polarization of radio source emission are important to an understanding of the source. The VLA should, therefore, be capable of measuring polarization and of operating over a range of frequencies, in order to determine the spectrum and the dependence of brightness distribution on frequency.

Since polarization and brightness as a function of position, frequency, and time are the only directly observable parameters of any celestial object (aside from discrete spectral lines), it is extremely important that the VLA have both polarization capability and the ability to be used at different frequencies.

### 4. Speed

The question of the rate at which a scientific instrument should be capable of collecting data is purely subjective, without any quantitative

answer. However, all past experience shows that the speed of an instrument is often a determining factor in its scientific value and usefulness. A 20-inch optical telescope, for example, has the same resolution and limiting sensitivity for many types of observations as does the 200-inch -- but the 200-inch telescope is two orders of magnitude faster. The speed of the 200-inch telescope is a major reason why it is the world's most powerful telescope.

Many other examples of the value and importance of speed could of course be given. The computer is an obvious one. The speed of computers has revolutionized many areas of scientific work and of a wide variety of other activities as well.

There is no doubt that the feasibility of undertaking a problem is directly related to the time needed to reach a solution and that the scientific value of an instrument is determined in part by its speed.

The use of the 140 ft and 300 ft telescopes at the NRAO, for spectral-line and mapping work, illustrates a different aspect of the speed question -- that of elapsed time. The 300 ft has twice the resolution and four times the collecting area of the 140 ft, and therefore is considerably more powerful. However, it is a transit instrument, while the 140 ft has full tracking capability. Thus scientists with programs requiring either long integration times or the mapping of an extended region of sky almost invariably prefer to use the 140 ft, because, although the total observing time required to accomplish the program is 16 times as long as with the 300 ft, it can be accomplished in shorter elapsed time due to the tracking capability of the 140 ft. Thus, a program requiring four hours of integration time on the 140 ft to reach a desired flux density limit would require only 15 minutes integration time on the 300 ft; but on the 140 ft the program could be accomplished in one continuous four-hour period, while on the 300 ft the required 15 minutes would have to be accumulated at the rate of one 40-second transit per day for 22 days. Many programs that are simply not feasible with the 300 ft because of the long elapsed times required can be readily accomplished with the 140 ft.

Both speed and elapsed time are important considerations in the VLA design. A goal of "reasonable speed" for obtaining an observation was

initially set for the VLA, without precise definition of what was "reasonable." In any of the various instrumental techniques which could accomplish the VLA performance goals, the cost of the instrument will be strongly dependent on the speed and elapsed-time requirements. There is a direct trade-off between cost and speed.

A variable-spacing, 2-element interferometer can produce all of the performance requirements established above, except "reasonable speed." To map one small region of sky with such an interferometer would require a total elapsed time of almost five months, which is clearly not reasonable for an instrument which is to be a national facility serving the needs of a large number of scientists. With 200 antennas, or a continuous aperture, the time required for an observation can be reduced to a few minutes, but only at prohibitive cost. Reasonable speed, therefore, lies somewhere between the extremes of a few minutes and five months.

As the design progressed, it became apparent for various reasons, including speed considerations, that the aperture supersynthesis correlator array was the most feasible system for the VLA. For such a system, the natural breakpoint between cost and time is 12 hours. To effect cost savings by using fewer elements than needed for a 12-hour observing time requires using the system in different configurations over a succession of days. Because of scheduling considerations and the time required to change the array configuration, any reduction in number of elements from that needed for a 12-hour observing time in practice probably means the total time interval to complete an observation of one region of sky becomes at least two to four weeks. Since the cost is proportional to the number of elements, while the rate of obtaining data is proportional to the square of the number of elements, the cost saving is very small compared to the increased time and decreased efficiency. At the other extreme, the cost to accomplish an observation in times much less than 12 hours rises steeply.

These considerations are illustrated in Fig. 2-2, which shows the cost of an array as a function of the observing time required to map one field of view. The cost has been normalized to unity for an observing time of 12 hours. In deriving the curve, it was assumed that one-half

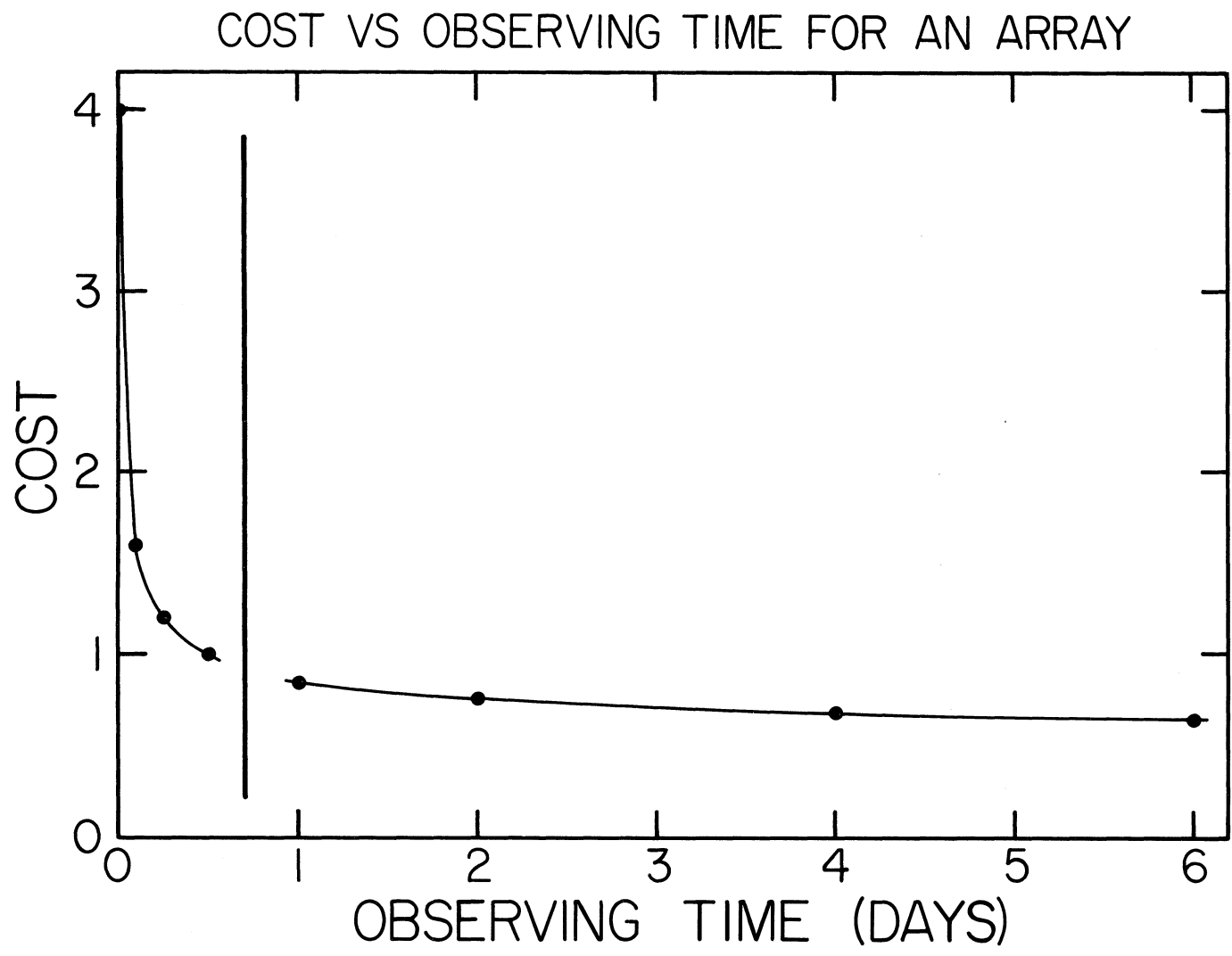


Figure 2 - 2

the total cost of the array was in items not directly related to the number of elements -- principally physical plant and railroad tracks on which to move the antennas. Actual cost and performance estimates of specific arrays adhere closely to the approximate relation of Fig. 2-2.

The abscissa of Fig. 2-2 is the total observing time. To the right of the vertical line, total elapsed time between start and finish of a given observation will be longer by a factor dependent on the time required to change configurations and the ratio of the time to be spent observing to the time to be spent moving. If the time to change a configuration is 12 hours and if a ratio of observing to non-observing time of 1 is acceptable, the times to the right of the vertical line must be doubled to get elapsed time. A more likely situation, however, is a ratio of observing to non-observing time of 10, and one to two days to change configurations, in which case the times must be multiplied by 10 to 20.

In view of these considerations, the speed requirement of the VLA has been set at 12 hours -- that is, it should be possible to map one field of view in one continuous observing period of no longer than 12 hours, without any change of array configuration.

#### 5. Spectral-line capability

Although the primary purpose of the VLA is the study of the continuum emission of radio sources, it should also be made useful for spectral-line work, if possible. This means that:

(a) provision should be made for a configuration that will permit obtaining the very low side-lobe levels required in galactic spectral-line work, even at the expense of lower resolution and/or longer observing time, if necessary;

(b) the selection of particular subsystems should not preclude the ultimate use of the instrument for line work.

#### 6. Versatility

The VLA should be as versatile an instrument as possible for at least the following three reasons:

(a) to allow application of the power inherent in its resolution, sensitivity, and speed to a wide range of diverse astronomical problems;

(b) to enable its capabilities to be readily modified to meet the changing, and not always easily predictable, needs of the science;

(c) to enable it to better fulfill its function of a national facility which can efficiently meet the varying requirements of a large number of radio astronomers.

This latter consideration -- that the VLA is a national facility to be used by large numbers of "visiting" scientists -- enhances the importance of various factors which are often relatively unimportant in an instrument used primarily by a resident staff. Versatility is one of these. Speed, reliability, and ease of operation are others, already mentioned. All take on greater importance at a national observatory used primarily by visitors than at a scientist's home institution where time and continuity of effort are possible for him. The flexibility, versatility, and speed must be provided in advance at the national facility, often at considerable cost, but with the reward of an instrument of great power available to all.

More than one hundred scientists and graduate students used NRAO telescopes in 1965-66. The doubling time for the number of radio astronomers is -- from several lines of evidence -- about four years. Thus, potential users of the VLA are expected to number more than two hundred by 1970, and more than four hundred by 1974. From experience at the NRAO thus far, they will generate a very great demand for diverse uses of the VLA, and the instrument should be as versatile as possible, to meet as many of the demands as possible.

### C. The VLA Performance

The design of a telescope system that will meet the performance requirements discussed in the preceding section is the subject of the bulk of this report. The results are summarized here in a description of the performance characteristics of the VLA that have been established by the design. In Section D of this chapter these characteristics are applied to specific radio astronomy problems to illustrate the potential power of the instrument.

The VLA will have the following characteristics:

#### 1. Wavelength

Eleven centimeters is the primary design wavelength. The system design is flexible enough to accommodate changes of wavelength with relative ease and for relatively low cost. In particular, provision for 5.5 cm wavelength has been made.

## 2. Resolution

Four configurations, giving 1", 3", 9", and 27" at 11 cm wavelength, are available for continuum observations. Each of these configurations will allow pencil-beam mapping of a region of sky of radius 30 to 60 times the diameter of the synthesized beam, depending on the bandwidth used. In the case of the configuration giving 27" resolution, the field of view is limited to a diameter of about 17' by the primary beam width of the individual elements of the array. In addition, fan-beam resolutions as good as 0.6" are available.

## 3. Side-lobe levels

In all configurations, including that giving 1" resolution, the mean side-lobe levels within the field of view are less than - 22 db. The rms side-lobe and grating-lobe level within the entire 17' field is less than - 30 db. The confusion due to sources in side-lobes is less than that due to unresolved sources in the main beam.

## 4. Sensitivity

A point source whose flux density is  $10^{-4}$  flux units will yield a signal-to-noise ratio of 5, in the absence of confusion. Assuming a static, Euclidean universe, and extrapolating from existing low-sensitivity source surveys, the array will also be resolution limited at about  $10^{-4}$  flux units.

## 5. Time required for an observation

To achieve the above resolution, side-lobe levels, and sensitivities requires an observing time of 8 hours. Observations of up to 12 hours may be made to further reduce side-lobe levels. No changes in the positions of the elements of the array are required. Observations not requiring such low side-lobe levels may be obtained in shorter observing times. Similarly, observations requiring still lower side-lobe levels may be accomplished by successive measurements with the array elements in complementary configurations, at the expense of more total observing time.

## 6. Polarization

Circular or linear polarization observations may readily be made. In particular, the speed of the VLA is great enough to make feasible the complete polarization synthesis of extended sources.

### 7. Versatility

The correlated outputs of all possible pairs of antennas are separately available. Every antenna is movable to any position within the array configuration. The individual antennas of the array are altitude-azimuth mounted paraboloids of revolution, operable to wavelengths as short as 3 cm. Thus, a very wide range of both electronic and geometric configurations can be achieved with at most minor modifications to the system. The system can, for example, be split into two or more smaller arrays to allow independent programs to be carried out simultaneously. In addition, the array is, by its nature, readily expandable to give increased resolution, sensitivity, or flexibility as future developments in radio astronomy dictate. Radio astronomy is a rapidly changing field. The instrumental needs of ten or fifteen years hence cannot be reliably predicted, but the instrument of five or ten years hence should, if possible, be capable of adapting to those needs.

### 8. Hydrogen-line configuration

A configuration with somewhat modified electronics can be provided to give an instrument with about 1.5' resolution at 21-cm wavelength, with multi-frequency spectrometer capability. The standard array can also be used in either of its two lower resolution configurations to give 54" or 18" resolution at 21 cm.

The VLA is by far the most powerful and versatile radio telescope system ever designed. It is of some interest to compare it with other existing or planned radio telescopes. The parameters characterizing a telescope system include resolution, sensitivity to point sources and extended objects, side-lobe characteristics, speed, polarization characteristics, frequency range, flexibility, and ease and economy of operation. The relation between these parameters is complicated. It is difficult to make a quantitative comparison of systems designed for somewhat different purposes or with different emphasis on various parameters. However, a good qualitative comparison is afforded through the following three basic parameters:

(1) The total physical collecting area of the system. This is a direct measure of the sensitivity per unit time of the system, for point-source observations.

(2) (a) For synthesis instruments, the number of Fourier components measured per unit time. This is a measure of the speed of the instrument for synthesizing a desired beam and observing an area of sky.

(b) For continuous-aperture instruments, the number of beams produced. In terms of speed in measuring an area of sky, this is equivalent to the number of simultaneous Fourier components in the synthesis case.

(3) The product of the maximum orthogonal linear dimensions of a system. This is a direct measure of the maximum resolution obtainable. In the case of a system consisting of a single line of elements and utilizing supersynthesis, the quantity used is one-fourth the square of the maximum linear dimension -- a rough approximation of the effective orthogonal dimension introduced by the supersynthesis.

The following systems are compared:

VLA: Thirty-six 25-m antennas in a Wye configuration, with each arm of the Wye 21 km long.

Cal Tech Array: Eight 130-ft antennas in a cross configuration of maximum dimensions 16,000 ft north-south by 9,000 ft east-west.

Westerbork Array: An east-west line array of twelve 25-m antennas. The maximum linear dimension is 1,600 m.

Cambridge One-Mile Telescope: An east-west line array of three 60-ft antennas. The maximum linear dimension is one mile.

NRAO Three-Element Array: A line array of three 85-ft antennas. The line is tilted  $28^\circ$  from east-west. The maximum linear dimension is 2,700 m.

All of the above systems are synthesis arrays. In principle, all can be operated at wavelengths as short as about 3 cm. Two quite different systems are also included to complete the comparison:

Molonglo Cross: A continuous-aperture Mills cross with dimensions one mile by one mile. The arms of the cross are 40 ft wide. Its wavelength limit is about 20 cm. It is operable with 11 simultaneous beams.

500-Foot Paraboloid: A conventional parabolic telescope, 500 ft in diameter. It is assumed that it is operated with five simultaneous beams.

Table 2-1 gives the quantities of A, B, and C for each of these systems.

Table 2-1

<u>System</u>	<u>A</u>	<u>B</u>	<u>C</u>
VLA	$1.8 \times 10^4$	630	$1.14 \times 10^3$
Cal Tech Array	$9.9 \times 10^3$	28	13.4
Westerbork Array	$5.9 \times 10^3$	66	.64
Cambridge One-Mile Telescope	$7.9 \times 10^2$	2	.65
NRAO Array	$1.6 \times 10^3$	3	1.8
Molonglo Cross	$4.0 \times 10^4$	11	2.6
500-Foot Paraboloid	$1.8 \times 10^4$	5	.02

A = collecting area, in  $m^2$

B = number of instantaneous Fourier components or beams.

C = product of maximum orthogonal dimensions, in  $km^2$ .

It is clear from the table that the VLA far exceeds any other instrument in resolution and speed. Furthermore, since the sensitivity of any instrument is ultimately set by one or the other of these parameters, the VLA also excels in this characteristic, although several other systems have comparable collecting area.

The VLA will provide radio astronomers, for the first time, with an instrument comparable in resolution, sensitivity, and speed to optical telescopes. It will allow a very wide range of investigations to be undertaken, many of which could not be contemplated with any other instrument. Some specific programs for which the VLA can be used are noted in the following section. The list is by no means complete, however. The capability of the VLA is so far beyond that of any existing instrument that it can be expected to open up vast new vistas and areas of research which cannot now be predicted.

#### D. Some Specific Capabilities of the VLA

##### 1. Array sensitivity

Before looking at some applications of the VLA to astronomical research, it is necessary to specify more precisely its limiting sensitivities for flux density and surface brightness measurements. These, in turn, depend on  $N(S)$ , the number of sources per steradian with flux density greater than  $S$ , at values of  $S$  several orders of magnitude below the present limit of

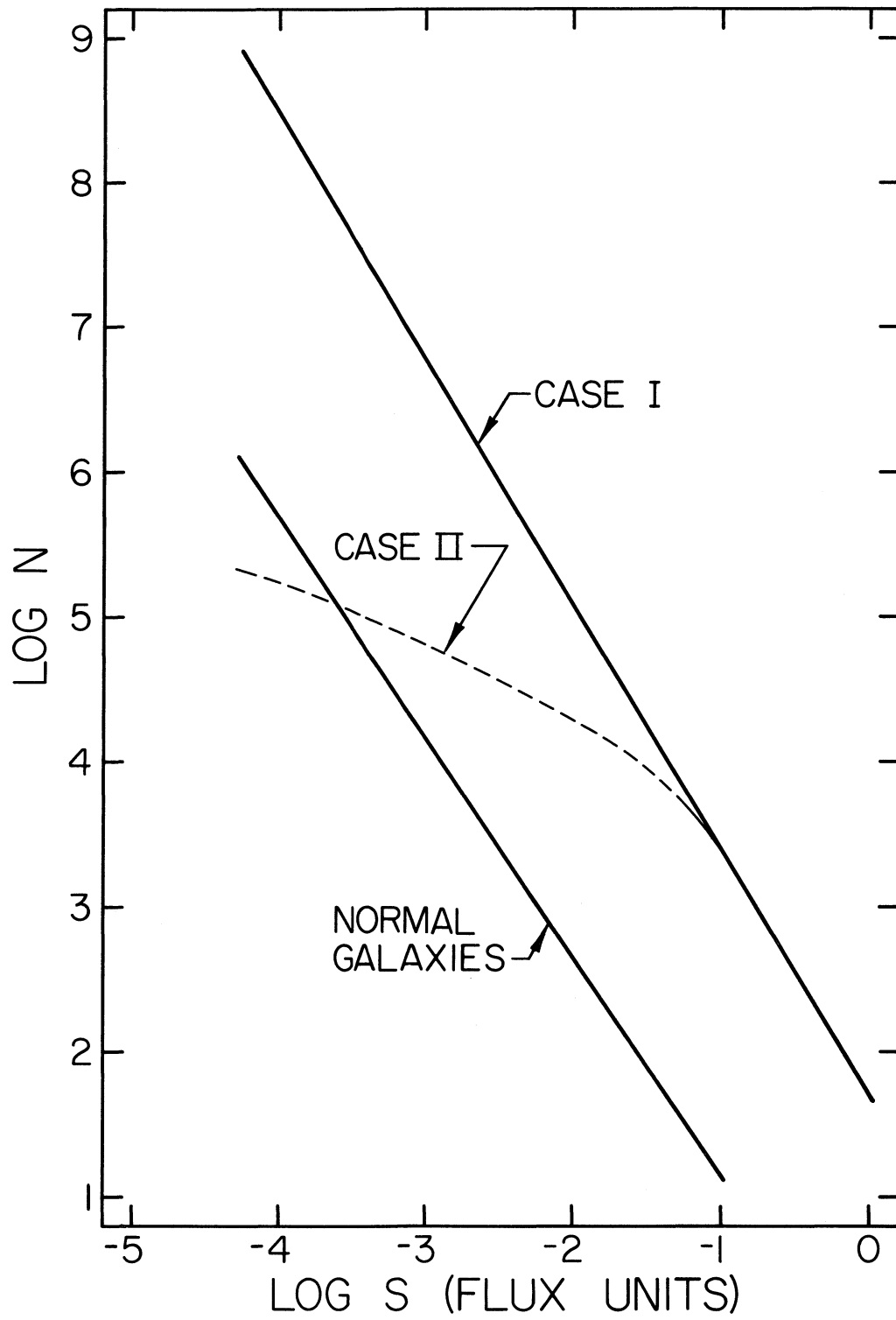


Figure 2 - 3

observations. Two extreme cases are considered, which should bracket the real, but unknown situation:

Case I:  $N(S) \propto S^{-1.8}$ , for  $S \geq 10^{-4}$  flux units;

Case II:  $N(S)$  flattens out at some value of  $S > 10^{-4}$  flux units in such a way that  $N(S=10^{-4}) = 4 \times 10^5$ . The exact form of  $N(S)$  for Case II is unimportant to the discussion. Fig. 2-3 shows  $N(S)$  for the two cases. The curve for Case II is an arbitrary extrapolation of Cambridge results (Gower, 1966) adjusted to 11-cm wavelength. Also shown in Fig. 2-3 is the  $N(S)$  for normal galaxies, with an assumed slope of  $-1.5$  and a zero point adjusted to the survey of Heeschen and Wade (1964). It is interesting to note that normal galaxies will dominate the  $N(S)$  relation at low flux densities if the  $N(S)$  curve for radio galaxies flattens out at  $N \sim 10^4 - 10^5$ . At  $\lambda$  11 cm the curve for normal galaxies must persist with slope  $-1.5$  to well below  $S = 10^{-4}$  flux units. At  $S = 10^{-4}$  flux units,  $z \approx 0.1$  for these weak radio emitters, so cosmological effects are still unimportant.

The array sensitivity is limited by the combination of system noise, main beam confusion, and side-lobe confusion. The limiting sensitivity due to system noise is  $1.65 \times 10^{-4}$  flux units, for a signal-to-noise ratio of 5 in an 8-hour observing time. Main beam confusion with signal-to-noise ratio of 5 occurs at that flux density which yields one source per 75 beam areas (von Hoerner, 1961). It therefore depends on both  $N(S)$  and the array resolution. The limiting flux density due to side-lobe confusion is given approximately by

$$\Delta S_s = \left( \frac{\Omega_e}{\Omega_m} \right)^{\frac{1}{2}} \cdot f \cdot \Delta S_m,$$

where  $\Delta S_m$  = limiting flux density due to main beam confusion;  
 $\Omega_e$  = solid angle subtended by the beam of a single antenna of the array;  
 $\Omega_m$  = solid angle subtended by the synthesized array beam;  
 $f$  = ratio of rms power in side-lobes to power in the main beam.

The limiting flux densities and brightness temperatures calculated from the above considerations are shown in Table 2-2 for the two N(S) assumptions and four array resolutions.

For Case I, the array is system noise limited at 1" resolution, and resolution limited in the lower resolution configurations. For Case II, the array is system noise limited for all configurations.

Table 2-2 also shows  $n$ , the number of sources brighter than  $S_{lim}$  in the field of view of the array. For Case I, the field of view is bandwidth limited to a diameter of  $100\beta$ , where  $\beta$  is the resolution, except at  $\beta = 27''$  where the field is that of a single element of the array -- 17'. For Case II, where side-lobe confusion is unimportant, the bandwidth may be decreased to give the full 17' field of view, with  $n \approx 10$ , for statistical studies requiring observations of many sources.

Table 2-2

$\beta$	Case I			Case II		
	$S_{lim}$	$T_{min}$	$n$	$S_{lim}$	$T_{min}$	$n$
1"	$2.0 \times 10^{-4}$	27 °K	16	$1.6 \times 10^{-4}$	22 °K	10
3"	$2.7 \times 10^{-4}$	4.1°K	98	$1.6 \times 10^{-4}$	2.5 °K	10
9"	$7.7 \times 10^{-4}$	1.3°K	151	$1.6 \times 10^{-4}$	.3 °K	10
27"	$2.8 \times 10^{-3}$	.5°K	19	$1.6 \times 10^{-4}$	.03°K	10

## 2. Structure of extragalactic sources

The brightness temperature, at 11-cm wavelength, of extragalactic sources ranges from about 0.1°K for the weakest normal galaxies to greater than  $10^8$ °K for some quasi-stellar sources. Table 2-3 gives the brightness temperatures of some radio galaxies, derived from published data or unpublished NRAO material. Comparison of the data of Table 2-3 with those of Table 2-2 suggests the kinds of studies that can be made of various types of extragalactic sources with the VLA.

Table 2-3

<u>Source</u>	<u>T<sub>B</sub> - °K</u>	<u>Component Diameter (seconds-of-arc)</u>	<u>Linear Dimension of 1" (pc)</u>
Cyg A	$\geq 9 \times 10^5$	30	850
Her A	$1.3 \times 10^3$	40	2350
NGC 1275	core $> 10^8$	$< 0.1$	270
	halo $\geq 40$	$\leq 100$	
M 87	core $1.7 \times 10^4$	20	55
	halo 85	300	
M 82	$2.5 \times 10^4$	5	16
NGC 598	.02	$10^4$	3.6
NGC 4278	$\geq 300$	$\leq 15$	50
NGC 7331	.85	300	72

Cygnus and Hercules A have the double component structure typical of many radio galaxies. The structure of the individual components of Hercules A is not known. That of Cygnus A is very complex, with features at least as small as 4", as shown in Fig. 2-1. It will be possible to study these objects, and many more like them, with the 1" beam of the VLA and, therefore, with spatial resolution corresponding to a small fraction of their overall dimensions and with a dynamic range of brightness and polarization of about 100:1. This dynamic range is limited by the effects of nearby side-lobes on the more intense source features. It can be extended considerably by making observations with the array in a second, complementary, configuration and thus greatly reducing the side-lobe levels. Although somewhat laborious, such a procedure should certainly be followed for a number of objects of the Cygnus A and Hercules A type, since the VLA is the only instrument capable of obtaining polarization and brightness structure to such levels. Until this is done for a reasonable number of sources, the true nature and history of these objects cannot be inferred with any confidence.

NGC 1275 is a peculiar galaxy with core-halo radio structure. The core is too small to be resolved with the VLA. The halo, however, should be observed with 1" or 3" resolution to determine the scale and nature of any brightness or polarization structure. Both the core and the halo of M 87 can be observed with the 1" beam of the VLA.

The large "halo" components of sources like M 87 and NGC 1275 probably should first be observed with the low-resolution VLA beam. Any evidence of structure could then be examined with higher resolution. If structure is present in the core or halo, it then becomes of great interest to compare optical and radio features as observed with similar resolution.

There are many bright radio galaxies with angular dimension in the range of 1" to 100" which can be studied in varying detail with the 1" resolution of the VLA. Polarization and brightness observations of these objects, and comparison with optical and other radio characteristics, are obviously of great importance.

NGC 598, NGC 4278, and NGC 7331, listed in Table 2-3, are "normal" galaxies with weak radio emission. NGC 4278 is an elliptical, the other two spiral, galaxies. The surface brightness of the spirals is quite low, and they are difficult objects to observe with the VLA. However, it is possible and should be rewarding to observe these objects with 27" resolution. There is at present no information about the distribution of brightness or polarization within these objects. If there are sources which rise significantly above the average brightness, they should be detected. A source like Cas A should be detectable in a galaxy as distant as 7 Mpc. Other galactic-type sources and strong HII regions could be detected in galaxies of the local group.

Although many quasi-stellar sources (QSS) have small dimensions, others are large enough to permit the study of their structure with the VLA. Nineteen of thirty-eight QSS studied recently by Hogg (1966) had angular dimensions greater than 6". Some examples are given in Table 2-4. The surface brightness of all these objects is high enough to permit detailed brightness and polarization studies with the 1" beam.

Table 2-4

<u>Source</u>	<u>Component Separation</u>	<u>Component Diameter</u>	<u>T<sub>B</sub></u>
3C 47	80"	10"	$2.6 \times 10^3$
3C 207	6"	3.5"	$1.7 \times 10^4$
3C 323.1	69"	2.7"	$2.1 \times 10^4$
3C 380	-	$4.5 \times 3''$	$1.3 \times 10^5$

### 3. Faint sources

Table 2-2 shows that, on the average, there will be at least 10 faint sources per field of view. Eight hours is required to observe one field. Thus, some 1,000 sources could be observed in one month, for statistical studies. The observations would yield positions to an accuracy of 0".2, flux densities to a limit of  $2 \times 10^{-4}$  flux units, and dimensions to a limit of about 0".25.

Table 2-5 shows values of red shift,  $z$ , for sources of observed flux density  $2 \times 10^{-4}$  flux units and absolute luminosity  $L$  at 11 cm, for various values of the deceleration parameter,  $q_0$ . The last column gives sources typical of that luminosity. It is apparent that for the most intense radio galaxies and QSS of the Cyg A and 3C 286 type cosmological effects are extremely pronounced, and observations of such sources will be of great interest.

Table 2-5

<u>L (W Hz<sup>-1</sup>)</u>	<u>z</u>				<u>Typical Source</u>
	<u>q<sub>0</sub> = -1</u>	<u>0</u>	<u>+ 0.5</u>	<u>+ 1</u>	
$6 \times 10^{27}$	14	20	150	280	3C 286
$3 \times 10^{27}$	12	17	100	200	Cyg A
$1 \times 10^{27}$	10	13	56	110	3C 48
$5 \times 10^{25}$	4	5	13	20	Hyd A
$2 \times 10^{24}$	1.4	1.8	2.6	3.5	NGC 1275
$6 \times 10^{23}$	.6	1.2	1.5	2.0	M 87

In deriving the numbers in Table 2-5, it was assumed that the radio spectrum was given by  $S \propto f^{-0.8}$  between the observed frequency,  $f_o$ , and the emitted frequency,  $f_o (1 + z)$ , which of course may not be the case for large  $z$ .

A wide variety of possible cosmological and evolutionary effects must be considered in evaluating any observations that reach to values of  $z$  as large as those indicated in Table 2-5. They are beyond the scope of this discussion, but it is just these effects which make observations of faint radio galaxies and quasi-stellar sources of such great potential interest.

At the other end of the luminosity scale, normal galaxies like NGC 598, NGC 4278, and NGC 7331 will be observable to distances of 300 Mpc. Nearby galaxies, to about the distance of the Virgo Cluster, will be observable if their intrinsic luminosity is within  $10^{-3}$  of that now considered "normal" for a spiral galaxy. This  $10^3$  extension of the luminosity scale should permit detection of many E, SO, and Sa galaxies not now observable.

#### 4. Galactic sources

Table 2-6 shows the emission measures, E, required of thermal sources to yield the limiting brightness temperatures shown in Table 2-2 (Case II) for different array configurations.

Table 2-6

<u><math>\beta</math></u>	<u>E</u>
1"	$7 \times 10^4$
3"	$8 \times 10^3$
9"	$1 \times 10^3$
27"	$1 \times 10^3$

---

At present only a few galactic objects with emission measures greater than  $10^5$  are known. A number of bright planetary nebulae have  $E \approx 2 \times 10^6$ , with dimensions of 1" to 20". These could be readily mapped with the 1" VLA beam. Other planetary nebulae would be detectable, but not resolvable, out to distances of 40 kpc. In addition, there

may be central cores or condensations in some HII regions with  $E > 10^5$ . The Orion Nebula is one example. These could also be mapped with the 1" beam. Many HII regions having  $E > 10^2$  and diameter greater than 27" would be observable.

There is also the possibility of detecting stellar envelopes, discussed recently by Weymann and Chapman (1965). If their theory is correct, stars of type K and M, luminosity class I or II would have detectable envelopes at distances of 600 pc. There may be 20 to 30 such stars within this distance.

The use of the VLA for studies of supernova remnants (SNR) depends on the scale of the structure in these objects, about which little is known. Cas A, the brightest SNR, is known from NRAO observations to have complex structure with a scale size less than about 10". Polarization and brightness observations of this object with a 1" beam should be very interesting. Proper motion in Cas A, due to expansion, is about 0".5 per year and should be easily measurable. Other SNR also show some indications of structure, still unresolved, and might be profitably examined with the high resolution of the VLA. Very large, low surface brightness objects like the Cygnus Loop will not be easily detectable with the VLA, unless they contain fine-scale structure of much higher than average surface brightness.

#### 5. Solar system studies

Although the VLA was not designed specifically for solar system work, its high sensitivity and resolution, and ability to make polarization maps, make it an extremely powerful instrument for some types of solar system studies.

For many planetary studies the VLA is nearly an ideal instrument. All of the planets except Pluto should be readily observable in varying degrees of detail, depending on the Planet's diameter and brightness temperature. Mercury, Uranus, and Neptune have small angular diameters (1" to 7") but at least crude measures of brightness distribution and polarization will be possible. It should also be possible to measure differences between the day and night hemispheres of Mercury.

Detailed polarization and brightness observations of Venus and Mars should provide a wealth of information concerning the physical

conditions of these planets. It will be possible to measure day and night effects, polar-equatorial temperature differences, and limb darkening or limb brightening. It will also be possible to check for temporal changes in the brightness distributions caused by dynamic processes on the planets. Measurements of the polarization of their thermal emission should give data on the nature of the Martian and Venusian surfaces at different locations, and allow the conversion of brightness temperatures into physical temperatures.

Observations of Jupiter and Saturn will require special techniques because of the rapid rotation of these planets. The low resolution, 27", configuration, and higher resolution fan beam configurations can be used profitably for some investigations. To obtain the highest-resolution polarization and brightness data, it will be necessary to observe the planets for many days. Since their rotation periods are not 24 hours, proper combination of the data from different days and different hour angles will yield all Fourier components for each central meridian longitude. The observations and reductions would be very laborious--impossibly so for any instrument except the VLA. The resulting brightness and polarization maps would be of inestimable value, however, for defining the structure of the radiation belts and disk components and the temperature structure of the atmospheres.

The ring structure of Saturn may also be observable, if the rings consist of particles of sufficient size.

Solar observations with the VLA, although complicated by the transitory nature of solar phenomena and the large diameter of the sun compared with the field of view of the instrument, should provide much new data of importance to solar physics. The high resolution of the VLA opens the possibility of a wide variety of interesting investigations. For example, it should be feasible to obtain detailed maps of flare emission regions with a resolution of a few seconds of arc. Such maps, showing the evolution of flaring regions on a short time scale, would be valuable in furthering the understanding of flare mechanisms. In addition, coronal hot spots associated with chromospheric plage regions have angular structure of 1' or less and brightness temperatures of  $10^5$  to  $10^6$ °K. It would be very useful to resolve such regions with the VLA and map their brightness distributions.

High-resolution observations of occultations of radio sources or artificial probes by the solar corona would provide new information about the structure, motion, and magnetic field of the corona.

#### 6. Dual frequency work

All of the preceding discussion is based on a single operating wavelength of 11 cm. The proposed system, however, would permit simultaneous observation at two wavelengths, 5.5 cm and 11 cm. Extension of the above discussion to 5.5 cm wavelength, or to any other wavelength for which the VLA may some day be instrumented, is fairly obvious and will not be undertaken here. The increased scientific value of the VLA, by addition of the second wavelength, is very great. Particular advantages include improved resolution, spectral information, and especially the data necessary to deduce the Faraday rotation across sources.

#### 7. Spectral line work

The resolution attainable with the VLA is of importance to spectral line observations. At present the smallest circular beam from a filled-aperture instrument used in 21-cm hydrogen-line observations is 10'. This represents a linear scale of 2 kpc at the distance of the Andromeda Nebula, the largest system in the local group of galaxies. At the distance of the Virgo Cluster, 10' corresponds to 36 kpc, the size of an entire galaxy. These linear scales should be compared with the thickness and spacing of spiral arms which, in our own galaxy, are about 1 kpc and 2 kpc, respectively. Higher resolution studies of spiral galaxies will allow an accurate comparison of the location of HI arms with respect to optical arms. Detailed line mapping will also supply information on the distribution of HI (i.e., as arms or an amorphous structure) beyond the optical extent of a galaxy. The hydrogen distribution in the direction perpendicular to the plane of a galaxy can be obtained from systems seen edge-on.

Other extragalactic line studies include: radial velocity maps, rotation curves, and possible large-scale circulation patterns of the interstellar material within galaxies. The systemic radial velocity and total HI content of a large number of systems could be determined. The former will enable optical radial velocities to be placed on a fundamental system. Special objects within the nearer galaxies will become

available for study, e.g. giant HII regions, including those seen in the nuclei of some spirals, dusty regions in elliptical galaxies, and the companion of M 51.

In our galaxy the overall hydrogen features have been delineated from observations obtained with telescopes having beam sizes of 10' to 2°. Much higher resolution will allow small regions and special objects to be studied. Examples include: obscuring clouds, especially globules and elephant trunks (typical sizes are 10" to several minutes-of-arc), material swept up by nova shells (sizes of such shells are  $\leq 20''$ ) and by planetary nebulae (typical sizes are 10" to 50"), regions close to stars shedding material, regions close to extremely young stars, HI dynamics at the edges of an HII region, and the fine-scale structure of the interstellar medium.

The recombination lines of hydrogen and helium allow quantitative chemical analysis of HII regions and will yield information on the structure and physical condition within these regions. OH sources appear to be intrinsically small and are obvious candidates for high-resolution line observations.

Quantitative examples of the detection capabilities of the VLA for the 21-cm hydrogen-line are given in Table 2-7. Listed there are the brightness temperatures for several cases of galactic and extragalactic objects. Corresponding values for VLA minimum detectable brightness temperatures are also given.

#### REFERENCES

- Gower, J. R. 1966, MN 133, 151.  
 Heeschen, D. S. and Wade, C. M. 1964, A. J. 69, 277.  
 von Hoerner, S. 1961, Pub. NRAO 1, 19.  
 Hogg, D. E. 1966, Nature in press.  
 Panel on Astronomical Facilities, 1964, Ground-Based Astronomy, a Ten-Year Program, National Academy of Sciences, Washington, D. C.  
 Ryle, M., Elsmore, B. and Neville, A. C. 1965, Nature 205, 1259.  
 Wade, C. M. 1966, Phys. Rev. Letters 17, 1061.  
 Weymann, R. and Chapman, G. 1965, Ap. J. 142, 1268.

Table 2-7

Peak Brightness Temperature  
for Various Hydrogen Distributions

	$M_{\text{HI}}/M_{\odot}$	Velocity Spread (km/s)	Distance (Mpc)	Beam Size	Peak $T_{\text{B}}$ (°K)	Minimum Detectable $T_{\text{B}}$ (°K)
(a)	$10^9$	200	12	54"	29	0.7
(b)	$10^9$	200	60	54"	1.1	0.7
(c)	$10^4$	20	0.69	18"	7.8	6.1
(d)	$10^4$	20	0.69	54"	0.9	0.7
(e)	$10^{-1}$	20	0.002	18"	9.3	6.1

(a) Hydrogen in average late-type galaxy at Virgo Cluster distance.

(b) As in (a) but five times more distant.

(c)

and Small regions in M 31 and M 33.

(d)

(e) A galactic hydrogen example.

The minimum detectable  $T_{\text{B}}$  is based on a 100 kHz bandwidth.

---

Chapter 3

POSSIBLE SYSTEMS

## Chapter 3

## POSSIBLE SYSTEMS

The performance specifications enumerated in the previous chapter clearly demand that an array of antennas be used, rather than a single reflector. The 3" telescope requires an array of linear dimensions of about 7 km. To extend the resolution to 1" requires about 21 km. The specification can be met, in principle at least, by any of the following types of array:

A. Continuous, Completely Filled, Phased Arrays

Examples: The MIT Lincoln Laboratory solar radar antenna at El Campo, Texas, and the incoherent ionospheric scatter radar antenna at Jicamarca, Peru. Both of these enormous antennas have been eminently successful; however, this system utilizing a continuous distribution of dipoles appears to be impossibly impractical for the high resolutions envisaged here. To achieve 10" resolution would require approximately  $10^9$  dipoles, and to achieve 1" resolution would require  $10^{11}$  dipoles, even at the maximum feasible spacing.

This array, and the Mills Cross type discussed below, have the disadvantage that polarization observations are, at best, extremely difficult to make.

B. Continuous Cross Type Arrays

Examples: The Mills Crosses at Fleurs and Molonglo, Australia; the Mills Cross formerly at the Carnegie Institution River Road Station in Maryland; the Serpukhov Cross in the USSR; the Italian Cross at Bologna.

This highly successful type of antenna can probably be expanded to achieve the extreme resolution desired. Whether it can do so economically remains to be demonstrated. For a symmetrical cross of the "classical" type, approximately 70,000 dipoles would be needed to achieve 10" resolution, together with a very large number of preamplifiers and an intricate network of phase shifters. For 1" resolution, 700,000 dipoles would be needed.

To achieve adequate speed of operation, many "beams" would necessarily be produced simultaneously, leading to great electronic complexity.

This type of system, together with a variant called the "Kilodish Cross," an array of 1,000 small paraboloids, has been analyzed in greater detail in a separate report (Clark, 1966). The conclusions reached are as follows:

Total cost of the 10" array is \$34 million. Expanding the array for more resolution is very expensive. The arms may be extended indefinitely at a cost of about \$8 million per mile, which is prohibitive for resolution as small as 1". A 1" by 2° fan beam, however, can be constructed by simply adding five large (about 100 ft) dishes to one end of the E-W arm, at appropriate distances.

To summarize, the Kilodish Cross has the following advantages:

(1) Very low sidelobe levels. The grating sidelobes are spaced 1.2°, and although only moderately discriminated against by the element beam, they are virtually eliminated by the delay pattern.

(2) Very high information rate. This cross could look at 50 sources per day as contrasted with the two per day of the tracking array.

To offset these, it has the following disadvantages:

(1) Changing the front ends of the receivers would be an enormous job, so that changing the frequency of the array or taking advantage of advances in the state-of-the-art would be enormously expensive.

(2) It cannot be expanded to give a narrower pencil beam except at great monetary cost.

(3) Maintenance costs will be much higher than for a 36-element system. Not only is each of 1,000 elements nearly as complicated as each of the 36, but the interconnection equipment must be rephased on occasion to preserve a clean sub-array beam.

(4) It is slightly more difficult than the tracking array to compact to give an array with higher filling factor for use on low brightness objects.

(5) Because of the greater number of elements, they cannot be monitored as precisely.

### C. Grating Cross Arrays

Examples: The Christiansen Cross at Fleurs, Australia; the Bracewell Cross at Stanford University; the Cross at Nançay, France. Several related instruments have been constructed, some having features of both continuous

arrays and interferometers, notably the arrays constructed by Covington at Ottawa and by Erickson at Clark Lake, California.

This type of array shares with the Mills Cross the ability to produce very narrow beams with great economy of materials and equipment. The conventional grating cross employs two sparsely-filled arms correlated with each other. Because of the wide spacing, a number of strong secondary lobes appear in the antenna pattern, the so-called "grating lobes." Provided one has some assurance that none of the grating lobes falls upon another source of radiation, the grating cross can be used very effectively to map the brightness distribution of an extended source. It is also required, of course, that the antennas comprising the arms of the cross be spaced closely enough so that the angular separation between grating lobes is greater than the angular extent of the source to be examined.

The grating cross principle can probably be extended to resolutions of 10" or 1". However, as such instruments to date have commonly operated in the transit mode, it will be necessary either to add phase tracking or a multiplicity of separately instrumented beams in both the hour angle and declination coordinates in order to achieve adequate integration time and speed of observation. The number of independent beams of a grating cross with  $m$  and  $n$  elements, respectively, in the two arms, is at most about  $m(n)$ . This is also the approximate number of correlators if the device is used as a correlator array. These two configurations deliver about the same information so that the choice between them is determined by the fact that correlators are more economical and reliable than phasing devices. It is also difficult to use the multiple-beam output information of the grating cross in any simple way to improve the sidelobe level as the earth rotates. Thus, the possibility of supersynthesis also favors the correlator array. It is interesting to note that the large grating cross built by Christiansen at Fleurs, Australia, is presently being converted to a correlator array, in order to increase its sensitivity and versatility.

#### D. Aperture Synthesis Antennas

This type of radio astronomy instrumentation had its origin in early interferometer experiments (Little and Payne-Scott, 1951), and its most

sophisticated development in recent experiments by the Cambridge radio astronomers led by Ryle (Ryle, et al., 1965).

The basic principle of aperture synthesis involves the Fourier analysis of the brightness of a finite area of the sky and the recording of individual Fourier components or of partial sums of components for later summation in a computing machine. It is easily shown (Bracewell, 1961) that an array of interferometers, each measuring a single Fourier component of a brightness distribution, can be used to simulate a very large antenna. As each interferometer determines and records one Fourier component, independently of all other interferometers in the array, it is unnecessary for all measurements to be made simultaneously. In fact, it is possible to synthesize a large antenna with only two small ones, by moving one of them about for successive observations in such a way that all necessary Fourier components of the brightness distribution are determined. Provided the area being mapped is of finite extent, its brightness distribution can be represented by a Fourier series, and the minimum baseline length and the interval between successive baseline lengths is determined by the finite angular dimension of the source. The maximum baseline length, of course, is determined by the angular resolution sought. Thus, the number of baselines needed is finite, even in a two-dimensional situation. The aperture synthesis principle has many ramifications. It has been successfully applied by several groups of researchers, including those at Cambridge, Cal Tech, NRAO, and Stanford. A particularly reliable and precise form of instrumentation, suitable to extremely long baselines and highly intricate arrays of antennas, was developed at Cal Tech (Read, 1963) and further perfected at NRAO (Wade, Clark, and Hogg, 1965).

A large array of antennas, connected into interferometer pairs by correlators, will be called a "correlator array." If  $M$  antennas are present, there can be as many as  $M(M-1)/2$  interferometers existing simultaneously. Such an array can be built using a number of steerable reflector antennas which can track a source for a considerable length of time, thus permitting relatively long integration time. As will be discussed later, this hour angle tracking can be utilized in the "supersynthesis" scheme to reduce the number of antennas required to synthesize a given equivalent antenna aperture. From the standpoints of speed, electronic simplicity,

sensitivity, ease of calibration, flexibility and versatility, and overall cost economy, the correlator array appears to be superior to all the other possible schemes for realizing seconds-of-arc resolution. Thus, the balance of this report will be devoted mainly to an investigation of a correlator array to achieve the parameters listed in Chapter 2.

#### REFERENCES

- Bracewell, R. N. 1961, IRE Trans., AP-9, 59.
- Clark, B. G. 1966, NRAO VLA Report No. 2.
- Little A. G., and Payne-Scott, R. 1951, Aust. J. Sci. Res., A4, 489.
- Read, R. B. 1963, Ap. J., 138, 1.
- Ryle, M., Elsmore, B., and Neville, Ann C. 1965, Nature, 207, 1024.
- Wade, C. M., Clark, B. G., and Hogg, D. E. 1965, Ap. J., 142, 406.

Chapter 4

THE CORRELATOR ARRAY

## Chapter 4

## THE CORRELATOR ARRAY

The number of antennas needed to yield complete brightness distribution information about a source can be determined by transforming from the aperture plane into the fringe visibility plane. The interrelationships among the various quantities are given in Fig. 4-1. The fringe visibility plane (u-v plane) representation, or "transfer function" of an array is the autocorrelation function of the aperture plane illumination. The "brightness spectrum" or complex coherence function of the brightness distribution is the Fourier transform of the brightness distribution. Only those components of the complex visibility of the source can be measured whose spatial frequencies correspond with spatial frequencies (vector spacings) represented in the u-v plane representation (transfer function) of the aperture illumination. The Fourier transform of the observed brightness distribution, as observed at the output of the array, is the product of the transfer function and the Fourier transform of the actual brightness distribution. It is necessary, therefore, to study the transfer function of any proposed correlator array in order to know how effectively it gathers the information needed to synthesize a portion of the sky.

The number of antennas needed to obtain all the necessary information in a finite area of the sky is determined by the angular extent of the area and by the angular resolution to be achieved. As the area of interest is finite in extent, it can be represented by a Fourier series whose fundamental term has its frequency determined by the angular width  $a$  of the area. It is, in fact,  $(a)^{-1}$  cycles per radian. In order to accommodate an arbitrary distribution of brightness within the area it is necessary that all harmonics be present; thus, spacings of antennas in the array must be at intervals of  $(a)^{-1}$  wavelengths. In other words, every antenna spacing corresponding with a term of the two dimensional Fourier series must be present. The finest detail that can be represented in the scanned area is determined by the highest-frequency term in the series, and this, in turn, is determined by the longest spacing in the array.

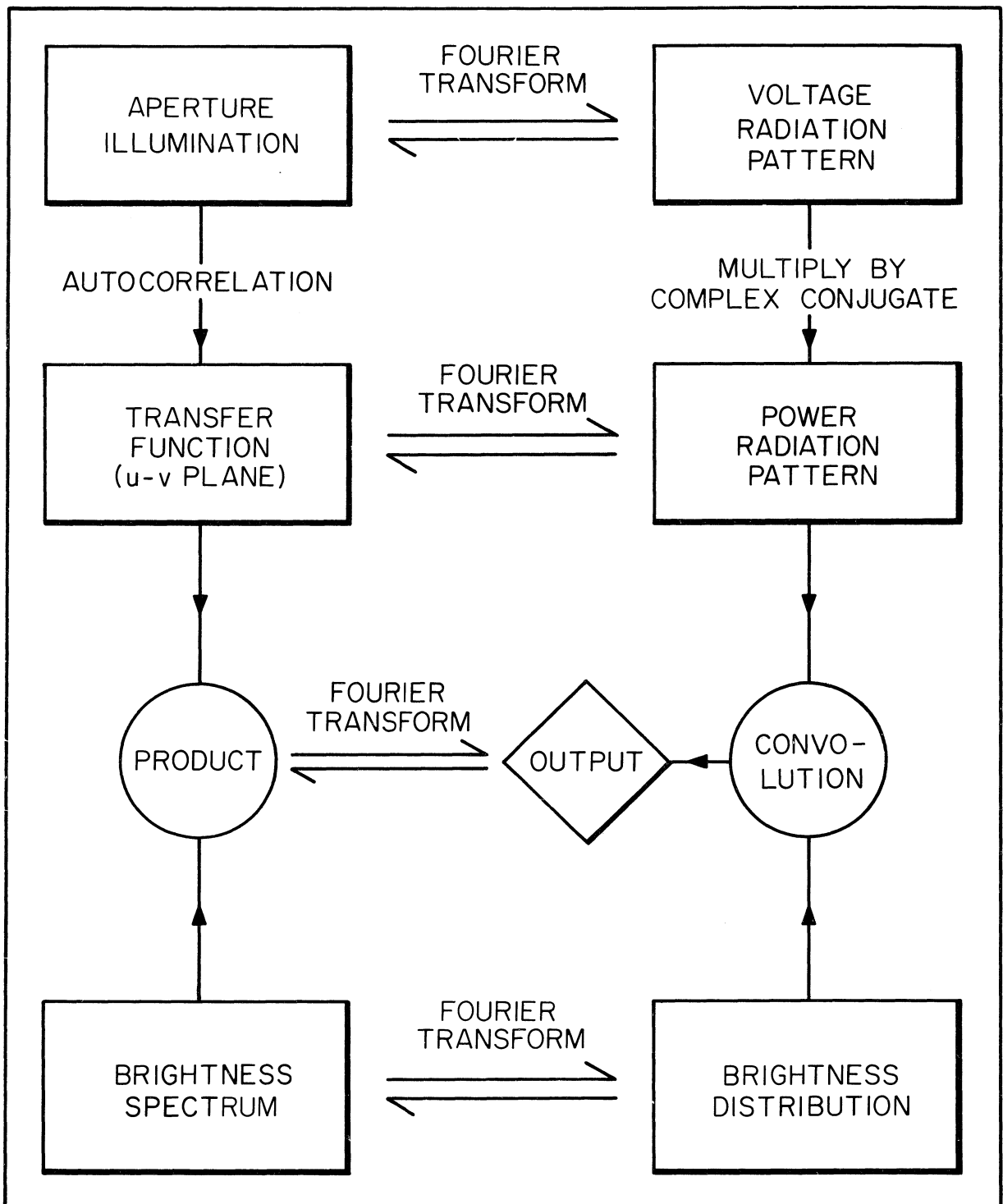


Figure 4 - 1. Transformations in a system linear in intensity.

It is assumed that "resolution" is defined in the Rayleigh sense; that is, that two point sources can just be resolved if they are separated by half the distance between the first-order nulls in the antenna's diffraction pattern. The separation of the first-order nulls (the "beamwidth between nulls") is determined not only by the width of the aperture but also by the weighting of the transfer function. The weighting function also controls the sidelobe level (as distinguished from the grating lobes) and it is customary for the weighting to be "tapered" from the center to the edges in order to achieve low sidelobes. This tapering increases the beamwidth over that obtainable with, say, uniform weighting. The relationship between beamwidth (between nulls) and ratio of the first-order sidelobes to the main beam, for well-chosen illumination functions, is given by Fig. 4-2, for rectangular apertures.

Much of the present chapter will be concerned with simplified examples of correlator arrays, in order to introduce the subject in a logical way. The reader should bear in mind that the actual VLA will have much more complicated geometry. Exact analysis in the latter case involves the use of a large digital computer; the results are given in Chapter 6.

#### A. The Transfer Function and The Radiation Pattern

The sampling in the Fourier transform plane is described conveniently by the transfer function  $W(u, v)$ . It has the following properties:

1.  $W(u, v)$  is real.
2.  $W(0, 0) = 1$ . This defines the numerical scale.
3.  $0 < W(u, v) \leq 1$  at sampled points, and  $W(u, v) = 0$  elsewhere.
4.  $W(u, v) = W(-u, -v)$ .

The value of  $W(u, v)$  is simply the weight given to the corresponding component in the Fourier inversion.

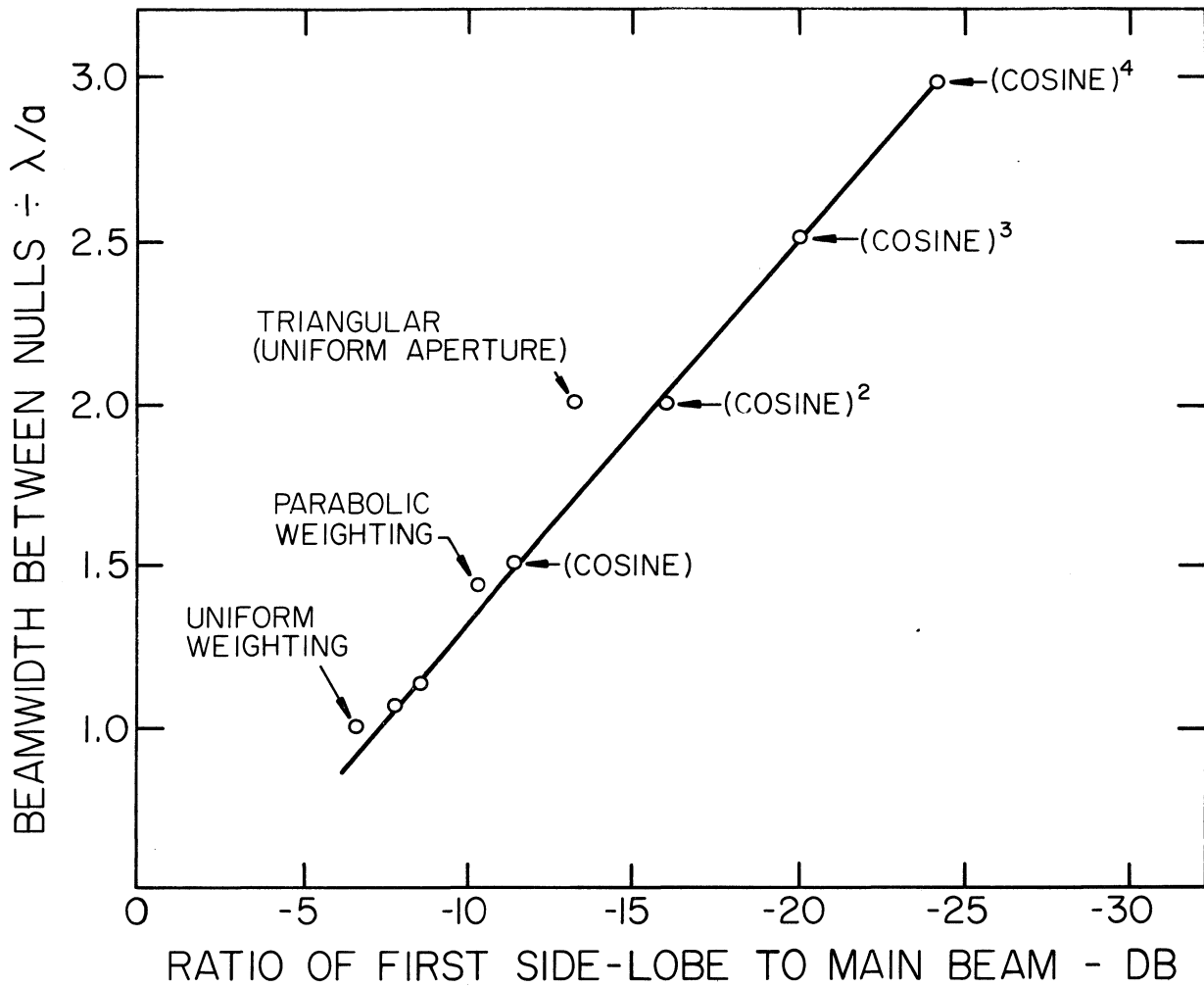


Figure 4 - 2. Beamwidth vs. sidelobe level for an array linear in intensity. Rectangular array in the transfer function plane. Transfer function weighted as shown. All sampling points are present.

The power radiation pattern of the synthesized aperture is the Fourier transform of the transfer function:

$$p(x, y) = \frac{1}{C} \int_{-\infty}^{\infty} \int_{-\infty}^{\infty} W(u, v) e^{-j2\pi(ux + vy)} du dv, \quad (4-1)$$

$$C = \int_{-\infty}^{\infty} \int_{-\infty}^{\infty} W(u, v) du dv. \quad (4-2)$$

When expressed in this way,  $p(x, y)$  is normalized so that

$$p(0, 0) = 1.$$

#### B. The Rectangular Sampling Grid

Since  $W(u, v)$  differs from zero only at a finite number of discrete points, the above integrals can be replaced by finite series. These points (the sampling grid) form a uniformly-spaced rectangular grid, one point of which is at the origin ( $u = 0, v = 0$ ). The sampling function is a two-dimensional sequence,

$$W(u, v) = W_{k, \ell} \delta(u - k\Delta u) \delta(v - \ell\Delta v) \quad (4-3)$$

with

$$k = -K, \dots, 0, \dots, K$$

$$\ell = -L, \dots, 0, \dots, L.$$

The largest spatial frequencies along the two coordinate axes are

$$u_{\max} = K\Delta u, \quad v_{\max} = L\Delta v.$$

Fig. 4-3 illustrates the arrangement.

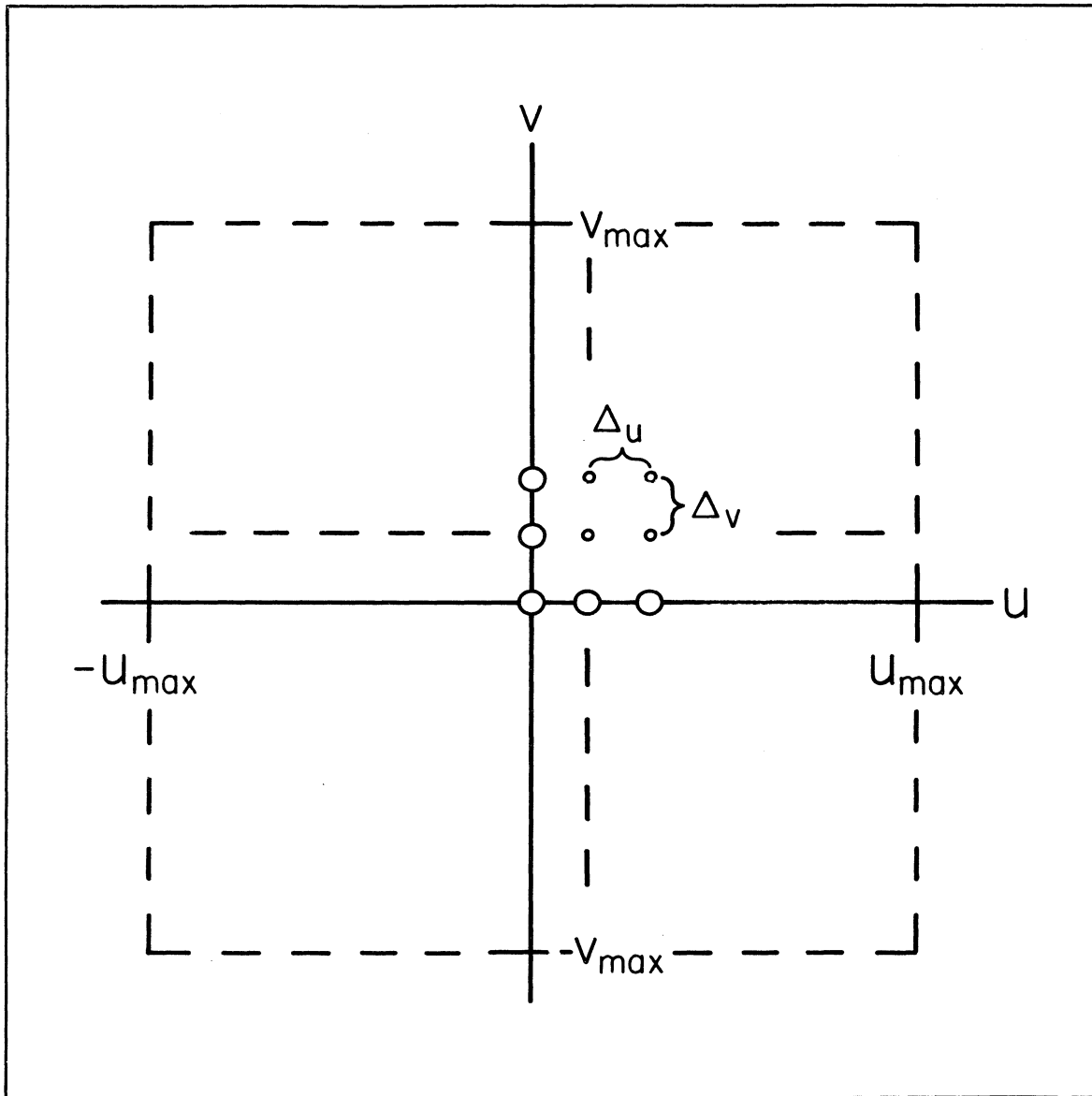


Figure 4 - 3. The rectangular sampling grid.

Using the four properties assigned to  $W(u, v)$  in Section A above, and equation (4-3), we can express equations (4-1) and (4-2) as

$$p(x, y) = \frac{1}{C} \left\{ 1 + 2 \sum_{k=1}^K W_{k,0} \cos 2\pi kx\Delta u + 2 \sum_{\ell=1}^L W_{0,\ell} \cos 2\pi \ell y\Delta v + 2 \sum_{k=1}^K \sum_{\ell=-L}^L W_{k,\ell} \cos 2\pi kx\Delta u \cos 2\pi \ell y\Delta v \right\} \quad (4-4)$$

$$C = 1 + 2 \sum_{k=1}^K W_{k,0} + 2 \sum_{\ell=1}^L W_{0,\ell} + 2 \sum_{k=1}^K \sum_{\ell=-L}^L W_{k,\ell}. \quad (4-5)$$

It is evident that the radiation pattern has the same kind of symmetry as the transfer function:

$$p(x, y) = p(-x, -y).$$

An important consequence of the rectangular sampling grid can be seen immediately from equation (4-4) - the radiation pattern is periodic, since

$$p\left(x \pm \frac{\mu}{\Delta u}, y \pm \frac{\nu}{\Delta v}\right) = p(x, y),$$

where

$$\left. \begin{matrix} \mu \\ \nu \end{matrix} \right\} = 0, 1, 2, \dots$$

Therefore the radiation pattern repeats at intervals

$$\Delta x = 1/\Delta u, \quad \Delta y = 1/\Delta v$$

radians. This self-replicating property is exactly analogous to that of a two-dimensional diffraction grating, and for this reason one speaks of

the family of repeated patterns as "grating lobes". These considerations bear directly on the manner in which the transfer function is to be specified, since separation of the grating lobes must be at least as great as the angular dimensions of the largest source to be mapped. If these are  $\phi_{EW}$  (east-west) and  $\phi_{NS}$  (north-south) radians,

$$\Delta u \leq 1/\phi_{EW}, \quad \Delta v \leq 1/\phi_{NS} . \quad (4-6)$$

In Chapter 6 it is shown that, because of the effect of the beam pattern of a single antenna element, grating lobes which fall outside the main beam of the element pattern are of little significance.

A further restriction on the effect of grating lobes arises from the non-zero bandwidth of the system. This is also treated in Chapter 6.

Advocacy of a rectangular sampling grid, when this leads inevitably to the unwanted grating lobes, requires justification. There are two strong points which favor the rectangular arrangement. First, varying the sampling interval over the Fourier transform plane in effect assigns a greater importance to some parts of the Fourier transform than to others. This is arbitrary and unreasonable in the absence of a priori knowledge of the structure of the source being observed; it follows that no such arrangement could be equally well suited to all sources. The second point is that any discrete sampling scheme must have unwanted response analogous to the grating lobes. While their shapes and positions can be altered, they cannot be eliminated; and this would be done at the expense of the real convenience which the rectangular scheme affords, particularly in the Fourier inversion.

### C. Separable Transfer Functions

A simplified situation is assumed here in order to illustrate the relationship between the transfer function and the beam pattern. In the array actually proposed, the transfer function is not, in fact, separable. In that case the beam pattern can only be computed by taking the Fourier transform of the transfer function.

If the transfer function is separable, i.e., if we can write

$$W_{k,\ell} = W_{k,0} W_{0,\ell} = W_k W_\ell,$$

equations (4-4) and (4-5) reduce to

$$p(x, y) = \frac{1}{C} \left\{ 1 + 2 \sum_{k=1}^K W_k \cos 2\pi kx \Delta u \right\} \left\{ 1 + 2 \sum_{\ell=1}^L W_\ell \cos 2\pi \ell y \Delta v \right\},$$

$$C = \left\{ 1 + 2 \sum_{k=1}^K W_k \right\} \left\{ 1 + 2 \sum_{\ell=1}^L W_\ell \right\}. \quad (4-7)$$

$$(4-8)$$

Therefore the radiation pattern is separable also:

$$p(x, y) = p(x, 0) p(0, y).$$

Two averages based on the transfer function will be needed in later sections of this proposal. These are the mean value  $\bar{W}$  and the rms value  $\rho = \sqrt{W^2}$ . If  $W_{k,\ell}$  is separable, we have

$$\bar{W} = \frac{C}{(1 + 2K)(1 + 2L)} \quad (4-9)$$

where C is given by (4-8), and

$$\rho_W = \sqrt{\left( \frac{1 + 2 \sum_{k=1}^K W_k^2}{1 + 2K} \right) \left( \frac{1 + 2 \sum_{\ell=1}^L W_\ell^2}{1 + 2L} \right)} \quad (4-10)$$

At this point, two specific examples of separable transfer functions will be studied. The first assigns equal weights to all Fourier components

and therefore corresponds to the so-called "principal solution". The second weights the Fourier components in inverse proportion to their spatial frequencies and is analogous to a uniformly-fed rectangular aperture.

1. Uniform weighting

$$W_k = W_l = 1 \quad \begin{cases} |k| \leq K \\ |l| \leq L \end{cases}$$

This gives

$$p(x, y) = \frac{\sin [(2K + 1) \pi x \Delta u]}{(2K + 1) \sin \pi x \Delta u} \cdot \frac{\sin [(2L + 1) \pi y \Delta v]}{(2L + 1) \sin \pi y \Delta v} \quad (4-11)$$

and

$$\bar{W} = 1,$$

$$\rho_W = 1.$$

2. Linear weighting

$$W_k = 1 - \frac{k}{K+1}, \quad k \leq K;$$

$$W_l = 1 - \frac{l}{L+1}, \quad l \leq L.$$

This gives

$$p(x, y) = \frac{\sin^2 [(K + 1) \pi x \Delta u]}{(K + 1)^2 \sin^2 \pi x \Delta u} \cdot \frac{\sin^2 [(L + 1) \pi y \Delta v]}{(L + 1)^2 \sin^2 \pi y \Delta v}, \quad (4-12)$$

$$\bar{W} = \frac{(1 + K) (1 + L)}{(1 + 2K) (1 + 2L)}, \quad (4-13)$$

$$\rho_W = \frac{1}{3} \left[ \left\{ 1 + \frac{K+2}{(K+1)(2K+1)} \right\} \left\{ 1 + \frac{L+2}{(L+1)(2L+1)} \right\} \right]^{1/2} \quad (4-14)$$

Since  $u_{\max} = K\Delta u$  and  $v_{\max} = L\Delta v$ , in the limit as  $(K, L) \rightarrow \infty$  and  $(\Delta u, \Delta v) \rightarrow 0$ , for constant  $u_{\max}$  and  $v_{\max}$ ,

$$p(x, y) = \left[ \frac{\sin \pi x u_{\max}}{\pi x u_{\max}} \right]^2 \left[ \frac{\sin \pi y v_{\max}}{\pi y v_{\max}} \right]^2 ,$$

$$\bar{W} = 1/4,$$

$$\rho_W = 1/3.$$

These are the familiar relations for a uniformly-fed rectangular aperture.

It should be noted that this transfer function gives a radiation pattern without negative sidelobes, since the right-hand side of equation (4-12) is an absolute square.

#### D. Beamwidth and Sidelobe Levels

Since the half-power beamwidth for any given transfer function is always inversely proportional to the highest spatial frequency,

$$\beta_{EW} = \kappa/u_{\max}, \quad \beta_{NS} = \kappa/v_{\max},$$

where  $\beta_{EW}$  and  $\beta_{NS}$  are respectively the east-west and north-south beamwidths in radians, and  $\kappa$  is a constant of the order of unity whose exact value depends on the transfer function.

An alternative way to specify the width of the synthesized main lobe is to give the angular distance between the first zeros. This is not as satisfactory conceptually as the half-power beamwidth, since some radiation patterns have sidelobes between the main lobe and the first zeros. On the other hand, the beamwidths between first zeros can often be found analytically, since these are the smallest values

of  $\theta_{EW}$  and  $\theta_{NS}$  for which

$$\sum_{k=1}^K W_k \cos \pi k \theta_{EW} \Delta u = -1/2, \quad (4-15)$$

$$\sum_{\ell=1}^L W_{\ell} \cos \pi \ell \theta_{NS} \Delta v = -1/2 \quad (4-16)$$

if the transfer function is separable.

The values of  $\theta$  are determined from equations (4-15) and (4-16), and the values of  $\beta$  from equations (4-11) and (4-12), under the assumption that M and N are large. For the two examples of Section C,

1. Uniform weighting

$$\theta_{EW} = \frac{1}{(K + 1/2)\Delta u} \approx 1/u_{\max}; \quad \beta_{EW} \approx 0.604/u_{\max};$$

$$\theta_{NS} = \frac{1}{(L + 1/2)\Delta v} \approx 1/v_{\max}; \quad \beta_{NS} \approx 0.604/v_{\max}.$$

2. Linear weighting

$$\theta_{EW} = \frac{2}{(K + 1)\Delta u} \approx 2/u_{\max}; \quad \beta_{EW} \approx 0.886/u_{\max};$$

$$\theta_{NS} = \frac{2}{(L + 1)\Delta v} \approx 2/v_{\max}; \quad \beta_{NS} \approx 0.886/v_{\max}.$$

E. A correlator Array Using Sidereal Tracking

The technique generally termed "supersynthesis" (Ryle, 1962; Ryle, et al, 1965) can make a significant reduction in the required number of antennas. When using a correlator array, one finds the complex coherence

$\tilde{V}(u, v)$  between the signals received from each pair of antennas. If there are  $M$  antennas,  $M(M-1)/2$  simultaneous pairs can be formed among them. Each pair can be treated as a two-element interferometer, and the array can be thought of as  $M(M-1)/2$  interferometers operating concurrently.

Each antenna pair has associated with it a set of four constants  $\{B_1, B_2, B_3, h\}$  (Wade and Swenson, 1964). These constants depend on the local-oscillator frequency and the length and orientation of the line joining the phase centers of the elements of the pair.  $B_1$  and  $B_2$  are respectively the components of the baseline parallel and perpendicular to the earth's rotational axis, in wavelengths;  $B_3$  allows for the difference in electrical path length between the local-oscillator and the two mixers; and  $h$  is the hour angle of the point where an extension of the line joining the antennas would strike the celestial sphere. The transform plane coordinates corresponding to a pair of antennas pointed at hour angle  $H$  and declination  $\delta$  are

$$u = B_2 \sin (H-h), \quad (4-17)$$

$$v = B_1 \cos \delta - B_2 \sin \delta \cos (H-h). \quad (4-18)$$

These are the parametric equations of an ellipse, with  $H$  as the parameter. Therefore, if the antennas are made to track a radio source along its diurnal circle, the position sampled in the  $u$ - $v$  plane will describe an elliptical arc (Rowson, 1963).

The elliptical track in the  $u$ - $v$  plane has the following properties:

1. Its major axis lies parallel to the  $u$ -axis.
2. Its center lies on the  $v$ -axis, at  $u = 0$ ,  $v = B_1 \cos \delta$ .
3. Its major and minor semi-axes are  $B_2$  and  $B_2 \sin \delta$ , respectively.
4. Its axial ratio is  $\sin \delta$  and its eccentricity is  $\cos \delta$ .

It is clear that the nature of the transform plane coverage offered by any such track depends strongly on the declination of the source being observed. At the celestial equator, the ellipse degenerates to a

straight line parallel with the u-axis, while at the pole it becomes a circle. Similarly, the u-v coverage given by an array using sidereal tracking is a function of declination. This is an important point which must always be kept in mind when discussing a tracking array. Generally speaking, it is most difficult to obtain a good u-v plane coverage for sources at low declination.

With an array of M antennas tracking a radio source, one obtains u-v plane samples on  $M(M-1)/2$  elliptical tracks simultaneously. These ellipses will have numerous points of intersection and, unless care is taken with the array plan, there will be appreciable areas on the u-v plane which are not sampled at all. An optimum array configuration will avoid such unsampled areas entirely while holding to a minimum the number of regions which are sampled by many tracks, and it will do so for all declinations within the range of the instrument. This problem will be treated in detail in Chapter 6.

The data sampling afforded by such an array is virtually continuous along the elliptical tracks. Prior to performing the Fourier inversion, one would organize the data in a suitable rectangular grid by determining the average  $\tilde{V}(u, v)$  for each grid cell. The grid dimensions would be made small enough that the number of grating responses within the primary (single-element) main lobe is not excessive, yet not so small that there would be an appreciable number of unsampled cells.

The signal-to-noise ratio of the correlator array must also be investigated. Blum (1959) has shown that the sensitivity of a single antenna pair, with correlated outputs, is

$$\Delta T = \frac{\gamma}{\sqrt{2}} \frac{T}{\sqrt{\tau B}} ; \gamma \approx 1$$

where  $\tau$  is the integration time, B is the bandwidth, T is the total system noise temperature and  $\Delta T$  is the thermal equivalent of the rms noise fluctuations. The correlator array antenna consists of a number of such correlated antenna pairs, or interferometers. If M antennas are available simultaneously,  $M(M-1)/2$  combinations of two are possible, although it may not be necessary or desirable to supply a correlator for every possible combination.

It has been shown (Clark, 1965, Faran and Hills, 1952) that in a correlator array the unwanted components (noise) of the outputs of any two correlators are uncorrelated, even if the correlators share a common antenna. Thus, as the noise outputs of all correlators are independent, each interferometer can be considered as a separate entity in calculating the sensitivity of the array.

For a point source, there is some point in the sky at which the fringe outputs of all baselines in an array are mutually in phase synchronism. This would occur at the center of the "main-beam" if there are a sufficient number of baselines to give this term any validity. Thus, when the output records of all available baselines are superimposed, the fringe amplitudes add numerically, while the noise amplitudes, being uncorrelated from one record to the next, add in quadrature. The signal-to-noise ratio, therefore, varies as the square root of the number of baselines. This statement is valid regardless of whether or not any antenna is common to two or more baselines. It is also immaterial whether or not all baselines exist simultaneously. As the number of baselines varies approximately as the square of the number of antennas, the signal-to-noise ratio varies directly as the number of antennas.

The signal-to-noise ratio and the "equivalent" antenna parameters of a correlator array utilizing sidereal tracking are analyzed in detail in Chapter 7.

#### REFERENCES

- Blum 1959 (Ann. d'Ap. 22, 140)  
 Clark, B.G. 1965, Appendix II, VLA Report No. 1, NRAO  
 Faran, J.J., Jr. and Hills, R., Jr. 1952, Tech. Memo. No. 28  
 Contract N5 ori-76, Project Order X, Harvard University  
 Rowson, B. 1963, Mon. Not. R.A.S., 125, 177  
 Ryle, M. 1962, Nature 194, 517  
 Ryle, M., Elsmore, B. and Neville, A. 1965, Nature 207, 1024  
 Wade, C.M. and Swenson, G.W., Jr. 1964, NRAO Report "Geometrical Aspects of Interferometry"

Chapter 5

THE FEASIBILITY OF THE CORRELATOR ARRAY

## Chapter 5

## THE FEASIBILITY OF THE CORRELATOR ARRAY

A. Introduction

Several problems may be anticipated in the construction and operation of an array capable of resolution as high as 1", the most important of which are as follows.

1. Stability of the mechanical structure

Mechanical dissimilarities between the antennas of a given baseline might result in unknown changes in the baseline parameters, giving rise to erroneous data.

2. Phase stability of the electronic system

Various possible sources of phase instability exist in the receiving system, the most critical of which is the transmission system for distributing local-oscillator signals from the central phase reference to the mixers at each of the antennas.

3. Delay tracking

The total time delay of signal transmission from the plane wavefront of the downcoming wave through the receiving system to the correlators must be the same for each antenna in the array. This requires the provision of a variable time delay for the output of each receiver, the delay to be varied in synchronism with the apparent motion of the source in the sky. For high resolution these delays must be relatively long and very precisely controlled.

4. Stability of the atmosphere

The possibility exists that the inhomogeneous structure of the atmosphere might introduce phase fluctuations which would seriously reduce the coherence between the downcoming waves reaching two different antennas. This could reduce the effective collecting area of the array, and could add to the total "noise" in the system.

In addition to these major problems, a number of less crucial ones exist. However, it has been adequately demonstrated that all these problems can be solved. In principle, the proposed array is merely an assemblage of interferometers capable of tracking a source for several hours. If an interferometer can be made to operate properly with

baselines equivalent in length to the longest baselines of the array, the stability of the atmosphere, the mechanical structure, and the electronic system can be considered adequate, and the delay tracking system clearly has suitable characteristics.

The existing instruments, whose experience confirms the feasibility of the correlator array, are the one-mile Cambridge radio telescope and the long baseline interferometers at the Royal Radar Establishment, NRAO, and Cal Tech. The Cambridge supersynthesis instrument perhaps bears most directly on the problem since it appears to have most of the capabilities of the proposed array, except the ability to supply a great deal of information very rapidly and a considerably lower resolving power. The maps published by Ryle (1965) and Ryle, Elsmore, and Neville (1965) are observations made with the equivalent resolution of a 23" pencil beam at 21 cm and demonstrate the feasibility of combining the various correlator outputs to produce a contour diagram of the brightness distribution of a source. The sensitivity of correlator arrays is also strikingly demonstrated in these observations. With three antennas of 60-ft (18 m) diameter and receiver temperatures of 450°K at 74 cm, sources as weak as 0.02 flux unit are visible on the map of a selected region of the sky. This is in accord with the theory of the array as developed herein.

#### B. The Green Bank Interferometer

The NRAO has operated a long-baseline, phase-synchronous interferometer at Green Bank, West Virginia since the fall of 1964. This instrument serves simultaneously as a very powerful research tool and as an engineering experiment to provide answers to problems of VLA design. It has been highly successful in both capacities.

From September 1964 to December 1966, the interferometer consisted of two 85-ft (26 m) paraboloidal antennas capable of tracking a celestial source whenever it is above the horizon. One antenna is fixed in position and the other can be moved along the ground on rubber-tired wheels. Six baselines are available, varying in length between 11,000 and 24,000 wavelengths. All baselines are collinear at a geographical azimuth of 62°. The wavelength is 11 cm. A simplified block diagram of the interferometer is shown in Fig. 5-1.

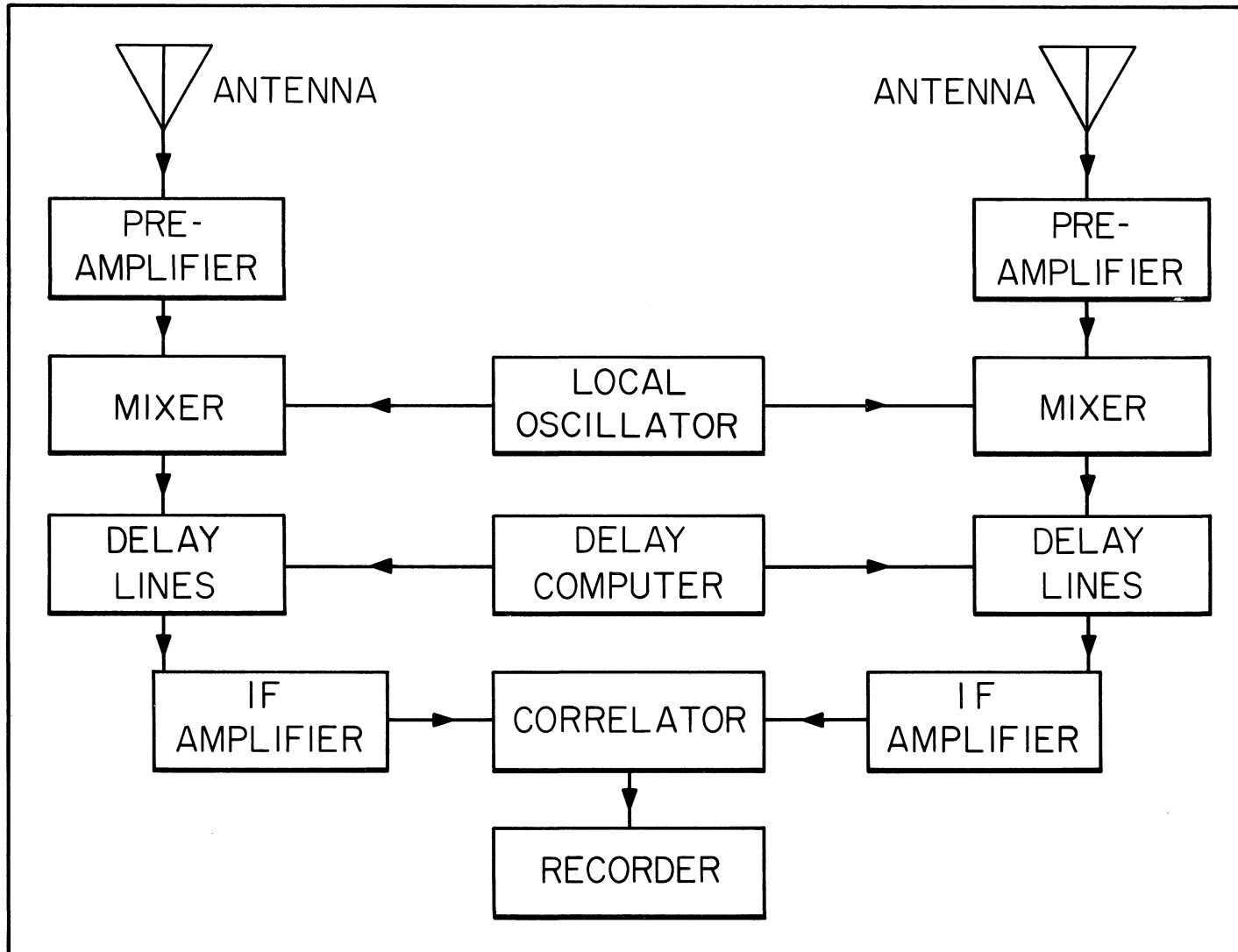


Figure 5 - 1. Simplified block diagram of a radio interferometer.

The receivers associated with the antennas are of state-of-the-art quality, involving solid-state parametric amplifiers. Automatically programmed delay lines provide the necessary time delays. A double side-band receiving system is used, in which small errors in phase-shift in the IF equipment have negligible effect on the phase of the interference fringes.

One of the most critical elements of the system is the local oscillator signal distribution system which must provide for minimal phase variations at the receivers. This problem is solved by "brute-force" methods in the present instance. The master oscillator is highly stable, the cables are buried deep in the ground to avoid temperature variations, and the pressure and humidity in the cables are regulated at constant absolute values.

The antennas themselves are of a type well-proven for general astronomical use, but not specifically designed for use in high-resolution interferometry. In particular, though the critical features of the two antennas are of identical design, no effort was made to improve upon the customary manufacturing tolerances. Thus, the distances between the phase center and the two rotational axes, respectively, must be slightly different for the two antennas.

The output of the correlator is recorded in digital form on magnetic tape for processing in a large digital computer. The computer determines the phase and amplitude of the interference fringes by a process of model fitting. Fringe parameters are routinely recovered from "signals" buried so deeply in noise that they are indistinguishable on an analog record.

The baseline parameters, that is, its length and its orientation in space, are determined by observations of optically identified, point sources of radio emission. While a very careful survey of the baseline parameters was made using the best available geodetic engineering techniques (Geodimeter and high-grade theodolite), it was quickly discovered that the radio observations gave much more rapid and accurate calibration.

#### C. Stability of the Mechanical System

It was mentioned earlier that no particular effort other than routine manufacturing practice was devoted to making the two antennas mechanically identical. Small differences in the corresponding lengths of critical

portions of the two antennas might result in unpredictable changes in baseline parameters, and thus in unknown errors in interference-fringe measurements. Experience with the interferometer has shown that this possibility need cause little concern.

In the winter of 1964-65 an experiment was conducted at Green Bank to determine the influence on the performance of the interferometer of errors in pointing the antennas. An error in pointing simulates in part an error in manufacturing which results in slight mechanical dissimilarities between antennas. The procedure was to observe a strong point source alternately with both antennas correctly pointed and with deliberate pointing errors in one or both antennas. Errors as great as half a beam width ( $7\frac{1}{2}'$ ) were used, so that at times the two lines of sight diverged or converged by as much as  $15'$ .

The phase of the interference fringes when both antennas were correctly pointed was compared with the phase when pointing errors existed. No difference in phase could be found. The phase of the fringes was plotted against pointing error as the latter was varied periodically. No periodic variation of phase was observed.

The negative results of this experiment are understandable in terms of the geometrical configuration of the tracking interferometer, which ensures that the effective change in baseline length is negligible for small error in pointing. In the Blaw-Knox 85-ft antennas at Green Bank, the distances between the polar and declination axes are relatively large. This would tend to accentuate the phase errors caused by pointing or manufacturing errors; the fact that no such errors were observed suggests that they are indeed higher-order effects.

Again it is emphasized that the Green Bank antennas were manufactured without extreme care to make them mechanically identical. In fact, the second antenna was manufactured and erected five years after the first. Nonetheless, the interferometer has performed with great precision. No errors have been discovered which can be attributed to mechanical dissimilarities. The inescapable conclusion is that great precision of manufacture is unnecessary; antennas which will perform individually with acceptable characteristics as single-element telescopes can be assembled into a large array with every expectation of satisfactory performance.

The Very Large Array (VLA) concept requires that its constituent antennas be mobile, and it is important to know whether or not they can be moved without suffering mechanical strains which would destroy their accuracy. One of the Green Bank interferometer antennas is movable on rubber tires along a rather uneven roadway. This antenna has been moved many times in the past two years, for a total distance of approximately 15 miles. It is evident that the pedestal of the antenna suffers severe wracking stresses during movement. In the observing position, the antenna rests upon carefully surveyed foundations with indexing plates. After every move the orientation of the polar axis is checked optically with respect to the stars. In each case to date, the axis was within one minute of arc of the pole, despite the rather rough treatment the structure had received. This is completely acceptable. The VLA mobility system is designed to minimize stresses due to movement. In view of this and the excellent experience with the Green Bank interferometer, no difficulty is anticipated in retaining the necessary accuracy while moving the VLA antennas.

D. Phase Stability of the Electronic System

The difficulty of transmitting a precise phase reference to two antennas has inhibited phase-synchronous, long-baseline interferometry until quite recently. Satisfactory techniques are now available which will permit satisfactory operation over baselines of the order of 20 km long. These techniques are elaborate and expensive -- radio interferometry has definitely progressed beyond the "string and sealing-wax" era.

The main sources of phase variation on a conventional metallic transmission line system are variations in ambient temperature, pressure, and humidity. Two general approaches to the problem can be used: by protecting the transmission lines against these external influences, or by compensating in some way for the phase variations so caused. The former method is feasible for baselines up to two or three kilometers in length and has been used in the Green Bank interferometer. In this instrument the interference fringes normally have constant phase and amplitude while a point source on the celestial sphere is being tracked. Any phase variation in the local-oscillator signal-transmission system or in the atmosphere above the site is visible on the interferometer output as

a variation in the phase of the fringes. Unfortunately, meteorological and electronic influences cannot be separated directly in the absence of a monitoring system, which could indicate the phase differences of the two local-oscillator signals as injected into the receiver mixers.

Phase variations were measured while the antennas were tracking point sources during 1964 and 1965. In general, the rms scatter in the phase was below  $30^\circ$  for any particular day, and much of the time it was less than  $10^\circ$ . These figures are upper limits on the rms electronic phase fluctuations, as they also include the meteorological effects. In fact, as will be discussed below, the phase variations are quite strongly correlated with meteorological parameters.

The interferometer, as it existed in 1964 and 1965, depended for its local-oscillator phase stability upon coaxial cables buried about one meter underground. The cables were filled with dry nitrogen, which was held at constant absolute pressure by a regulating system. At each antenna, however, the cable ran up the structure without protection from the weather and was subject to flexing as the antennas rotated. Computation shows that these exposed lengths of cable could be responsible for the largest part of the observed phase fluctuations.

The fact remains that the interferometer has performed very well, despite the above-mentioned deficiencies. Source positions have been measured routinely with internal consistencies of the order of one second-of-arc (Wade, Clark, and Hogg, 1965; Clark and Hogg, 1966). Certain obvious improvements to the electronic system are expected effectively to eliminate the electronic component of phase variation, leaving only the atmospheric component.

The VLA local-oscillator distribution system will incorporate a phase-compensating scheme in addition to the buried cables used in the first version of the interferometer. Exposed and flexible cables will be avoided. The phase-compensation concept has been tested thoroughly under laboratory conditions, and two different compensation systems are presently being installed in the Green Bank interferometer. The VLA system is confidently expected greatly to exceed the performance of the former interferometer system, which has already demonstrated its ability to produce fringe stability adequate for one-second position measurements.

Thus, the VLA electronic system will assuredly perform adequately.

E. Delay Tracking and IF Signal Transmission

The delay tracking problem, in common with most of the other significant problems of the VLA, is also encountered in a long-baseline, phase-synchronous interferometer. In the Green Bank instrument, the problem was solved in a highly satisfactory way through the use of a binary array of coaxial delay cables. The appropriate combination of cable lengths, at a given instant, is connected in cascade by solid-state switches under the control of an analog computer. For the VLA much longer delays are needed than for the interferometer; too long, in fact, to allow the economical use of coaxial cables. Fortunately, the problem can be solved by using acoustical delay lines constructed of quartz. Experiments in the laboratory (see Chapter 17) have confirmed that acoustical delays are technically and economically feasible for the longer delays required.

Chapters 16 and 17 explain the delay-tracking and IF signal transmission systems in detail. The double-sideband system is used in order to take advantage of its insensitivity to errors in phasing in the IF amplifiers, delay-lines, and transmission lines.

The double-sideband system does not lend itself to spectral-line radio astronomy. For this reason, consideration has been given to the use of a single-sideband system as well. It appears that the IF equipment can be controlled accurately enough in phase to be usable in the single-sideband mode, particularly in the lower-resolution configurations of the array which are likely to be used in spectral-line work. This topic is considered in detail in Chapter 21.

Transmission of the IF signals from the antennas to the central computing facility does not pose any critical technical problems, particularly if the double-sideband mode is used. The simplest system involves a coaxial cable for each antenna, plus appropriate IF amplifiers spaced at intervals along each cable. Unfortunately, this is a relatively expensive solution. Chapter 16 details a more economical scheme, and one which is technically feasible.

F. Stability of the Atmosphere

The fluctuations in phase observed on the interference fringes produced by the interferometer are apparently caused partly by the electronic

system and partly by the atmosphere. These fluctuations are for the most part below  $30^\circ$  rms for all baselines and for all weather conditions. Under present conditions it is not possible to separate the fluctuations by cause, although phase-monitoring equipment is presently being installed which should accomplish this.

Phase fluctuations as large as  $30^\circ$  would be a severe handicap in the operation of the correlator array. By averaging several observations it will be possible to improve the data to usable form in any event, provided that the phase fluctuations are less than about  $\pi$  radians. As the most of the Fourier coefficients are measured many times during a series of supersynthesis observations, the rms fluctuations are automatically reduced in the fringe-processing computation. Even so, it is conceivable that atmospherically-induced phase-fluctuations might require repeated observations of some coefficients, especially during adverse weather. This could increase the observing time considerably.

The atmosphere at Green Bank has been studied by means of phase-fluctuation data from the interferometer at several baselines during 1964 and 1965 (Baars and Lites, 1966). Concurrently, the temperature, pressure, and relative humidity were measured at ground level. Meteorological information was also obtained from the Weather Bureau station at Elkins, 50 miles north of Green Bank. The rms phase fluctuation was calculated for each day when strong point-sources were observed, and the resulting numbers plotted against specific humidity, rate of change of specific humidity, refractivity, temperature, frontal activity, and general weather type. Significant correlations (above 0.5) were noted with frontal activity, temperature, specific humidity, and general weather type, as shown in Figs. 5-2, 3, 4, 5.

The phase-fluctuations are definitely higher in humid weather and are particularly high during rainfall. It is difficult to see how humidity or rainfall could affect the stability of the electronic system; thus, a large part of this effect can be assigned to the atmosphere. Temperature is the meteorological parameter most likely to affect the electronic system so that the influence of temperature on atmospheric stability is uncertain. No correlation was found between rms phase scatter and surface refractivity. Large discontinuities in phase are common during frontal activity.

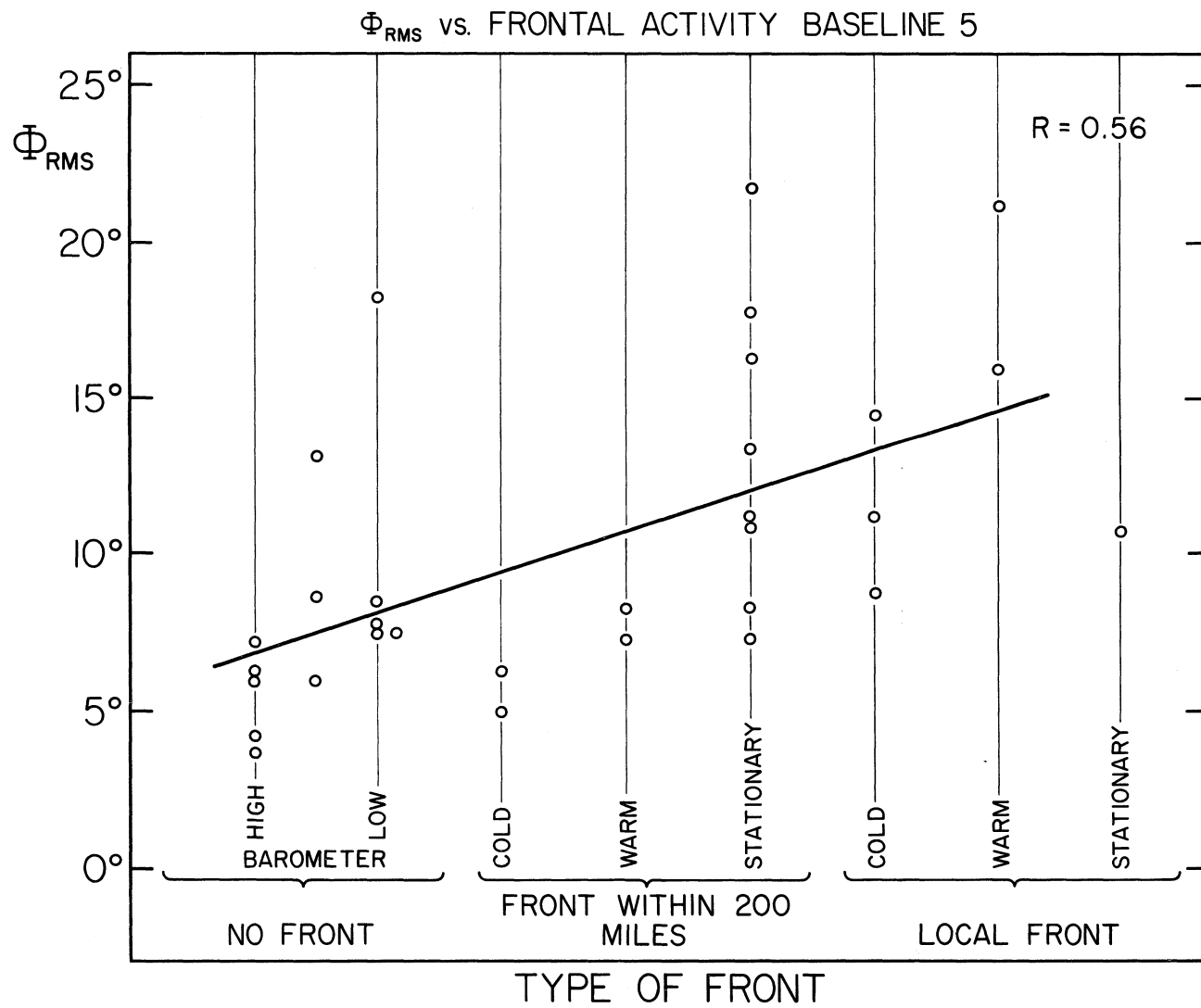


Figure 5 - 2

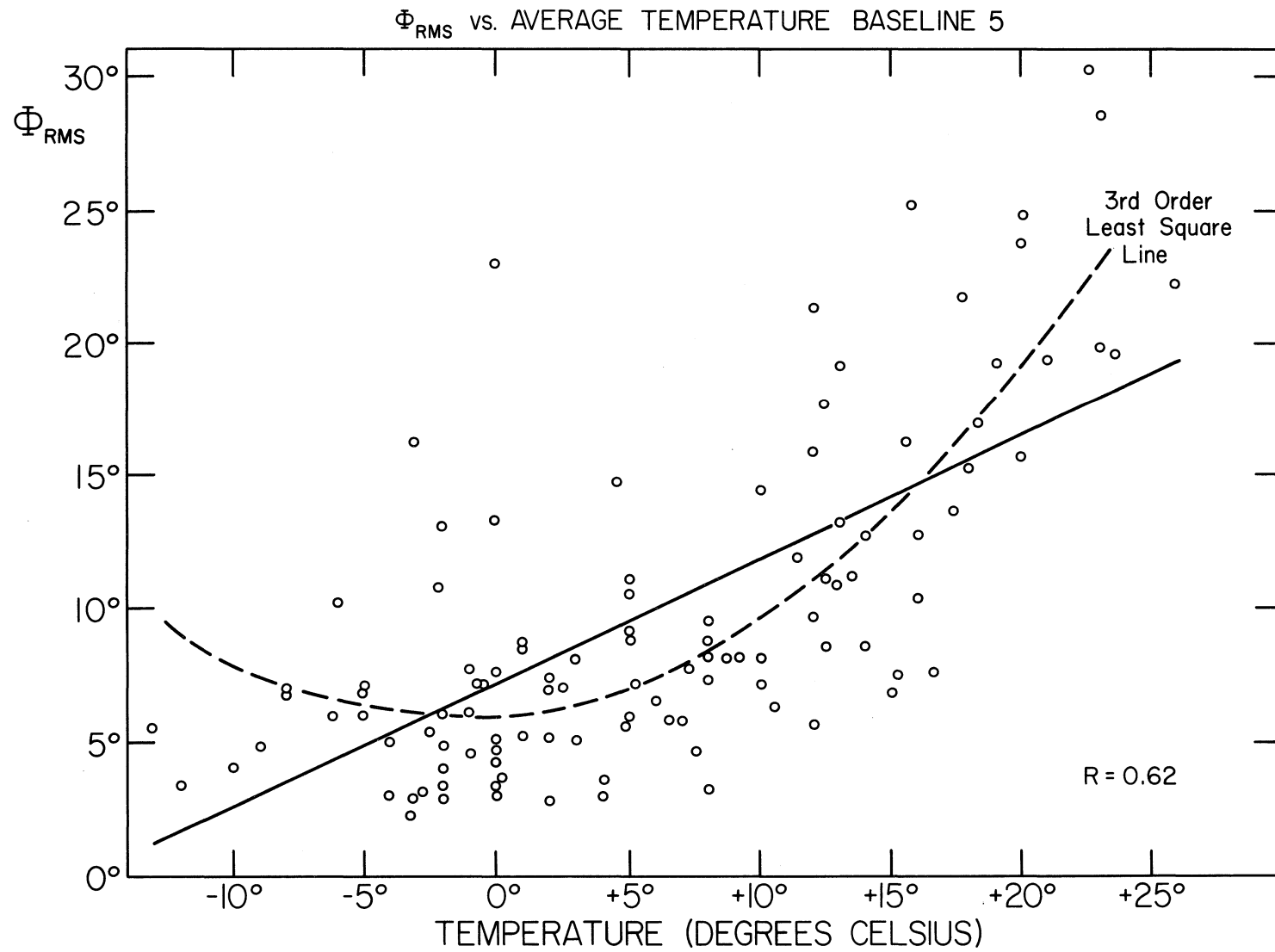


Figure 5 - 3

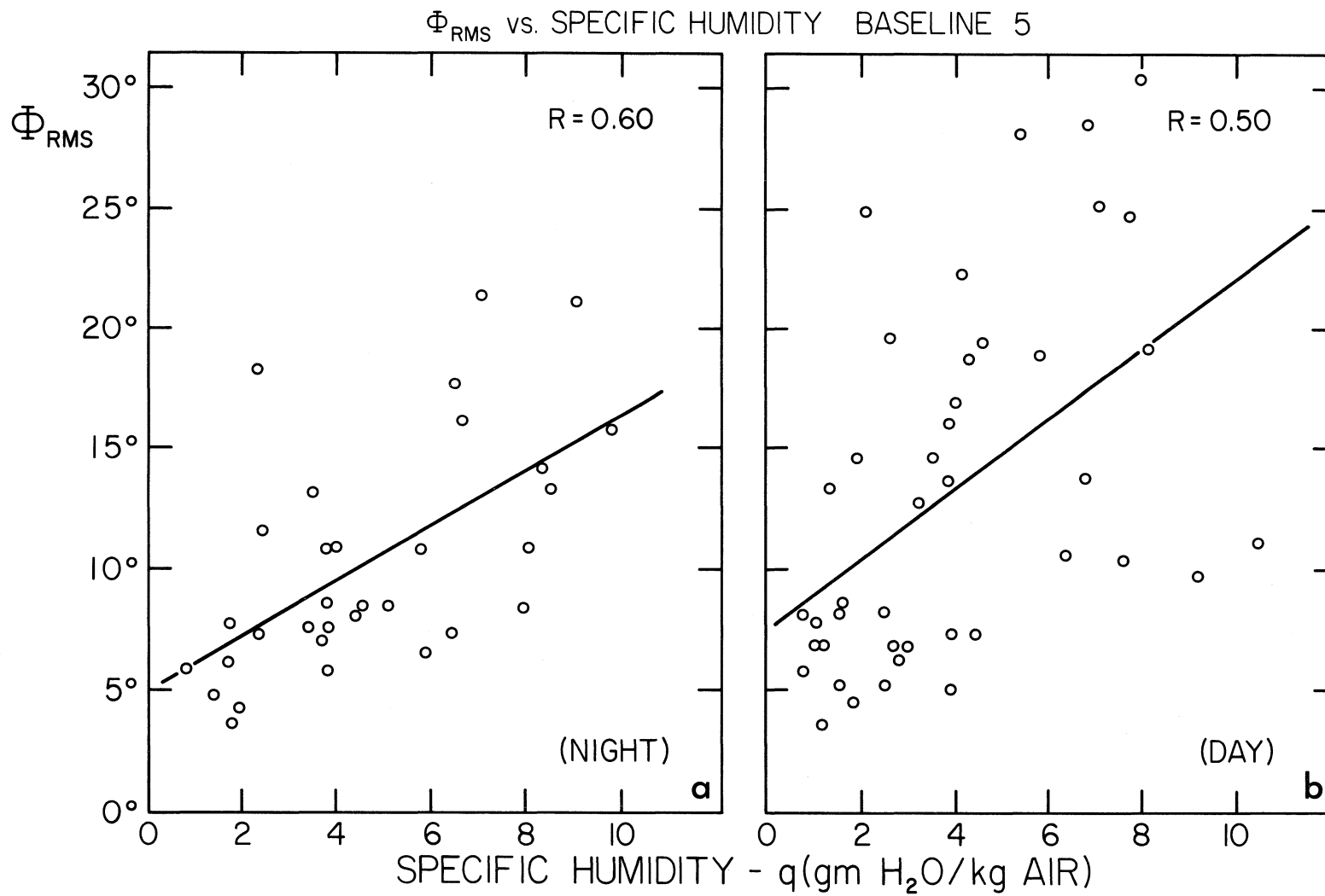
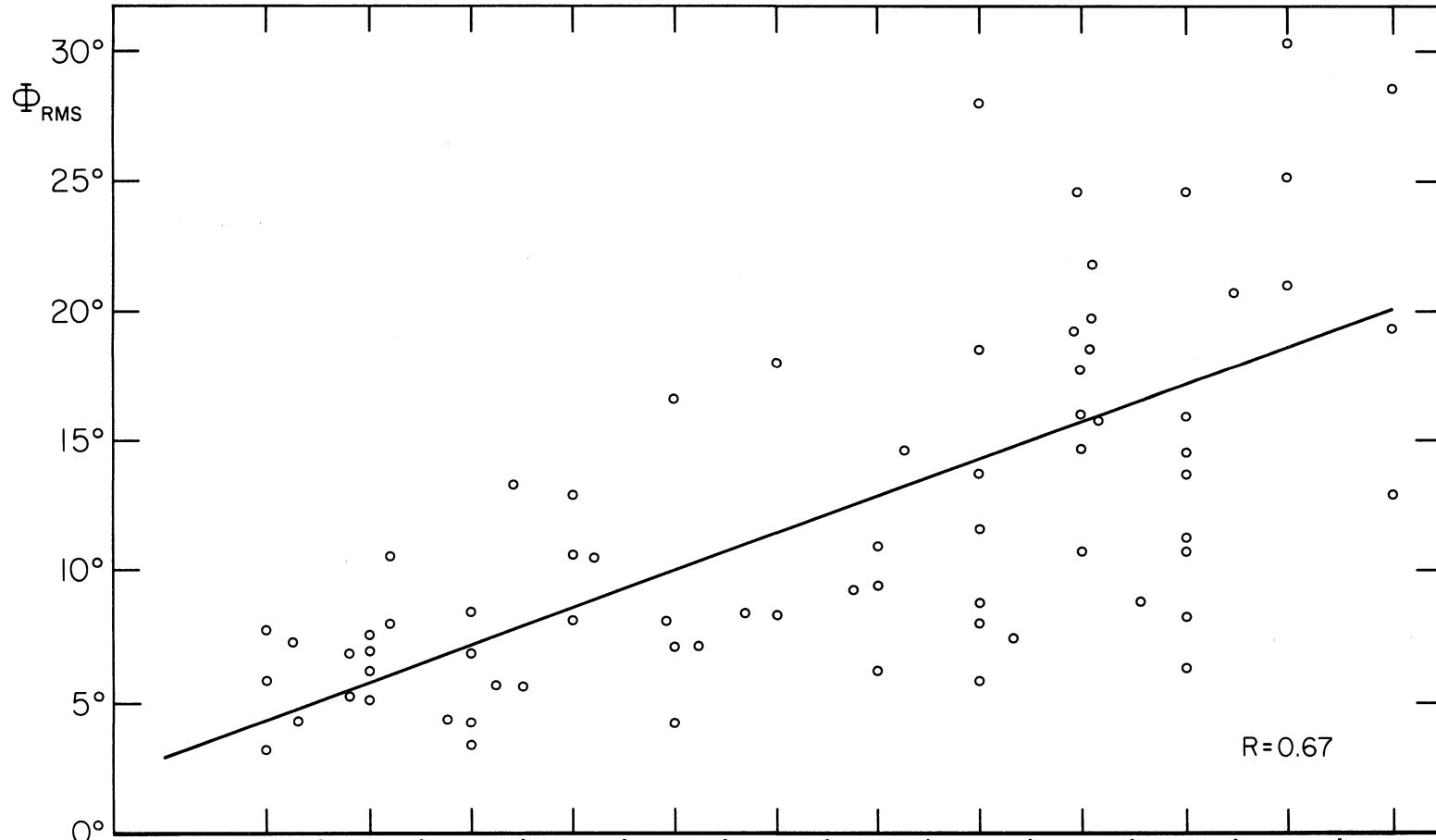


Figure 5 - 4

$\Phi_{RMS}$  vs. WEATHER BASELINE 5



WEATHER	CLEAR	CLEAR	CLEAR	CLOUDY	CLOUDY	FOG	CLOUDY	CLOUDY	CLEAR	RAINY	RAIN	RAIN
BAROMETER	STAT.	STAT.	MOVING	STAT.	STAT.		MOVING	MOVING	MOVING			RAIN LATER
TEMPERATURE	LOW	HIGH	LOW						HIGH			

Figure 5 - 5

It is believed that there is evidence of tropospheric influence on the fringe phase-fluctuations at 11 cm wavelength and baselines of about 2400 m. The order of magnitude of the rms phase scatter over a time of a few hours ( $\phi_{\text{rms}} \sim 4-40^\circ$ ) is as expected from the theory of wave propagation in a turbulent atmosphere (Tatarski, 1961). A direct application of this theory to a one second-of-arc array gives six times larger phase scatter. This extrapolation is not warranted, however, because the distances involved exceed the ones for which knowledge on the scale size of tropospheric turbulons is available.

It does not seem possible in view of these results to predict from surface measurements of meteorological data the amount of phase scatter to be expected at a specific site. It can be concluded, however, that a high altitude site (less water vapor in the line of sight) with little cloud formation, a stable pressure regime, and little frontal activity will yield the best obtainable phase stability. For these reasons, site selection activity has been concentrated mainly in the high altitude deserts of the southwestern United States.

A survey of total atmospheric water vapor content was made during 1963 at several sites in the United States, using portable spectral hygrometers (Low, 1964; Fowle, 1912). The data, averaged over one year, are plotted in Fig. 5-6, which shows that the southwestern, high-altitude sites have considerably less total precipitable water vapor than does Green Bank. It is therefore expected that the phase fluctuations will be less troublesome at such sites.

It is regrettable that the atmospheric phase-scatter data are so strongly contaminated by electronic effects. The experiment will be performed again early in 1967, when the interferometer will have adequate phase-control equipment. In addition, a 14 m portable antenna has been procured, together with a phase-locked local-oscillator system capable of operation over a baseline 40 km long. This antenna will be used as an interferometer element with one of the existing antennas at Green Bank to determine the influence of the atmosphere at fringe spacings as small as 0.5". From these data it should be possible to determine how much, if any, repetitive observing will be necessitated by atmospheric phase-fluctuations.

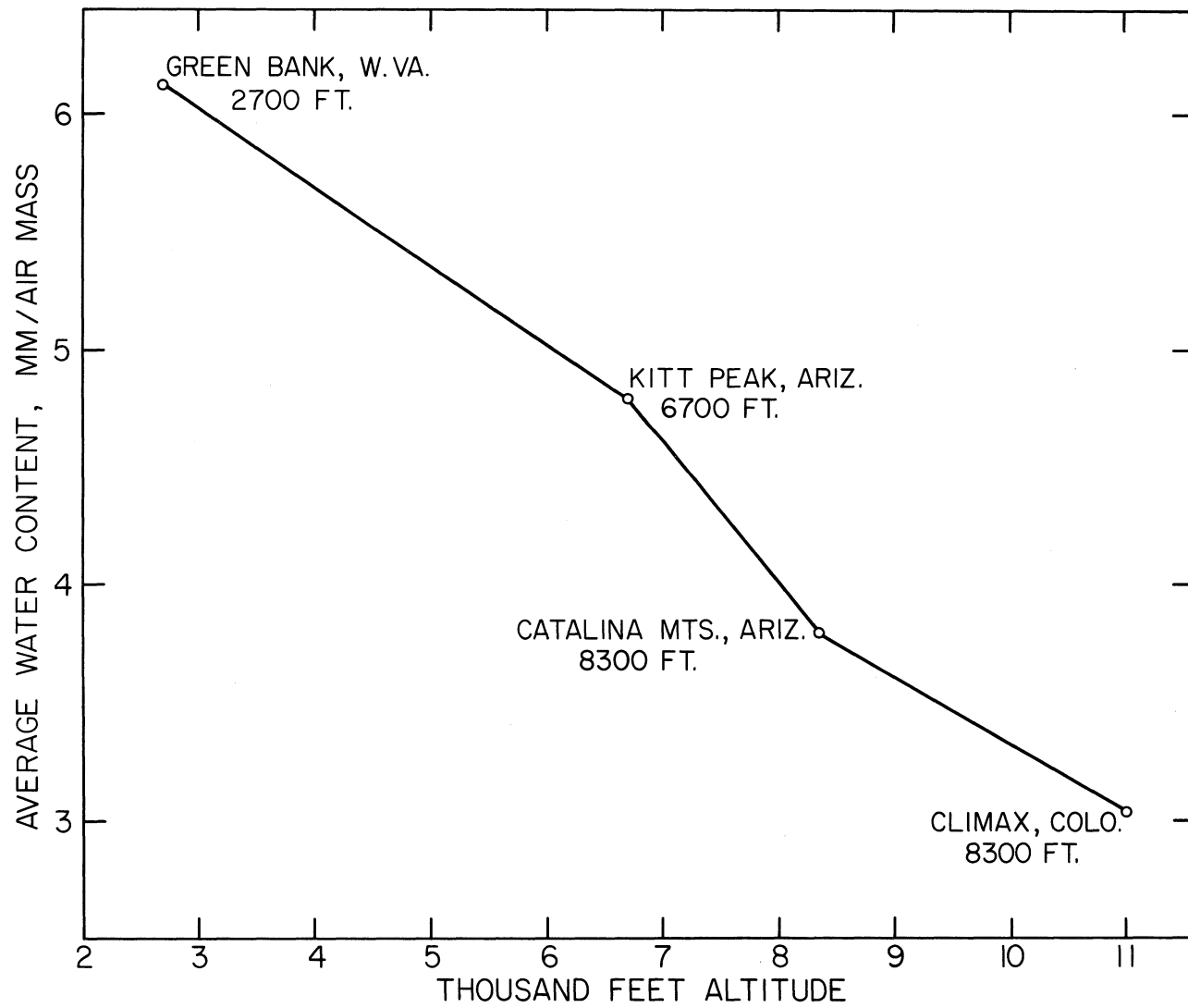


Figure 5 - 6

The interim conclusion of the atmospheric phase-fluctuation study is that, while the inhomogeneous atmosphere produces fluctuations sufficiently large to be of some concern, the problem is of manageable proportions, even in the unfavorable environment of Green Bank. In the arid Southwest the fluctuations are expected to be considerably smaller. During the more favorable seasons, the water vapor content is extremely low, and the effect of the atmosphere is expected to be negligible.

G. Organizational and Computing Problems

Observing with an array with approximately 36 antennas, and thus approximately 630 simultaneous output-information channels, might be a very complex operation. Furthermore, it is contemplated that three channels of information might be required from each baseline in order to measure polarization, so that the total number of output channels is 2040. Each of these channels produces one complex number every minute, and a typical observation will require, say, eight hours. The numbers must be sorted to correspond with their respective baselines and must be arranged for convenient summation of the Fourier series they constitute. The desired output is a map of a region of the sky, probably in the form of contours of equal brightness.

The correlator array is inherently tied to a large computer facility. The computing requirements have been examined in detail (see Chapter 20), and a system has been designed which will solve the computer problem satisfactorily.

An observer wishing to use the instrument must decide which of the available array configurations is most suitable for his problem. This could be a formidable problem, particularly for a person not intimately familiar with the instrument and its mode of operation.

The user of the VLA will have at his disposal an extensive library of transfer functions, covering all standard array configurations, declinations, and hour angle intervals. With some advance knowledge of the nature of the source to be investigated, an array can be chosen which has an appropriate transfer function. Computer programs will be available to determine (1) the beam pattern from the transfer function and (2) the effect of convolving the beam pattern with an assumed source-brightness function.

By judicious preparation for his observations, a visiting astronomer should be able to make effective use of the VLA just as he does an instrument of a more familiar type. Clearly it will be necessary to have a staff of trained operators to run the instrument. Probably the scientific observer will choose an array configuration and prepare a list of coordinates to be observed. After the observations and data reduction have been completed by the VLA staff, the scientist will receive his data in the form of contour maps, computer printouts, or magnetic tape, usually within 12 hours of the start of an observation.

The observatory will be an isolated site, and the astronomer will have little to do at the site. As the output data will be in suitable form for digital transmission, it is feasible to consider sending output data to the astronomer at his home office, by means of facsimile or digital data transmission over the public telephone system.

#### REFERENCES

- Baars, J.W.M. and Lites, B. W. 1966, NRAO VLA Report No. 4.  
Clark, B. G. and Hogg, D. E. 1966, Ap.J., 145, 21.  
Fowle, F. E. 1912, Ap. J., 35, 149.  
Low, F. J. 1964, NRAO Millimeter-Wave Internal Report.  
Ryle, M. 1965, Nature, 205, 1259.  
Ryle, M., Elsmore, B., and Neville, A. 1965, Nature, 207, 1024.  
Tatarski, V. I. 1961, "Wave Propagation in a Turbulent Medium,"  
McGraw-Hill Book Co., New York.  
Wade, C. M., Clark, B. G., and Hogg, D. E. 1965, Ap. J., 142, 406.

Chapter 6

THE ARRAY CONFIGURATION

## Chapter 6

## THE ARRAY CONFIGURATION

A. The Computer Program for the Selection of an Array Configuration1. The basic program

Optimization of the array configuration involves, in essence, a compromise between an array with a large number of elements, giving complete sampling of the desired Fourier components at a high cost, and an array with a small number of elements, which is less expensive but has large side-lobe levels, because of the incomplete sampling. For a one-dimensional array yielding an instantaneous fan-beam, the optimum number and location of the elements have been given by a number of people (e.g., Leech, 1956). For example, 11 elements can be arranged to give all (integer) baselines between 1 and 42, with only twelve redundant spacings. However, the extension of this analysis to a two-dimensional array yielding an instantaneous pencil-beam has not been made; the problem is even more complex in the present case because the ability to track allows each pair of elements to contribute many baselines to the synthesis. The study of the configuration has therefore been made empirically, by computing on a high-speed digital computer the transfer functions of a large number of arrays and determining what factors most seriously affect their performance.

The basic computer program which has been used for this study accepts as input the locations of the elements in the proposed configuration and computes the transfer function of the array for specified observing conditions. The program has the following constraints:

(a) The beam width is 10", assuming that the Fourier components are weighted in inverse proportion to their spatial frequencies. Since this is analogous to the case of uniform illumination of the aperture plane, the usual expression for a circular aperture (Silver, 1949) may be used to determine the maximum baseline (measured in wavelengths) required.

$$D/\lambda = \frac{0.5145}{\theta} = 21220$$

where  $\theta$  is the beam width in radians.

(b) The array should be capable of mapping the entire region included in the primary beam of an element in the 10" configuration. The half-power width of a 25 m dish at 11.1 cm is approximately 20'. According to Bracewell (1958), this requirement can be met by sampling the brightness spectrum at intervals  $\Delta u$ ,  $\Delta v$  which correspond to  $\frac{1}{20'}$ , or 172 cycles per radian.

(c) The latitude assumed for the array is 34°. The computations are not very sensitive to this value.

The transfer function produced by the program is a semi-circle of radius 21,223 cycles per radian. It is divided into 24,100 discrete squares, or cells, of dimension 172 cycles per radian on a side.

The program treats the array as a large number of simple two-element interferometers. For each pair of elements, it computes the spatial frequency which is sampled at each minute during the observation, using (4-20) and (4-21), and assigns one minute of integration to the appropriate cell of the transfer function. One minute was chosen as the interval in order that the change in the spatial frequency during the integration time is less than one-half the length of the unit cell. After the computation has been made for all possible pairs of elements, the distribution of integration time over the cells in the transfer function has been obtained and is printed out. Two samples of such a transfer function are given in Fig. 6-1a and 6-1b; the array used was a hollow circle with 37 elements, observing at a declination of + 30° and 0°, respectively, over an hour angle range of  $\pm 4$  hours. A more detailed description of these figures is given in Section C.

It is important to emphasize that although the computer program is written specifically for a resolution of 10" and field of view of 20', the results transform exactly for any other resolution, if the ratio of resolution to field of view is preserved. In particular, the conclusions reached for the 10" array apply equally well to arrays with a 30" beam in a 60' field, 3" beam in a 6' field, and 1" beam in a 2' field.

## 2. The effect of element size

It is assumed in the program that the elements are geometric points. Since the actual elements will be many wavelengths in diameter, a given pair will instantaneously sample a range of Fourier components of the brightness spectrum, rather than the single component which is computed

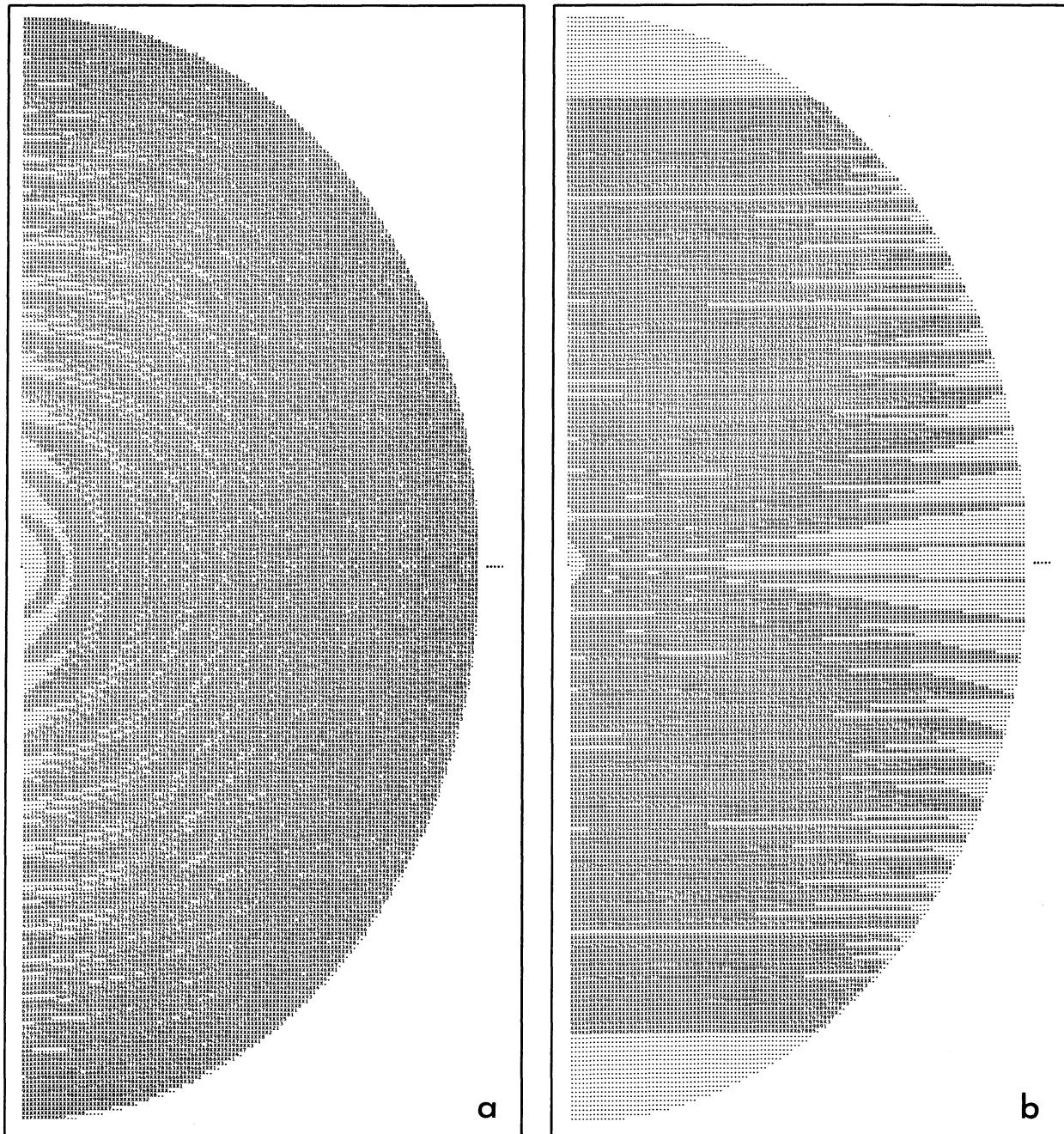


Figure 6 - 1. The transfer function of a 37 element circle (a)  $\delta = +30^\circ$  (b)  $\delta = 0^\circ$ .

in the program. An allowance for this effect can be made in either of two ways:

(a) The transfer function can be modified. If  $W_p(u,v)$  is the transfer function of the array with point elements and  $W_e(u',v')$  is the transfer function of an element, the actual transfer function of the array is

$$\begin{aligned} W_a(u,v) &= W_p * W_e \\ &= \int_{-\infty}^{\infty} \int_{-\infty}^{\infty} W_e(u',v') W_p(u-u', v-v') du' dv' \end{aligned}$$

(b) It is more satisfactory to consider the effect on the power pattern of the array. The power pattern of the actual array will be the product of the patterns of the element and the array with point elements. It is clear that the only effect of element size is to restrict the field of view.

Thus, there is no need to make an explicit correction for the element size. It is sufficient to note that for configurations with beam width larger than 10", the field of view will be defined by the primary pattern of the element.

### 3. The effect of bandwidth

The program assumes operation at a single frequency; in fact, the bandwidth is large, possibly 50 MHz at the IF. The effect is more complex than the smearing due to element size, since it is not a simple convolution of transfer functions. A detailed discussion of the bandwidth effect has not been made, but an estimate of the limitation on the field of view follows from consideration of a simple interferometer.

For a two-element correlator interferometer, having a rectangular IF bandpass, the output is, after Burns (1964),

$$r(\tau) \propto \frac{\sin [2\pi \frac{B}{2} \tau]}{2\pi \frac{B}{2} \tau} \cdot \cos \omega_{IF} \tau \cdot \cos \omega_{LO} \tau$$

where  $B$  is the IF bandwidth

$2\pi \omega_{IF}$  is the IF center frequency:  $[\frac{B}{2} \sim 2\pi\omega_{IF}]$

$2\pi \omega_{LO}$  is the RF frequency  $\nu_0$

$\tau$  is the delay of the signal reaching one antenna with respect to the other.

Let  $x, y$  be the angular displacement in the sky plane from the position of zero delay

$u, v$  be the spatial frequencies sampled

then  $\tau = (ux + vy)/\nu_0$

$$r(\tau) = \frac{\sin \left[ \frac{2\pi B}{\nu_0} (ux + vy) \right]}{\frac{2\pi B}{\nu_0} (ux + vy)} \cdot \cos 2\pi(ux + vy)$$

The modulation of  $r(\tau)$  due to the bandwidth is most pronounced towards the edge of the field of view (large  $x, y$ ), for large baselines (large  $u, v$ ) and large IF bandwidth. Strictly speaking, the bandwidth smears the sample only in the direction of the line joining the elements; practically, it appears that the combination of the bandwidth and a number of other effects will limit the field of view in any direction to the distance for which the quantity

$$\frac{\sin \left[ \frac{2\pi B}{\nu_0} (ux + vy) \right]}{\left[ \frac{2\pi B}{\nu_0} (ux + vy) \right]}$$

has its first null (Section F). For a 1" array, operating at 2695 MHz

with a bandwidth of 50 MHz, the corresponding field of view has a radius

$$x = 33''$$

This is approximately one-half of the field of view for which the array is being designed. To utilize the full capability of the array, the bandwidth should be restricted to 25 MHz. Alternatively, if the bandwidth limitation on the field of view is accepted, somewhat lower side-lobe levels can be achieved.

#### B. The Figure of Merit of an Array Configuration

Because the empirical study of array configurations was based on the computation of transfer functions, it was necessary to define a figure of merit which would quickly distinguish the better arrays. Such a figure of merit could be very complicated, involving for example the distribution of integration, the completeness of sampling, and the number of redundant baselines; in the end, it was decided that the percentage of unsampled cells in the transfer function would provide a quick and reasonably sensitive measure of the performance of an array. The physical interpretation of an unsampled cell, or hole, is clear; it means that the corresponding Fourier component in the brightness spectrum of the source will be missing in an actual observation, and this will produce "hole" side-lobes in the final brightness temperature map.

To a potential observer the knowledge that the transfer function has some distribution of unsampled cells is not very useful. He requires a more explicit statement of performance, perhaps in the form of the power radiation pattern. This information has been obtained for a few selected arrays, and some examples are given later in the report. The inversion required to produce such a pattern is time-consuming, however, and cannot be applied to the large number of arrays which have been tested. An alternative approach is to consider the statistical relation between the number of holes in the transfer function and the mean side-lobe levels.

For a semi-circular transfer function of diameter  $N$  cells in which there are  $n$  randomly distributed unsampled cells  $(u_i, v_i)$ , with linear weighting in  $u$  and  $v$ , it is shown in Section F that the statistical properties of the side-lobe levels may be described by the following expressions:

Maximum Possible Side-lobe

$$\frac{n}{\frac{\pi N^2}{8} - n}$$

RMS Side-lobe Level at a  
Large Distance from the  
Main Lobe

$$\frac{\sqrt{\frac{n}{2}}}{\frac{\pi N^2}{8} - n}$$

Strongest "Distant" Side-  
lobe (within the field of  
view)

$$\frac{\sqrt{n}}{\frac{\pi N^2}{8} - n} \operatorname{Erf}^{-1} \frac{1}{2} \left( 1 - \frac{2}{\pi N^2} \right)$$

The side-lobe levels predicted by these expressions are given as a function of the percentage of holes in Fig. 6-2. Included for comparison are actual side-lobe levels which have been computed for a number of different arrays. It is seen that the statistical relations are well satisfied by the observations for regions far from the main beam. The near side-lobes are high, as was expected; they are, however, between 5 and 10 db lower than the maximum possible if the holes added in phase.

The percentage of holes is therefore a reasonably good indicator of the quality of an array, provided that the number of holes in the center and in large clusters (those that are most likely to add in phase) is not too large. It is difficult to place an upper limit on the number of holes which would be acceptable, since this must depend upon the astronomical problem under consideration. For a general-purpose array, a maximum distant side-lobe level of about - 20 db, corresponding to 15% holes, would be satisfactory. The permissible distribution of holes is determined by the size of the near side-lobes, which should be below - 15 to - 17 db.

### C. The Hollow Circle

An array which will have an excellent transfer function is a hollow circle of diameter in wavelengths equal to the radius of the transfer function. For any given declination, the array can be made to give a circular transfer function by making the shape elliptical to allow for foreshortening; then all element pairs sample entirely within the transfer function, so that little observing time is wasted. By proper choice

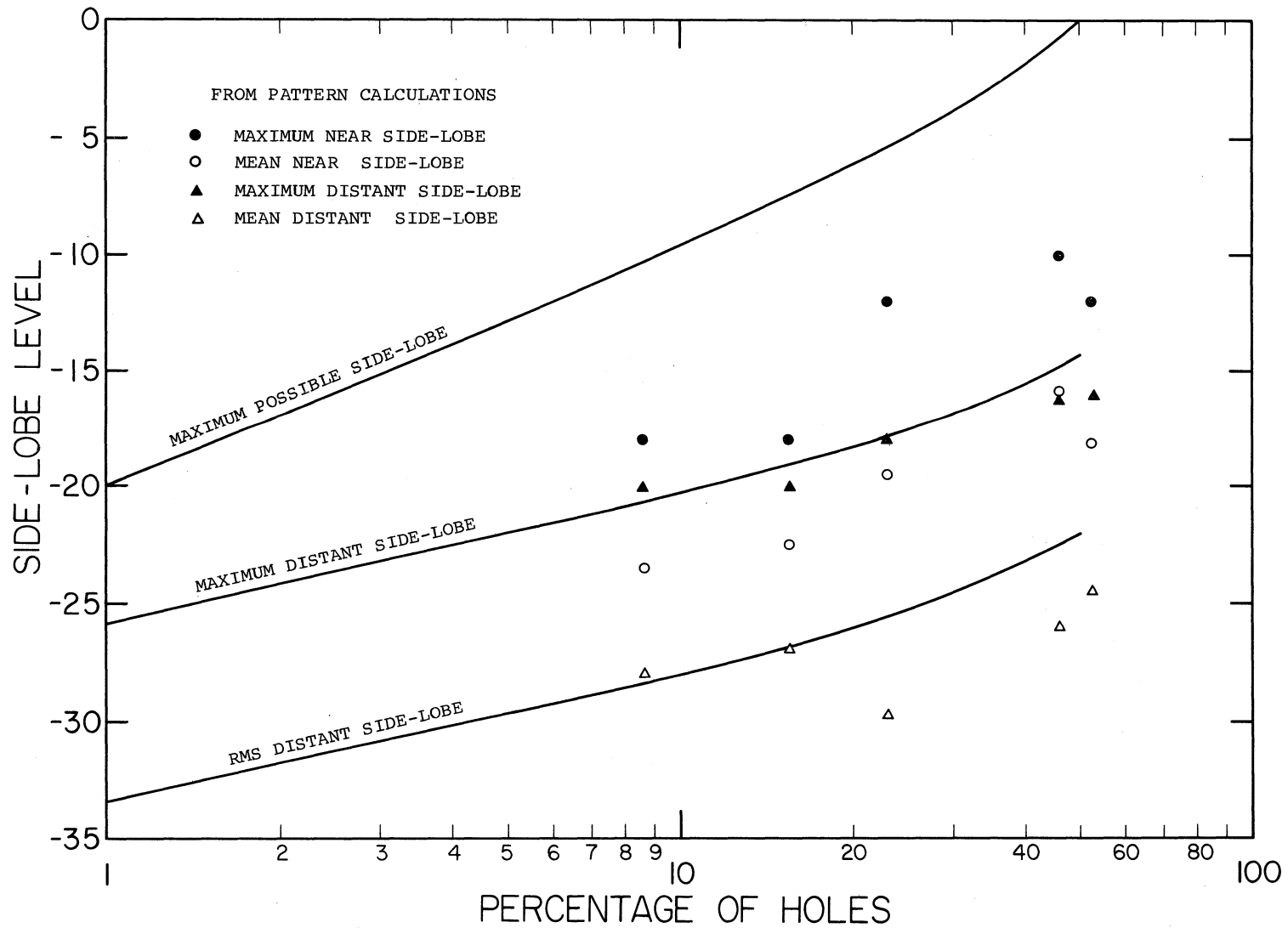


Figure 6 - 2. Side-lobe levels as a function of percentage of holes in the transfer function.

of element spacing around the ellipse, the number of redundant baselines can be reduced.

The overriding disadvantage of this configuration in the present application is that it cannot be easily adjusted to give the various resolutions which are required. Expansion would require either a large number of radial tracks or a series of circular tracks appropriate to each resolution. In each case the cost would be prohibitive, requiring, even in the second case, about 70% more track than a Wye configuration. This problem arises for most closed configurations.

Nevertheless, since the hollow circle is such a good configuration, it is useful to study its transfer function, in order to establish a standard against which the performance of other arrays may be compared. A comparison of two circular arrays is given in Table 6-1. One array has 37 elements; the other, 41. In each case the diameter is 2,400 m, and the elements are distributed at equal intervals around the circumference of the circle.

Table 6-1  
Percentages of Holes for Circular Arrays

Declination	Hour Angle Range (hours)	Percentage of Holes	
		37 Elements	41 Elements
+ 30°	± 2	36.7	31.1
	± 4	7.4	4.3
	± 6	1.1	0.4
0°	± 2	42.8	37.7
	± 4	22.8	19.9
	± 6	21.6	18.8
- 15°	± 2	36.9	32.1
	± 4	20.9	19.2
	± 5.5	16.8	15.7

Figs. 6-1(a) and 6-1 (b) show the transfer functions for a circular array of 37 elements operating over the hour angle range  $\pm 4$  hours, for declinations + 30° and 0°, respectively. The desired transfer function should be circular, with radius 21,200; the array at + 30° exactly satisfies this requirement. Unsampled cells are denoted by dots, and sampled

cells by characters, coded in order to give the number of minutes of integration in the cell.

There are some general features in these diagrams which appear again and again in the transfer functions of other array configurations. In the transfer function of Fig. 6-1(a) there are a significant number of holes near the origin. It is always difficult to completely sample the low spatial frequencies, both because the elements must be widely dispersed in order to give the desired resolution and because the track corresponding to a short baseline covers a very small area in the transfer function. In the transfer function of Fig. 6-1(b), there are long rows of cells where the sampling is incomplete. For sources near declination zero, the sampling track (in the transfer function) of a two-element interferometer is a straight line, rather than the ellipse which is obtained at other declinations. This means that for operation near declination  $0^\circ$ , the array must have instantaneously all desired N-S spacings. In contrast, for declinations far from the celestial equator, each element pair gives a range of N-S spacings, and complete sampling is more easily obtained. In both cases, of course, the range in E-W spacings is obtained by tracking in hour angle. Finally, again in Fig. 6-1(b), the sampling is incomplete near the top and bottom of the transfer function, an effect produced by the foreshortening due to projection. To compensate, the array should be elliptical, rather than circular. This will improve the performance for southern declinations and degrade the performance for declinations near  $+30^\circ$ , since in the latter case some of the correlators will sample outside the circular transfer function. Optimization of the configuration will involve a balance between these two effects.

The results shown in Table 6-1 suggest that the percentage of holes can be more rapidly decreased by allowing a greater tracking range than by adding a few more elements. Further studies tabulated in the following section support this idea.

#### D. Configurations with Three Arms

Since closed configurations are unacceptable, because of the requirement of expansibility, the most suitable classes of arrays are those having elements arranged along a small number of arms. Configurations using only one or two arms have poor performance for declinations near the celestial equator. The simplest successful array is one with three arms.

The three-arm array has been studied for a wide range of configurations. In order to keep the amount of computation within reasonable bounds, the various tests were carried out for three declinations only:  $+30^\circ$ , where the array has its full resolution;  $0^\circ$ , where the array performance is poorest because the elliptical tracks degenerate into lines; and  $-15^\circ$ , where the effects of foreshortening are important. If an array can be designed which has a good radiation pattern for these three declinations, then it will be good over most of the observable sky.

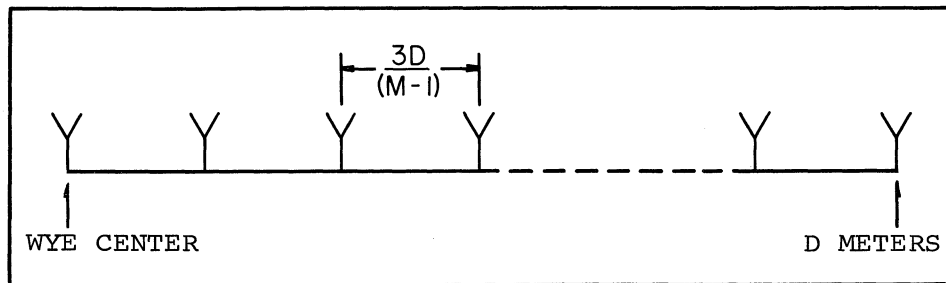
In the following studies it has been assumed that the optimum configuration of the arms is independent of the distribution of elements along the arms. Two configurations have been used for the majority of the studies. One is the uniform M-element Wye, which has an element at the center and  $\frac{(M-1)}{3}$  elements spaced uniformly along each arm, as shown in Fig. 6-3(a). The other, the M-element supplemented Wye, has no central element. Each arm has  $M/3$  elements, with the inner elements spaced more closely than the outer ones, as shown in Fig. 6-3(b).

1. The optimum orientation of the arms

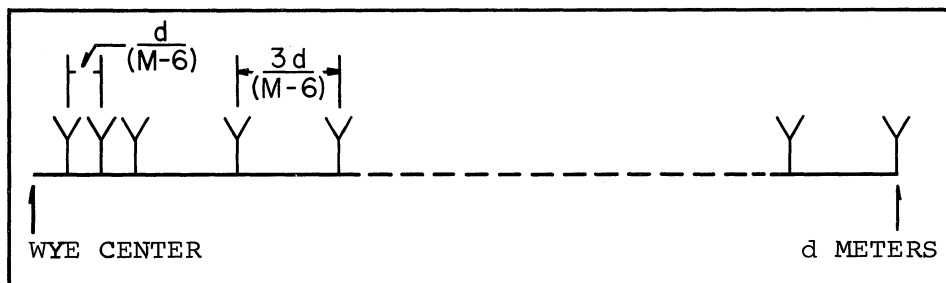
Although the Tee array has been used successfully in radio astronomy, its performance for sources near the equator is not good, because the available number of N-S baselines is small. This effect could be overcome by rotation of the entire Tee, or by rotating only the E-W arms, to form a Wye. It appears, therefore, that the first parameters of the general three-arm array which must be determined are the arm orientations.

The array used in the determination of the optimum values of the orientation parameters  $\theta$  and  $\phi$ , defined in Fig. 6-3(c), was a uniform Wye with arm length 2,400 m. In all cases the tracking range was  $\pm 4$  hours. The percentages of unsampled cells as a function of the angle of rotation  $\theta$  and the angle between the oblique arms  $2\phi$  are given in Table 6-2, for the three standard declinations  $+30^\circ$ ,  $0^\circ$ , and  $-15^\circ$ .

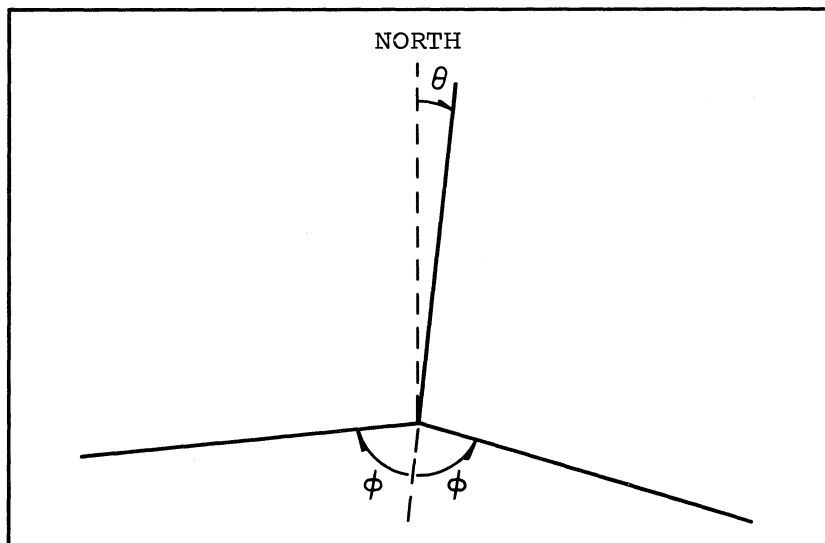
There is no single value of  $(\theta, \phi)$  which minimizes the percentage of holes simultaneously at all three declinations. For example, the orientation  $\theta = 80^\circ$ ,  $\phi = 60^\circ$  gives the lowest percentage at  $\delta = +30^\circ$ , but fails at the other two declinations. The best compromise is to take the value which minimizes the number of holes at declination  $0^\circ$ , which is the most difficult declination for the array, and accept the slight deterioration for the other declinations. In this case  $4^\circ \leq \theta \leq 8^\circ$ ,  $\phi = 120^\circ$ .



(a) Distribution of elements along one arm of an M-element uniform Wye. The arm length is D.



(b) Distribution of elements along one arm of an M-element supplemented Wye. The arm length is d.



(c) Definition of the orientation parameters  $\theta$  and  $\phi$ .

Figure 6 - 3. Geometrical aspects of a wye array.

Table 6-2

Percentage of Holes as a Function of Orientation of the Arms

Dec.	Rotation Angle	Angle between Oblique Arms									
		20	40	60	80	100	120	140	160	180	
+30°	0	69.3	52.1	34.9	27.5	28.3	22.9	22.3	19.4	29.0	
	2	68.6	49.8	34.3	26.2	26.5	21.0	20.4	18.0	27.4	
	4	68.1	49.2	33.7	25.6	25.0	20.7	19.9	17.4	26.0	
	6	67.8	50.0	33.0	24.8	23.6	20.2	19.9	17.4	25.5	
	8	67.4	49.5	32.2	23.8	22.7	20.5	20.1	17.0	25.5	
	10	67.2	49.4	32.3	23.6	22.0	20.6	20.3	17.8	26.0	
	20	62.8	44.8	27.2	24.1	20.2	21.2	18.8	17.9	26.4	
	30	56.8	39.9	25.1	21.9	20.5	23.4	20.4	17.7	25.8	
	40	51.8	35.5	23.0	21.1	21.3	21.2	19.8	21.4	26.4	
	50	47.5	31.8	20.1	18.7	20.3	20.6	19.5	21.1	26.5	
	60	43.3	30.0	20.6	18.4	18.9	22.9	22.1	23.0	26.0	
	70	39.8	27.6	17.5	17.2	18.7	20.6	22.1	24.5	26.6	
	80	38.0	26.3	16.0	16.5	18.3	21.3	22.2	25.1	26.3	
	90	36.5	25.8	19.1	17.7	23.6	23.4	24.3	27.7	29.5	
	0°	0	89.3	71.7	56.6	51.6	47.4	77.1	54.6	28.5	89.1
		2	85.6	64.0	48.2	42.7	38.3	30.5	21.0	25.1	63.2
		4	80.6	57.1	43.9	31.3	21.1	14.6	19.3	26.4	40.9
		6	74.2	53.3	37.6	27.4	21.0	22.9	24.7	26.7	27.9
8		68.2	49.1	38.4	32.1	27.7	14.3	27.1	40.0	28.5	
10		63.4	47.3	37.7	32.8	36.9	34.8	32.2	62.0	26.8	
20		56.9	47.8	45.8	43.8	24.6	17.3	63.4	24.4	28.7	
30		55.6	48.2	46.5	33.0	27.2	86.7	21.4	26.8	25.2	
40		56.3	47.7	36.1	22.8	58.4	17.3	21.1	48.0	25.3	
50		55.8	45.9	30.7	66.8	19.8	34.8	25.9	52.5	25.8	
60		61.2	45.8	58.7	25.6	37.0	77.1	35.0	32.7	26.1	
70		66.4	70.0	33.8	38.0	22.6	34.8	29.5	29.3	30.3	
80		81.6	55.9	40.2	26.0	25.4	17.3	24.0	24.5	27.9	
90		81.1	80.4	79.8	82.2	85.0	86.7	87.8	88.3	88.5	
-15°		0	66.3	34.9	21.5	14.8	14.4	14.8	25.1	21.9	32.0
		2	61.8	33.9	19.8	13.1	10.6	12.8	22.4	21.7	30.2
		4	57.8	33.8	19.9	12.6	10.1	12.7	18.7	22.4	30.3
		6	53.8	34.2	19.7	12.9	11.1	13.3	15.5	22.7	29.8
	8	53.3	35.0	19.7	12.7	11.4	14.0	13.5	22.2	29.6	
	10	53.5	37.5	20.0	11.9	12.3	16.8	12.4	20.7	28.5	

This is an equiangular Wye with its line of symmetry rotated  $4^\circ - 8^\circ$  from the N-S line.

It is interesting to consider the effects of a small amount of rotation of the array. Fig. 6-4 gives the percentage of holes as a function of declination for two arrays -- a supplemented Wye of 42 elements with a line of symmetry N-S, and a supplemented Wye with 42 elements rotated  $5^\circ$  away from N-S. In each case the array used an hour angle tracking range of  $\pm 4$  hours and had arm lengths of 2,400 m.

Rotation of the array has drastically reduced the percentage of holes for declination  $0^\circ$ . The effect of the rotation is to give a much larger range in instantaneous N-S baselines, thus breaking up the heavy redundancies and improving the sampling. For the N-S array 80% of the cells sampled have more than ten minutes of integration, while for the rotated array only 47% of the cells sampled have that much redundancy.

There are two subsidiary maxima in the number of holes for the array with rotation. This is a "resonance" which occurs when the minor axes of the elliptical tracks in the transfer function are a size comparable with the spacing between antennas; then, because the elements are uniformly spaced in the outer parts of the arm, the tracks will overlap, much as they do for a N-S Wye at declination  $0^\circ$ . The declination at which these secondary maxima occur is a function of the element spacing. In view of the improved performance of the rotated array both at  $\delta = 0^\circ$  and for  $|\delta| > 5^\circ$ , these small increases are acceptable.

After the entire array has been rotated, further movement of the individual arms has little effect. A test was made in which each of the three arms was moved  $\pm 15^\circ$  away from its position in an equiangular Wye. The test array was a 42-element supplemented Wye, having arm length of 2,200 m and  $\pm 4$  hours of track, with the line of symmetry rotated  $5^\circ$  from N-S. The percentages of holes at two declinations are given in Table 6-3. It should be noted that the percentages for the equiangular Wye (angle of rotation  $0^\circ$ ) differ slightly from those found in other tables in this chapter, since the computation was done with an early version of the program. The relative percentages within the table are accurate.

The data show that further rotation of the north arm has almost no effect, even if it is brought back to the N-S line. Rotation of the array serves mainly to break up the redundancies between the two south arms.

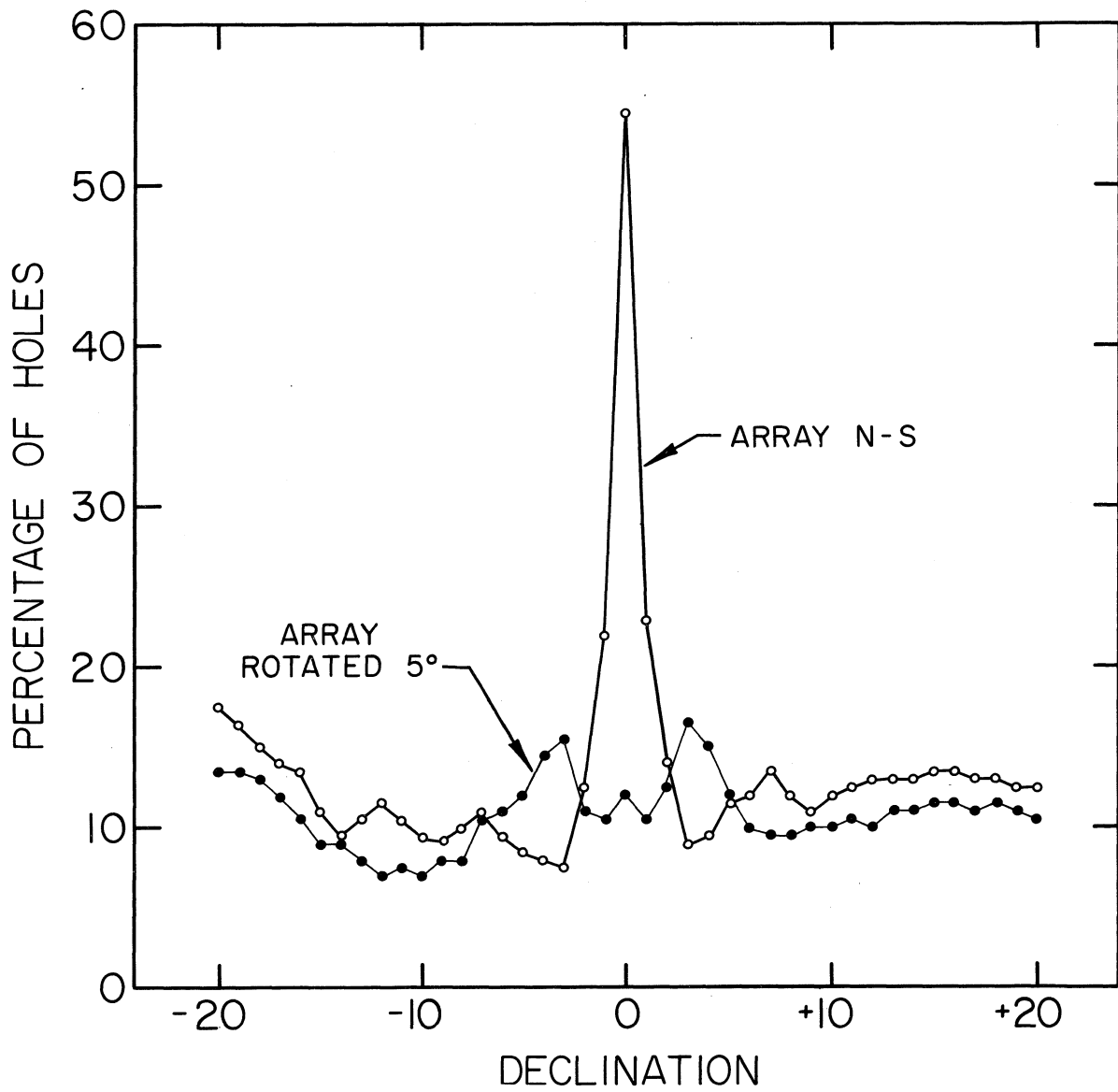


Figure 6 - 4. The effect of array rotation on the percentage of holes.

Table 6-3

Percentage of Holes when One Arm of an Array is Rotated

Arm Rotated	Declination	Angle of Rotation Relative to Equiangular Configuration						
		-15°	-10°	- 5°	0°	+ 5°	+10°	+15°
Southwest	+ 30°	6.6	6.4	6.7	7.4	7.4	8.4	9.0
	0°	14.5	18.3	17.2	12.0	23.2	30.8	21.9
North	+ 30°	6.8	7.1	7.3	7.4	6.9	6.7	6.7
	0°	13.0	12.3	12.3	12.0	12.6	13.3	13.3
Southeast	+ 30°	6.7	6.0	6.4	7.4	7.9	7.9	8.6
	0°	20.3	24.5	20.9	12.0	20.0	13.9	18.1

The slight improvement for  $\delta = + 30^\circ$  which might be obtained by a small amount of rotation of one of the arms is more than offset by the poor performance for  $\delta = 0^\circ$ . The conclusion is that the equiangular Wye is the best.

On the basis of the preceding studies, it is recommended that the array for the VLA shall be an equiangular Wye, with the line of symmetry rotated approximately  $4^\circ$  off the N-S line.

## 2. The distribution of elements along the arms

All efforts to adapt the optimum one-dimensional distribution of elements to the present array have failed. Since two-thirds of the correlations result from inter-arm pairs, any distribution of the elements which requires large separations, as is the case in the one-dimensional array of Leech, produces large regions in the transfer function which are unsampled. Accordingly, the starting point for the study of the distribution of elements was the uniform Wye.

Of the configurations that were tried, only five are worth describing in detail. For all of these, the arm length was 2,400 m; the hour angle,  $\pm 4$  hours; and the array rotation,  $4^\circ$  off N-S. The percentage of holes achieved by each array is given in Table 6-4, and the outstanding features in the transfer functions are as follows:

(a) The uniform 43-element Wye. This array has the best performance near the celestial equator, at least as far as the percentage of holes is

concerned. The chief disadvantage is that there are many holes near the origin, as is shown in the transfer function for  $\delta = +30^\circ$  (Fig. 6-5(a)) and for  $\delta = 0^\circ$  (Fig. 6-5(b)).

Fig. 6-6 shows sections through the power radiation pattern of this array, for  $\delta = +30^\circ$ . The pattern has been computed from the transfer function of Fig. 6-5(a), with uniform weighting in  $u$  and  $v$ , but with a Gaussian taper of 15 db superimposed on the whole transfer function. No corrections for the effect of bandwidth have been made in this or any of the other patterns shown. The sections are made in declination, and extend over  $20'$ , centered on the beam. The separation of the sections is  $4.7'$  in right ascension; the section through the beam center is marked in the figure. The vertical scale is linear in power; a level of 0.050 of the main beam is denoted by the vertical bar.

The most prominent feature of this power pattern is the large negative side-lobe surrounding the main beam. The side-lobe reaches a peak of 8% of the main beam. This is a direct consequence of the large number of holes near the origin. In addition, there are numerous side-lobes of between 3 and 5%, caused by the string of holes stretching from the origin towards the upper right.

(b) The 43-element Wye with tapered spacings. In order to break up the redundancies produced by the uniform spacing and to fill in the central regions of the transfer function, the spacings along the arm should be a function of distance from the center. Let the elements along an arm be numbered outwards from the array center. Then, the distance of the  $n^{\text{th}}$  element from the center is given by  $sn^k$ , where  $s$  is a constant chosen to give the desired arm length and  $k$  is the tapering power. A value  $k = 1.0$  corresponds to the uniform Wye. The performance of this configuration is given in Table 6-4, for a number of values of  $k$ . It is much better than the uniform Wye for northern declinations. In particular, the chain of holes stretching to the upper right in the transfer function of the uniform Wye (Fig. 6-5(a)) has been completely removed for a value  $k = 1.3$  (Fig. 6-7(a)). The holes are more numerous at  $\delta = 0^\circ$ , as is shown in Fig. 6-7(b), the transfer function for  $k = 1.3$ .

The tapered array with  $k = 1.3$ , for  $\delta = +30^\circ$ , has the power pattern given in Fig. 6-8. The pattern is excellent, with no side-lobes greater than 1% anywhere in the field of view. The pattern for  $\delta = 0^\circ$  is much poorer.

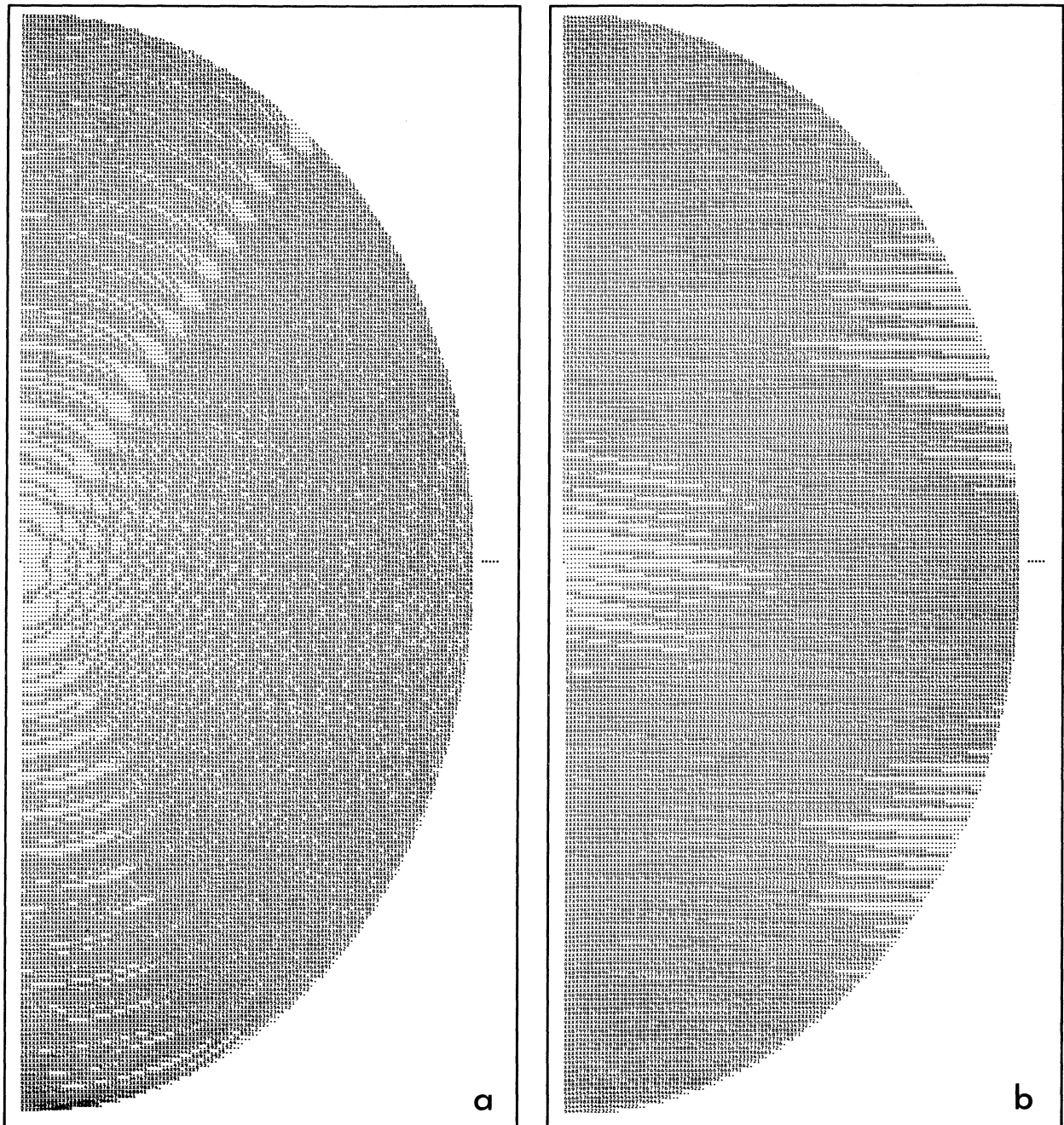


Figure 6 - 5. The transfer function of a 43 element wye  
(a)  $\delta = +30^\circ$  (b)  $\delta = 0^\circ$ .

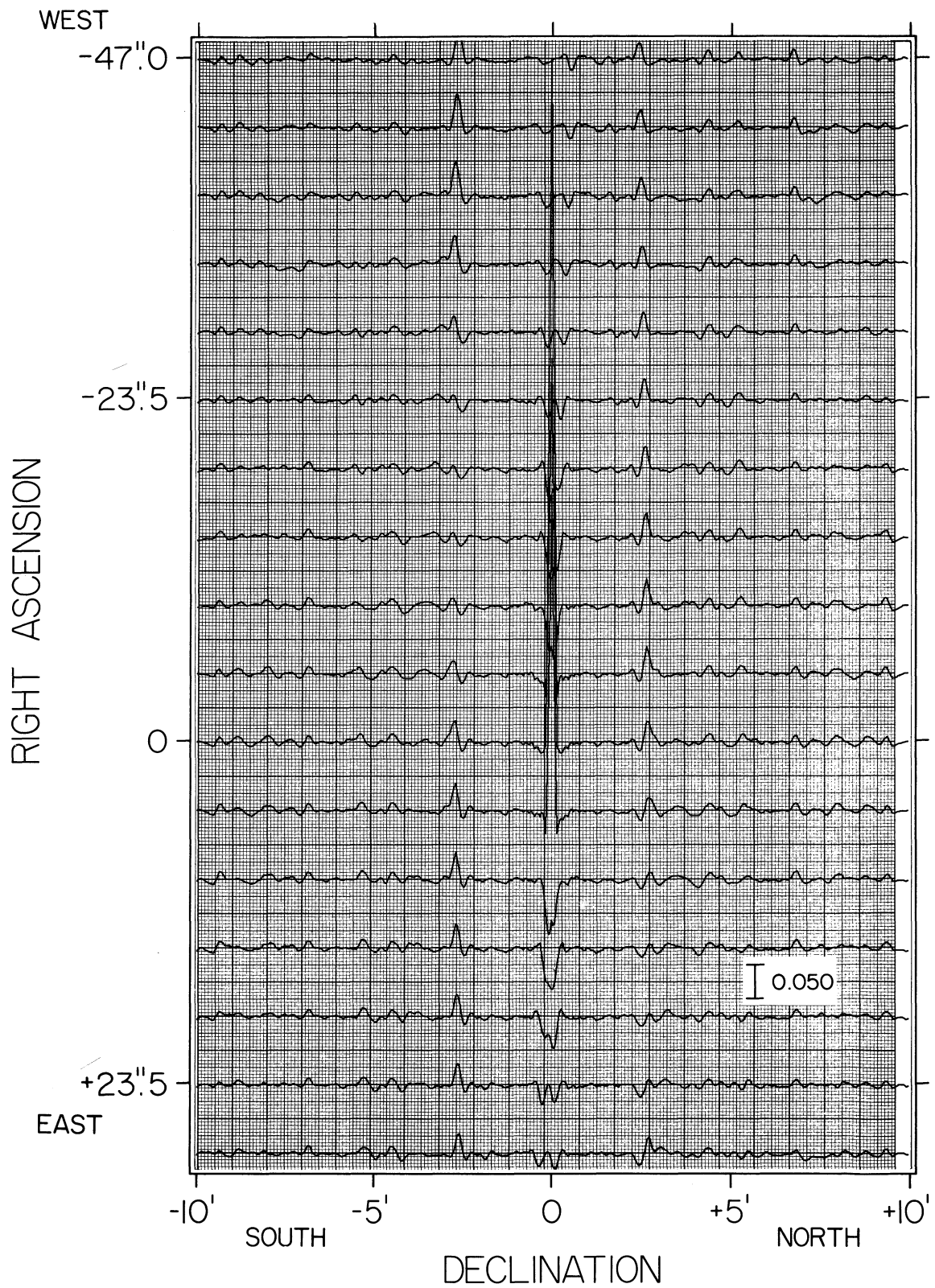


Figure 6 - 6. The power pattern corresponding to the transfer function Figure 6 - 5 (a).

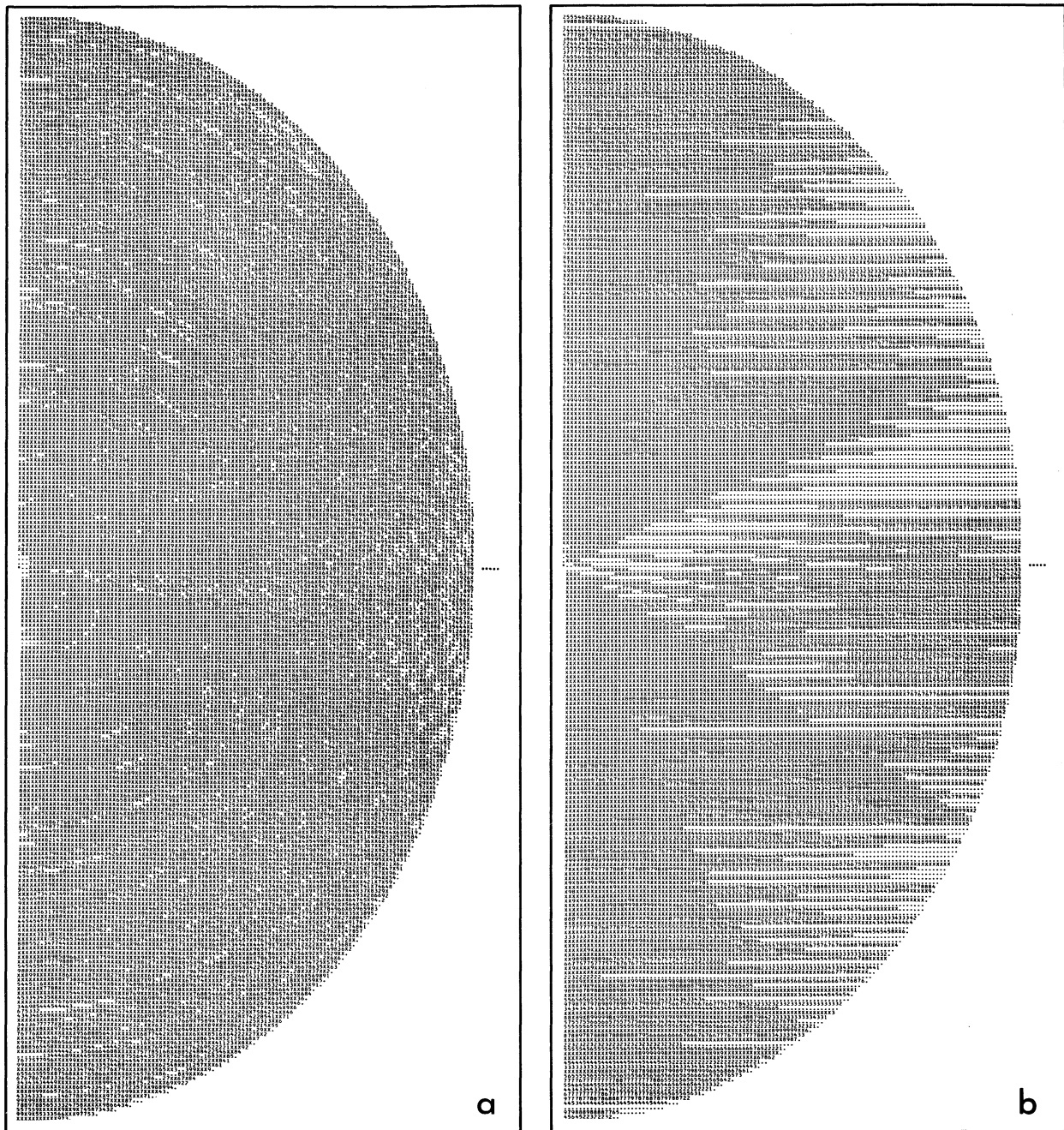


Figure 6 - 7. The transfer function of a 43 element (tapered) wye (a)  $\delta = +30^\circ$  (b)  $\delta = 0^\circ$ .

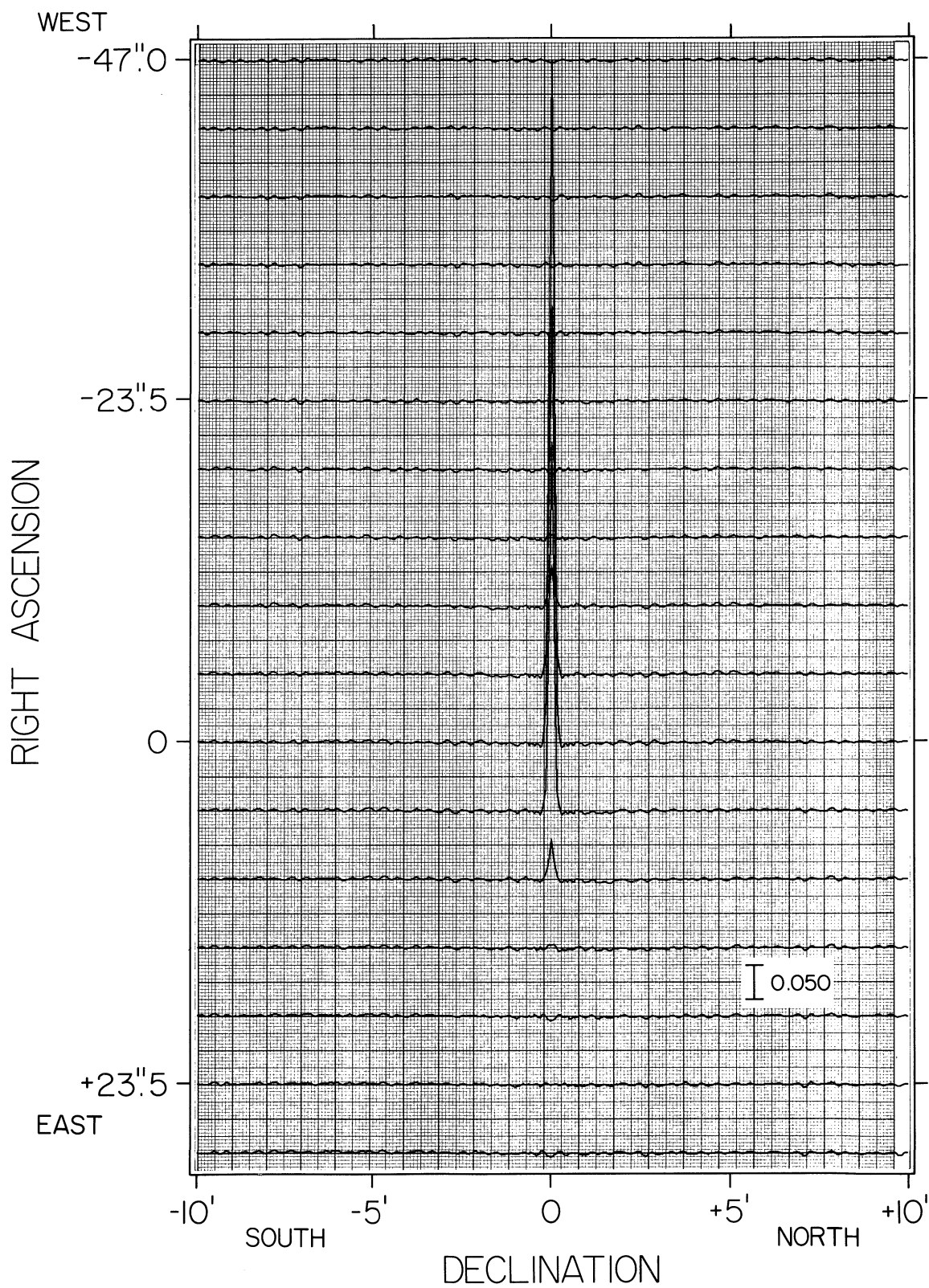


Figure 6 - 8. The power pattern corresponding to the transfer function Figure 6 - 7 (a).

(c) The 42-element supplemented Wye. The distribution of elements in this array is shown in Fig. 6-3(b). It represents an attempt to get more short baselines than are present in the uniform Wye, in order to fill the central portion of the transfer function. The transfer function at  $\delta = +30^\circ$  (Fig. 6-9(a)) does indeed have fewer holes near the center, but the chain of holes stretching towards the upper right is still prominent. The transfer function at  $\delta = 0^\circ$  (Fig. 6-9(b)) continues to show horizontal strings of holes.

The power patterns corresponding to the transfer functions of Fig. 6-9 are given in Fig. 6-10 and 6-11, for  $\delta = +30^\circ$  and  $\delta = 0^\circ$ , respectively. There is no negative side-lobe near the main beam in Fig. 6-10, because the central portion of the transfer function has been filled by the inner elements; there are still a few side-lobes of about 2.5%, produced mainly by the large groupings of holes in the upper right of the transfer function. The negative side-lobe at the center is present in Fig. 6-11, at a level of about 6%. In addition, there are numerous side-lobes to the north and south, produced by the strings of holes which are aligned parallel to the u-axis. This is a failing of all of the arrays described in this section and can be corrected only by the addition of more elements or by allowing a greater tracking range.

(d) The 42-element supplemented Wye with tapered spacings. The inner three elements on each arm are in the same position as in the supplemented Wye, but the outer elements are spaced according to the tapering power  $k$ . A sample transfer function of the array with  $k = 1.3$  is given in Fig. 6-12(a), for  $\delta = +30^\circ$  and Fig. 6-12(b), for  $\delta = 0^\circ$ . Again, the chain of holes present for northern declinations has been broken up, but the array has more holes near  $\delta = 0^\circ$ .

The power pattern of the array with  $k = 1.3$  and  $\delta = +30^\circ$  is shown in Fig. 6-13. It is quite similar to the pattern of the tapered 43-element Wye (Fig. 6-8). Again, the side-lobe levels are less than 1% anywhere in the field of view. The performance of this array at  $\delta = 0^\circ$  is poorer than that of the supplemented Wye with uniform spacings.

(e) The 42-element supplemented Wye with tapered spacings on the north arm only. For  $\delta = 0^\circ$  the sampling in the region of the u-axis is controlled by both the intra-arm and inter-arm correlations of the south

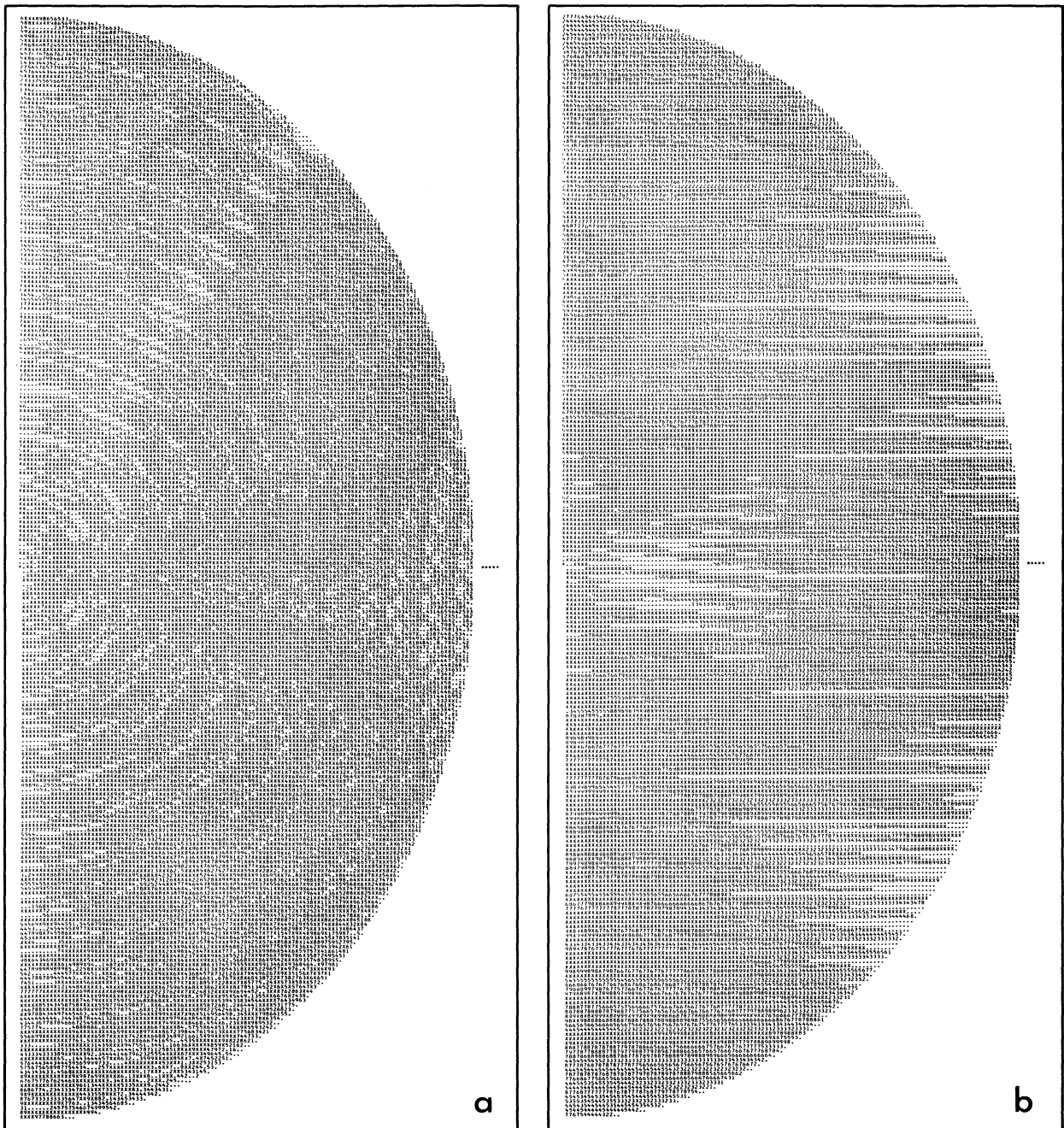


Figure 6 - 9. The transfer function of a 42 element supplemented wye (a)  $\delta = +30^\circ$  (b)  $\delta = 0^\circ$ .

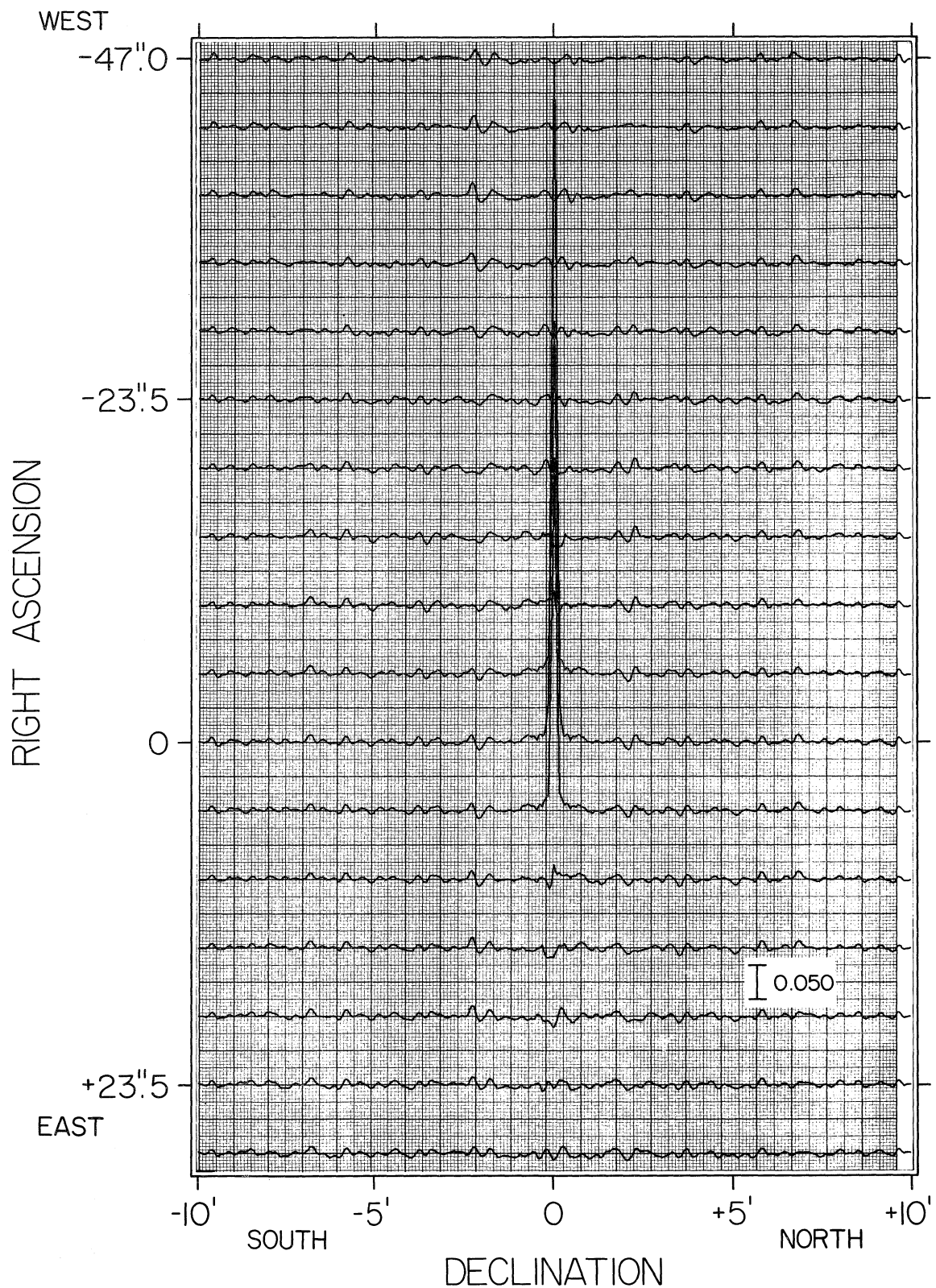


Figure 6 - 10. The power pattern corresponding to the transfer function Figure 6 - 9 (a).

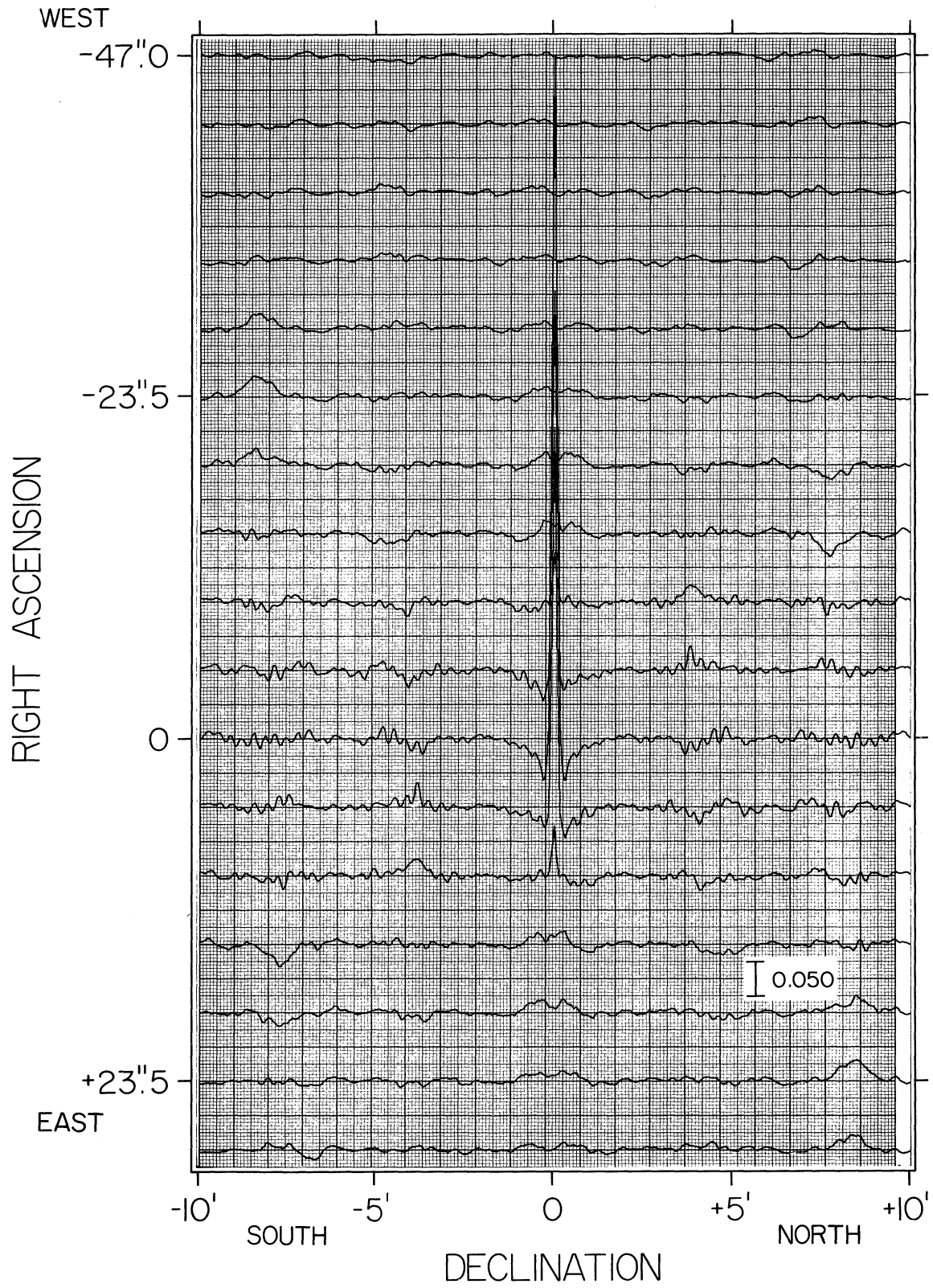


Figure 6 - 11. The power pattern corresponding to the transfer function Figure 6 - 9 (b).

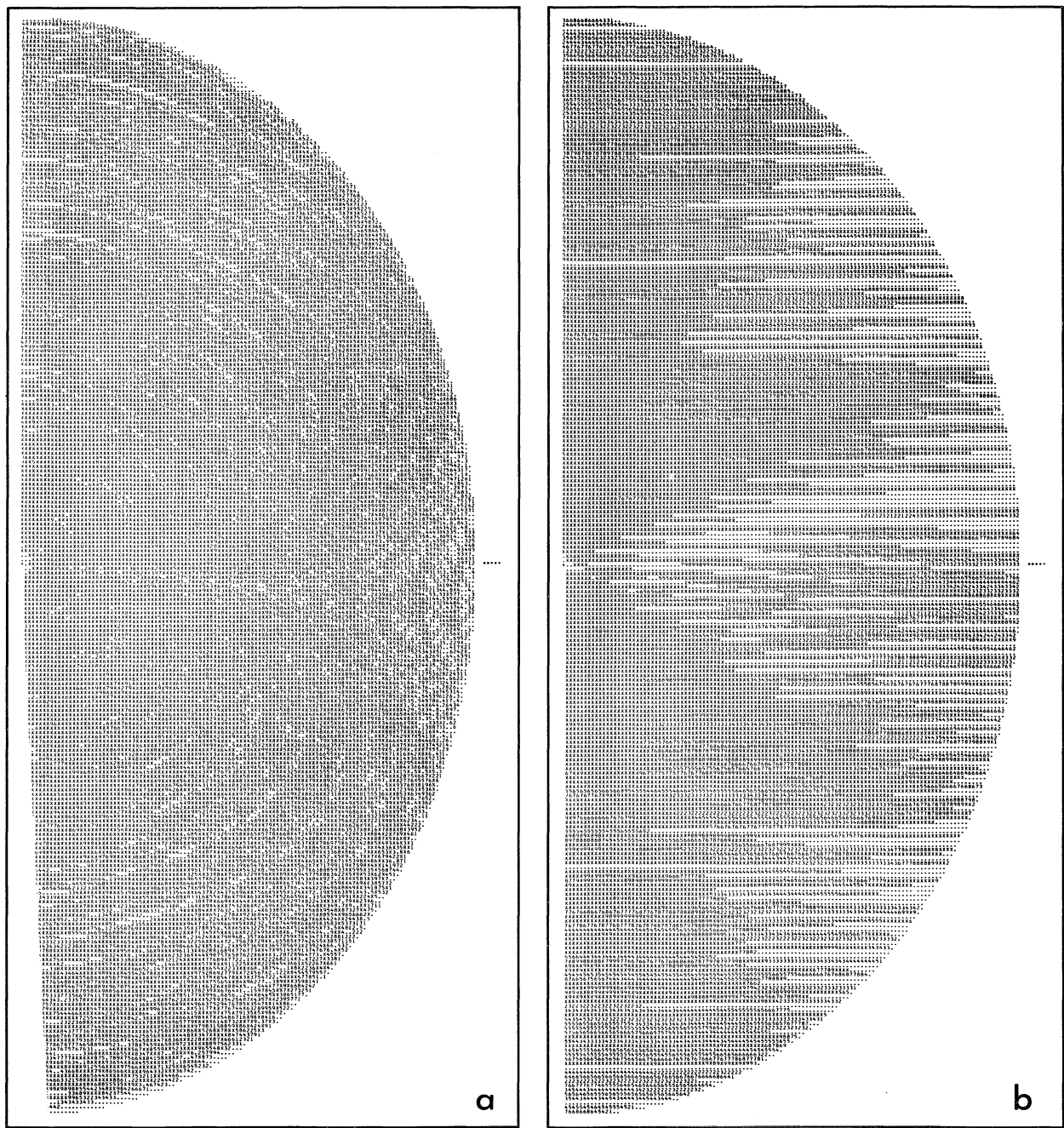


Figure 6 - 12. The transfer function of a 42 element (tapered) wye (a)  $\delta = +30^\circ$  (b)  $\delta = 0^\circ$ .

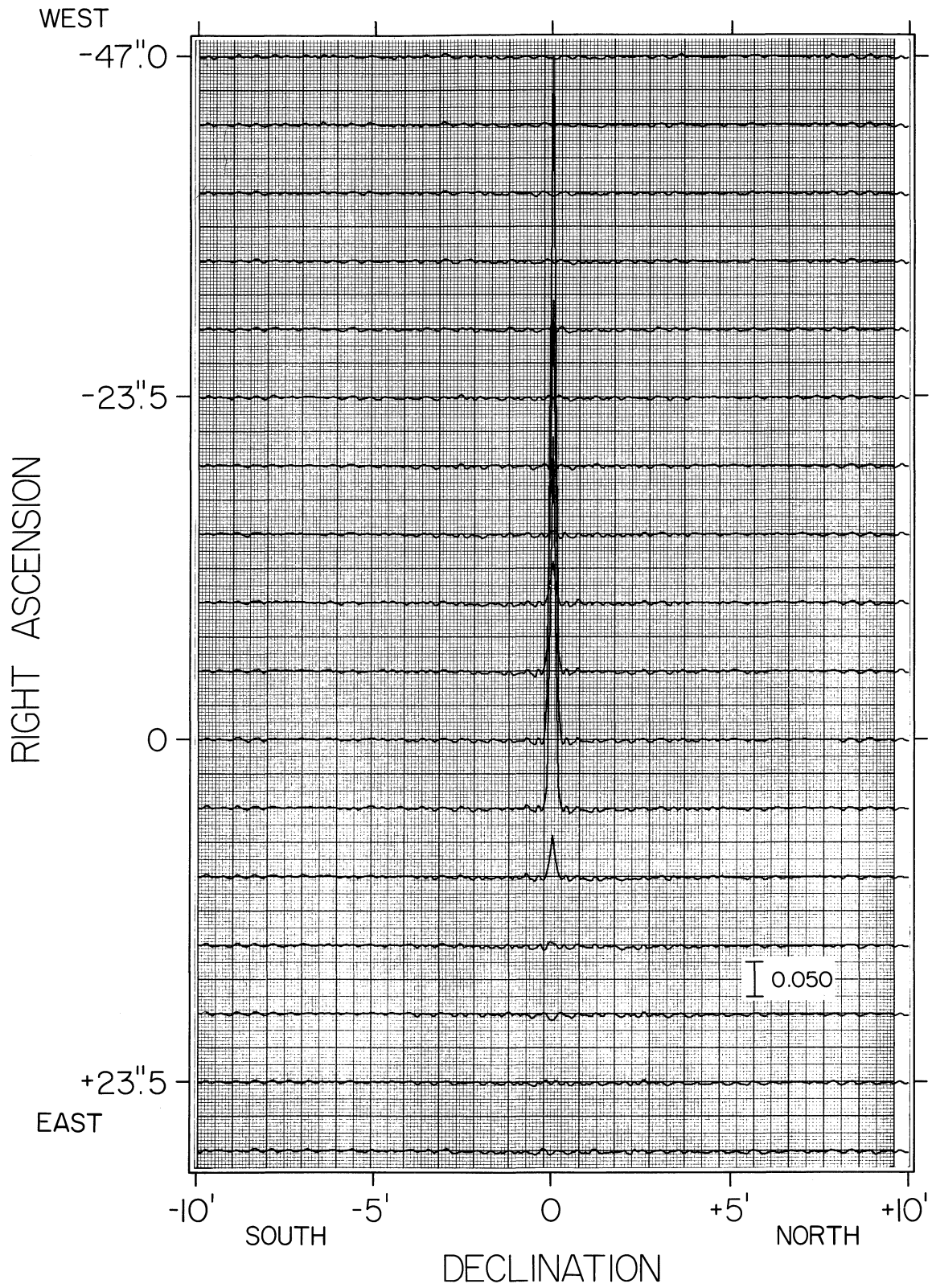


Figure 6 - 13. The power pattern corresponding to the transfer function Figure 6 - 12 (a).

arms. In contrast, the north arm is important in the region  $v = v_{\max}$ ,  $u = \frac{1}{3} u_{\max}$ . It seemed reasonable, therefore, to let the element spacing for the south arms be that of the supplemented Wye, and to taper the spacings of the north arm. The results are not too surprising, as is seen in Table 6-4; the percentages of holes are intermediate to those of the supplemented Wye and the supplemented Wye with tapering.

Table 6-4

## Percentages of Holes for Various Array Configurations

Number of Elements	Length of Arm (meters)	Array Model		Hour Angle Range $\pm 4h$	
				$\delta = +30^\circ$	$\delta = 0^\circ$
43	2400	Uniform Wye	k=1.0	12.44	8.51
43	2400	Wye with Taper	k=1.1	3.67	13.34
43	2400	Wye with Taper	k=1.3	3.05	17.60
43	2400	Wye with Taper	k=1.5	4.63	18.10
43	2400	Wye with Taper	k=2.0	6.29	23.21
42	2400	Supplemented Wye	k=1.0	8.17	9.87
42	2400	Supp. Wye with Taper	k=1.1	5.73	16.67
42	2400	Supp. Wye with Taper	k=1.3	5.40	20.04
42	2400	Supp. Wye with Taper	k=1.5	5.61	22.45
42	2400	Supp. Wye with Taper	k=2.0	7.95	25.61
42	2400	Supp. Wye, N Arm Tapered	k=1.1	7.23	13.15
42	2400	Supp. Wye, N Arm Tapered	k=1.3	6.28	12.55
42	2400	Supp. Wye, N Arm Tapered	k=1.5	5.97	13.44
42	2400	Supp. Wye, N Arm Tapered	k=2.0	6.39	14.33

Of all configurations tested, the best is the supplemented Wye (Figs. 6-9 to 6-11), since it has reasonably good patterns for both  $\delta = 0^\circ$  and  $\delta = +30^\circ$ . It is this configuration that is recommended for the VLA.

Studies of the array configuration will be continued. The percentage of holes is at this stage not a sufficiently sensitive criterion, and the actual power patterns will have to be computed for each proposed configuration. It does not seem likely, however, that an array can be found whose performance is so much better than that of a supplemented Wye that a significant number of elements can be saved. Therefore, although the supplemented Wye may not have the optimum distribution of elements, it will provide a good estimate of the number of elements required.

### 3. The optimum arm length

This array parameter has been treated last, because it is slightly dependent upon the distribution of elements along the arm. Since the best length is also a function of the declination and hour angle tracking range, optimization required an extensive amount of computation, the results of which are summarized in Table 6-5. The array configuration is the one recommended for the VLA -- a supplemented Wye, with equal angles between the arms, rotated  $4^\circ$  off north-south.

The best arm length, judged solely on the percentages of holes obtained at the three declinations, is about 2400 m. However, this value is strongly influenced by the percentage of holes at  $\delta = -15^\circ$ , where the effects of foreshortening are important; most of the holes at this declination are at the edge of the transfer function, and their effect is merely to broaden the synthesized beam, rather than to produce random side-lobes. On the other hand, the performance of the array for northern declinations is degraded if the arms are too long, since in this case many of the correlators sample outside the desired transfer function. More detailed studies based on a few power patterns show that a good compromise is an arm length of 2100 m. The array then has low side-lobe levels at  $+30^\circ$  and  $-15^\circ$ , yet the north-south beam width at  $\delta = -15^\circ$  has been increased by only 15%.

Since the north-south length of the array is set primarily by the north arm, it appeared that some gain in performance might be achieved by making the north arm longer than the south arms. This should keep most of the baselines within the transfer function for  $\delta = +30^\circ$ , while providing a long enough dimension north-south to compensate for the projection effects at  $\delta = -15^\circ$ .

The results of this test, made with a 39-element supplemented Wye, and  $\pm 4$  hours tracking range, are disappointing. As Table 6-6 shows, the performance of the array cannot be improved by making the north arm of a length different from that of the south arms.

It is recommended that the VLA have arms of equal length. The length should be 2100 m for the 10" arrays described above, corresponding to 21 km for the VLA when used at its maximum resolution of 1".

Table 6-5

Percentage of Holes for a Number of Supplemented Wyes

Number of Elements	Declination	Range in Hour Angle (hours)	Arm Length (meters)			
			2000	2200	2400	2600
33	+ 30°	± 2	46.1	47.8	51.3	54.9
		± 4	18.0	18.5	20.2	22.8
		± 6	9.1	8.0	7.7	8.0
	0°	± 2	55.9	56.7	58.3	60.0
		± 4	28.7	27.5	26.5	26.2
		± 6	23.3	20.9	17.8	15.7
	- 15°	± 2	50.3	47.9	47.4	47.8
		± 4	28.8	23.1	19.8	18.4
		± 5.5	22.7	16.6	12.3	9.7
36	+ 30°	± 2	40.3	42.4	45.5	49.8
		± 4	13.7	14.0	14.9	18.0
		± 6	6.8	5.7	4.9	5.7
	0°	± 2	49.2	49.7	51.3	54.5
		± 4	22.7	20.1	20.0	21.3
		± 6	19.7	15.8	13.6	13.7
	- 15°	± 2	45.4	42.8	41.9	42.5
		± 4	24.9	19.2	15.3	13.9
		± 5.5	20.3	14.0	9.8	7.2
39	+ 30°	± 2	34.3	36.5	40.1	44.8
		± 4	9.6	10.1	11.3	13.6
		± 6	4.6	3.7	3.4	3.8
	0°	± 2	43.1	42.9	44.6	48.2
		± 4	17.7	14.9	14.3	15.2
		± 6	15.9	12.4	10.1	9.1
	- 15°	± 2	40.9	40.0	36.8	37.2
		± 4	22.1	15.6	11.8	10.0
		± 5.5	18.2	12.0	7.6	5.0
42	+ 30°	± 2	28.7	31.1	35.1	39.7
		± 4	6.4	7.0	8.2	10.3
		± 6	3.0	2.4	2.2	2.2
	0°	± 2	38.7	37.1	38.6	41.9
		± 4	15.1	11.0	9.9	10.4
		± 6	13.4	9.5	7.3	6.2
	- 15°	± 2	36.9	33.5	32.2	32.5
		± 4	19.7	13.3	8.8	7.0
		± 5.5	16.4	10.2	6.0	3.5
45	+ 30°	± 2		26.2	30.2	35.0
		± 4		4.7	5.9	7.4
		± 6		1.6	1.4	1.5
	0°	± 2		32.8	33.5	36.2
		± 4		8.8	6.5	6.5
		± 6		7.7	4.9	3.8
	- 15°	± 2		29.8	28.0	28.2
		± 4		11.1	7.0	4.9
		± 5.5		8.7	4.8	2.5

Table 6-6

Percentage of Holes as a Function of the Length of the North Arm

Length of Oblique Arms	Declination	Length of North Arm (meters)					
		1800	2000	2200	2400	2600	2800
1800	+ 30°	10.60	10.67	10.57	10.67	10.91	
	0°	25.28	25.45	24.04	24.03	23.16	
	- 15°	30.24	29.58	29.09	28.91	28.38	
2000	+ 30°		9.58	9.87	10.05	10.21	10.59
	0°		17.72	17.88	17.85	17.32	17.52
	- 15°		22.14	21.70	21.23	20.82	20.48
2200	+ 30°		9.98	10.13	10.34	10.86	10.95
	0°		15.88	14.91	14.76	15.47	15.55
	- 15°		16.46	15.62	15.29	14.98	14.51
2400	+ 30°		11.81	11.01	11.31	11.49	12.10
	0°		15.08	14.66	14.33	15.45	14.77
	- 15°		12.40	12.06	11.82	11.23	11.07

#### E. The Recommended Configuration

The last step is to determine the number of elements that are required. The percentages of holes for the arrays with arm length 2100 m have been computed and are plotted in Fig. 6-14. It is clear that for all arrays the range in hour angle should be at least  $\pm 4$  hours and that a large reduction in the percentage of holes can be obtained for arrays with fewer than 40 elements by tracking from horizon to horizon.

The percentage of holes as a function of number of elements, for various declinations and hour angle ranges, is given in Fig. 6-15. Recalling that the array should have a maximum distant side-lobe level of - 20 db or less, corresponding roughly to 15% holes, it is obvious that 30 elements are not enough and that the 33 elements cannot meet the requirements, even if the full 12-hour tracking range is used. In contrast, the arrays with 45 and 42 elements are more powerful than are needed at the present time, since they can achieve the desired side-lobe levels with 8 hours of tracking or less. The decision thus rests between the arrays with 36 and 39 elements.

At this point it is necessary to consider the power radiation patterns of the two arrays for a number of declinations. In all cases the arrays

SUPPLEMENTED WYE, ARM LENGTH 2100 METERS

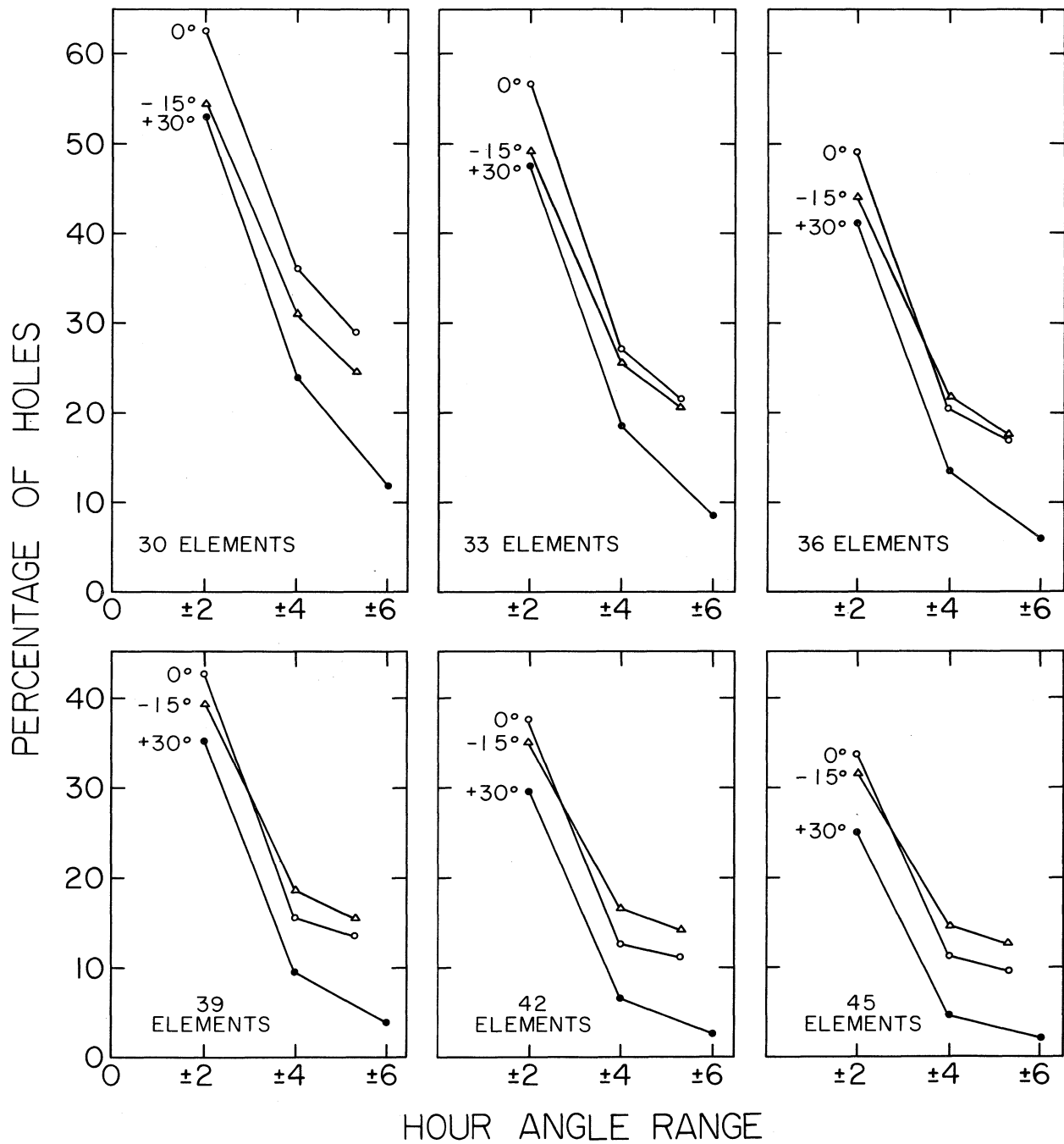


Figure 6 - 14. Variation of the percentage of holes in the transfer function with number of elements and tracking range.

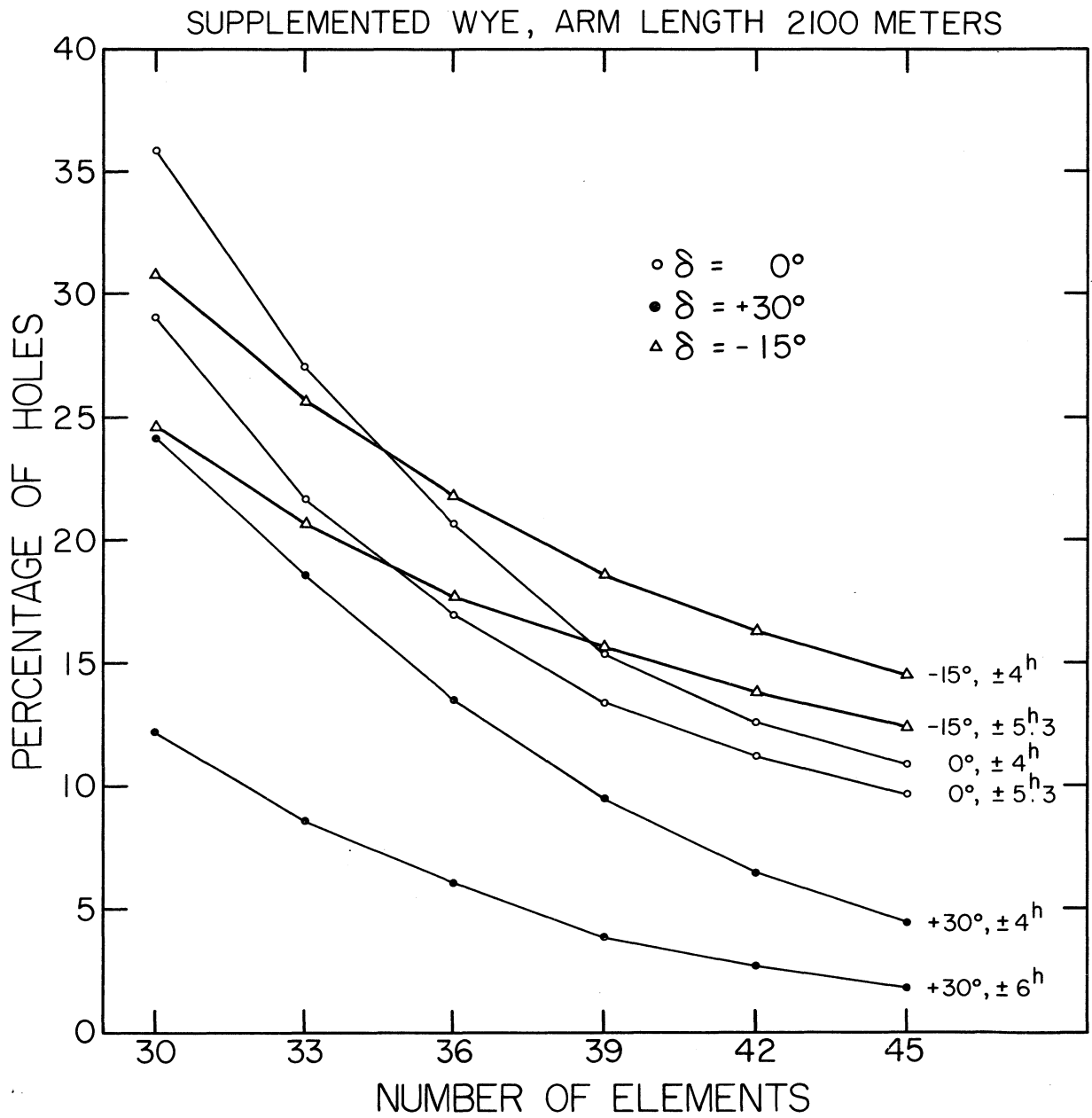


Figure 6 - 15. Variation of the percentage of holes in the transfer function with number of elements and tracking range.

have equal arms 2100 m long. The power patterns of the 39-element array are given in Figs. 6-16 to 6-18, as follows: Fig. 6-16,  $\delta = + 30^\circ$ , tracking  $\pm 4$  hours; Fig. 6-17,  $\delta = 0^\circ$ , tracking  $\pm 4$  hours; and Fig. 6-18,  $\delta = - 15^\circ$ , tracking  $\pm 4$  hours. The corresponding patterns for 36 elements are as follows: Fig. 6-19,  $\delta = + 30^\circ$ , tracking  $\pm 4$  hours; Fig. 6-20,  $\delta = 0^\circ$ , tracking  $\pm 4$  hours; and Fig. 6-21,  $\delta = - 15^\circ$ , tracking  $\pm 4$  hours. In addition, the power patterns for the 36-element array at  $\delta = 0^\circ$ , tracking  $\pm 5.3$  hours, and  $\delta = + 30^\circ$ , tracking  $\pm 6$  hours, are shown in Fig. 6-22 and 6-23, respectively.

As expected, the 39-element array has fewer large side-lobes and a lower mean side-lobe level than the 36-element array. However, the improvement is not great. The mean level is between 0.5 db and 1 db lower for the 39-element array, while the peak side-lobe is often about 2 db lower. More details of the side-lobe levels predicted for these arrays are given in Table 6-7.

The 36-element array does achieve the desired performance at  $\delta = 0^\circ$  for a total observing time of 11 hours and is acceptable at  $\delta = + 30^\circ$  and  $\delta = - 15^\circ$  with just 8 hours of observation. For those programs where a low side-lobe level is particularly critical, the observer might wish to utilize the full 12-hour tracking range even at  $\delta = + 30^\circ$ ; in this case the array is outstanding, as is seen in Fig. 6-23. The mean side-lobe levels are - 26 to - 31 db, with the maximum side-lobe anywhere in the field of view less than - 20 db.

The fact that the full tracking range must be used in order to reduce side-lobes of the 36-element array to levels of - 20 db implies that arrays with fewer elements would require two different configurations and two days of observation to achieve a clean pencil beam. It is, therefore, recommended that the VLA have at least 36 elements.

It must be emphasized again that these results, although calculated specifically for the 10" configuration, apply equally well to the other configurations that the array will adopt. For example, Fig. 6-23 shows the power pattern of 3" configuration, for  $\delta = + 30^\circ$  and  $\pm 6$  hours range in hour angle. The sections are separated in right ascension by  $1^m4$  and cover a range in declination of  $6'$ . Similarly, Fig. 6-23 shows the power pattern of a 1" array ( $\delta = + 30^\circ$ ,  $\pm 6^h$ ). The sections are separated by

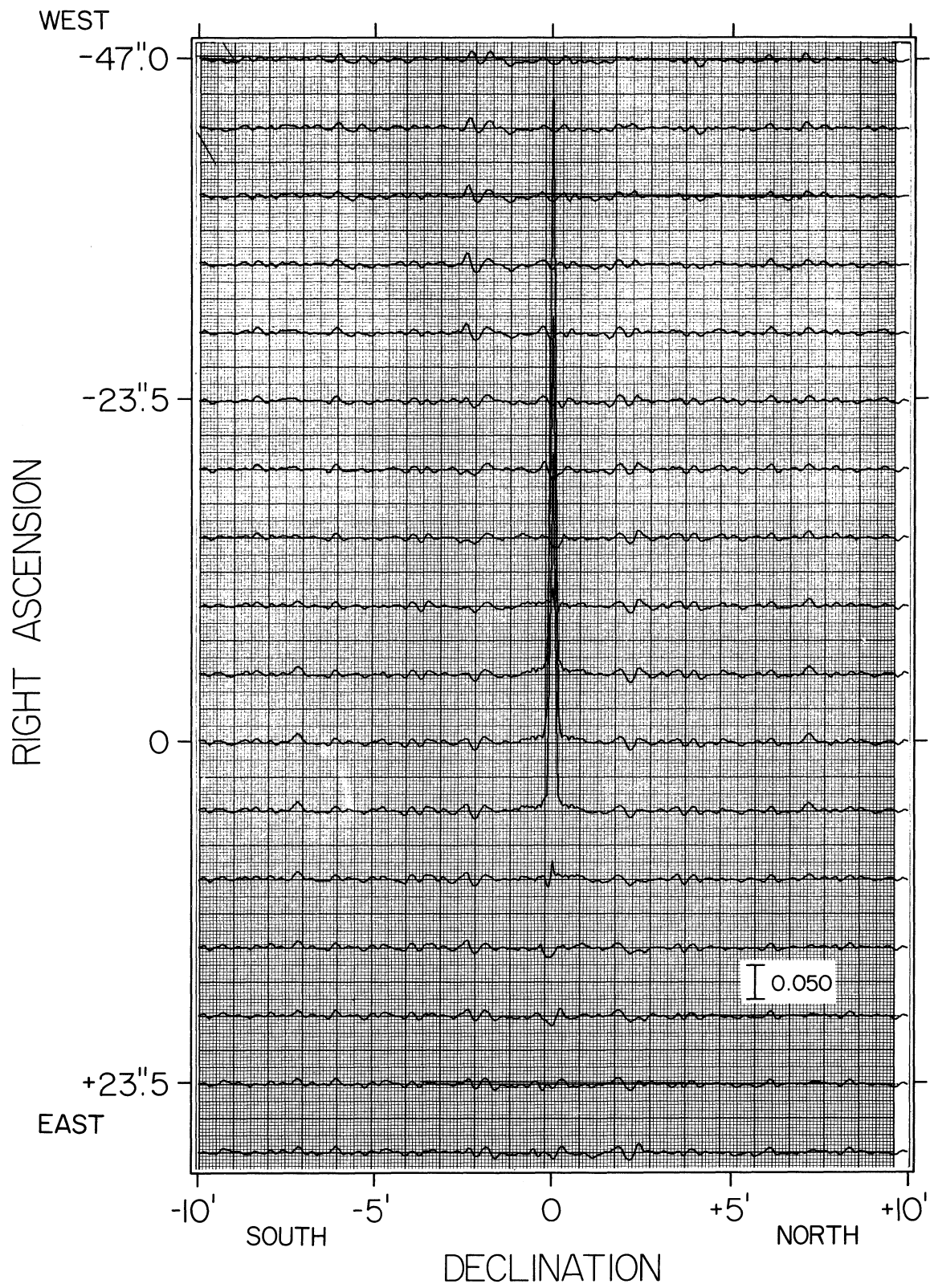


Figure 6 - 16. The power pattern of a 39 element wye for  $\delta = +30^\circ$  and  $H = \pm 4$  hours.

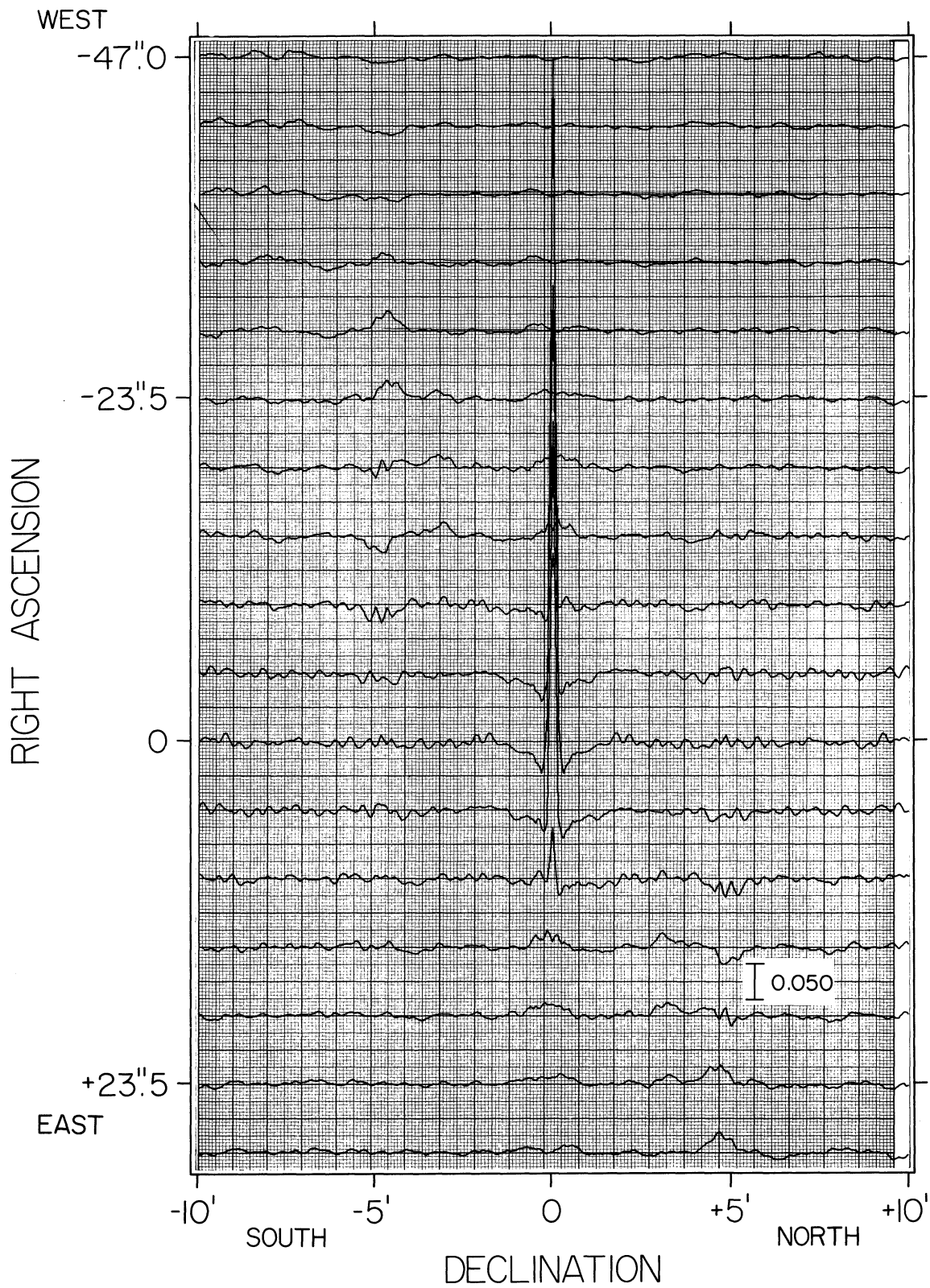


Figure 6 - 17. The power pattern of a 39 element wye for  $\delta=0^\circ$  and  $H=\pm 4$  hours.

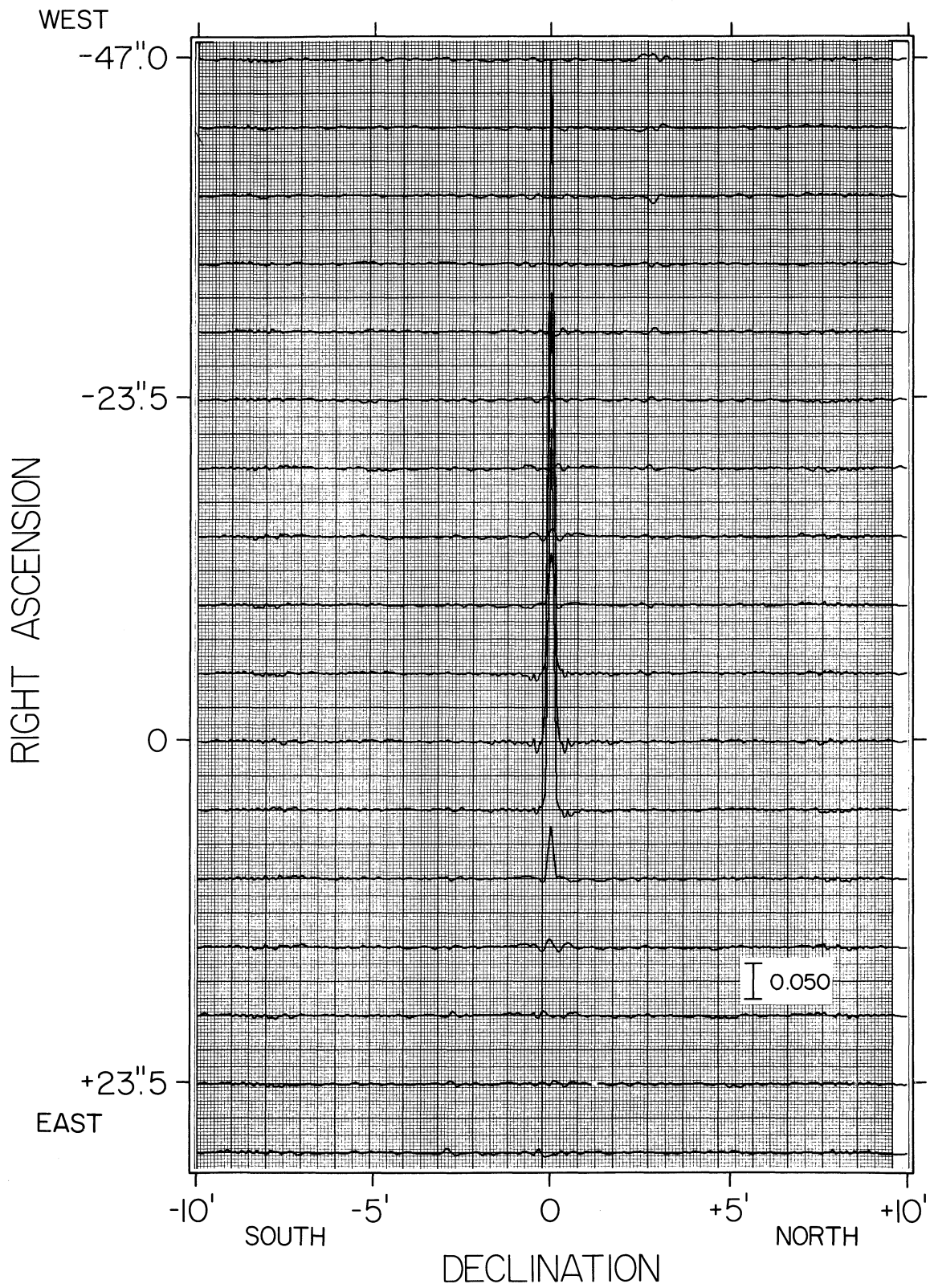


Figure 6 - 18. The power pattern of a 39 element wye for  $\delta = -15^\circ$  and  $H = \pm 4$  hours.

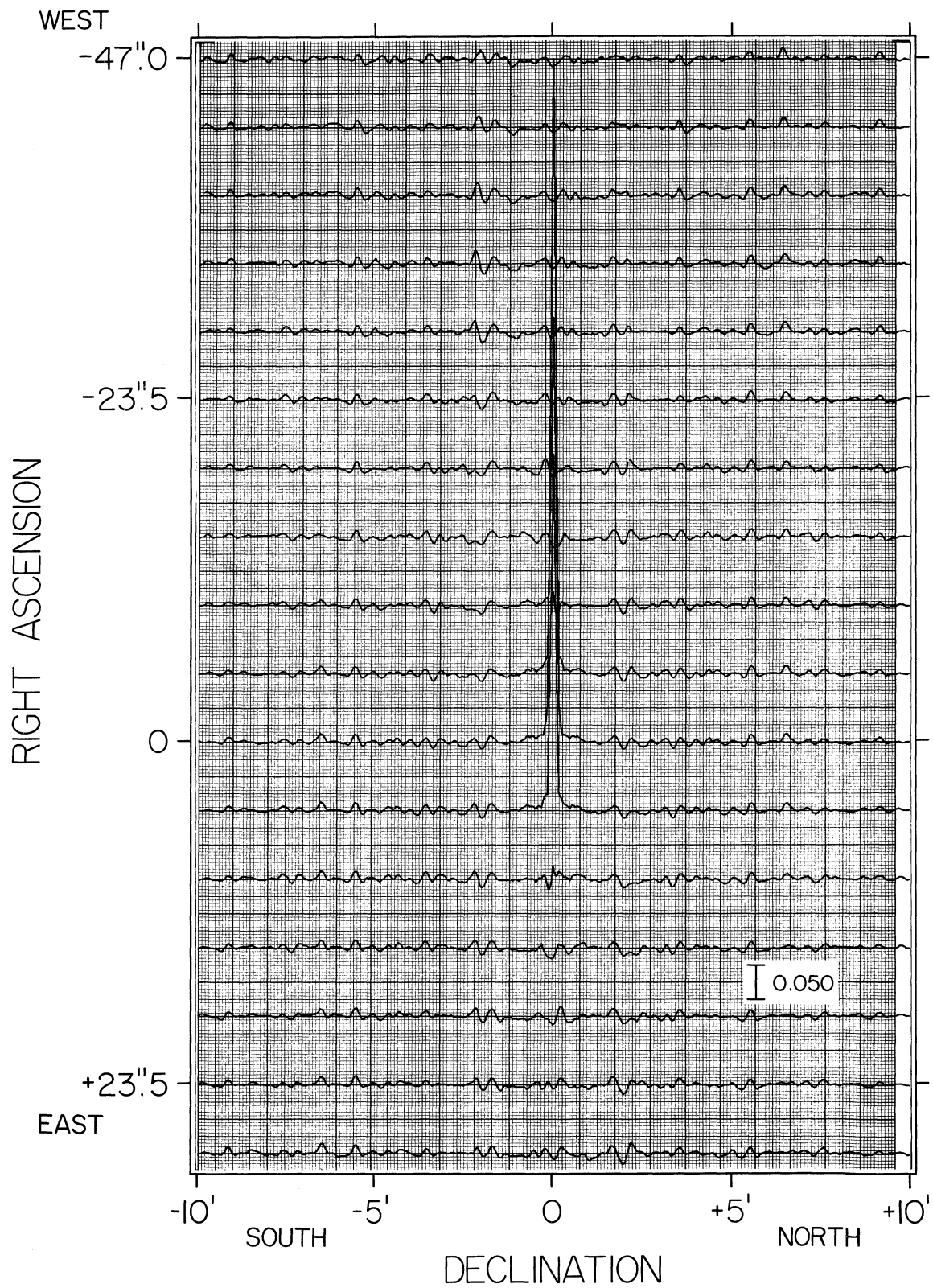


Figure 6 - 19. The power pattern of a 36 element wye for  $\delta = +30^\circ$  and  $H = \pm 4$  hours.

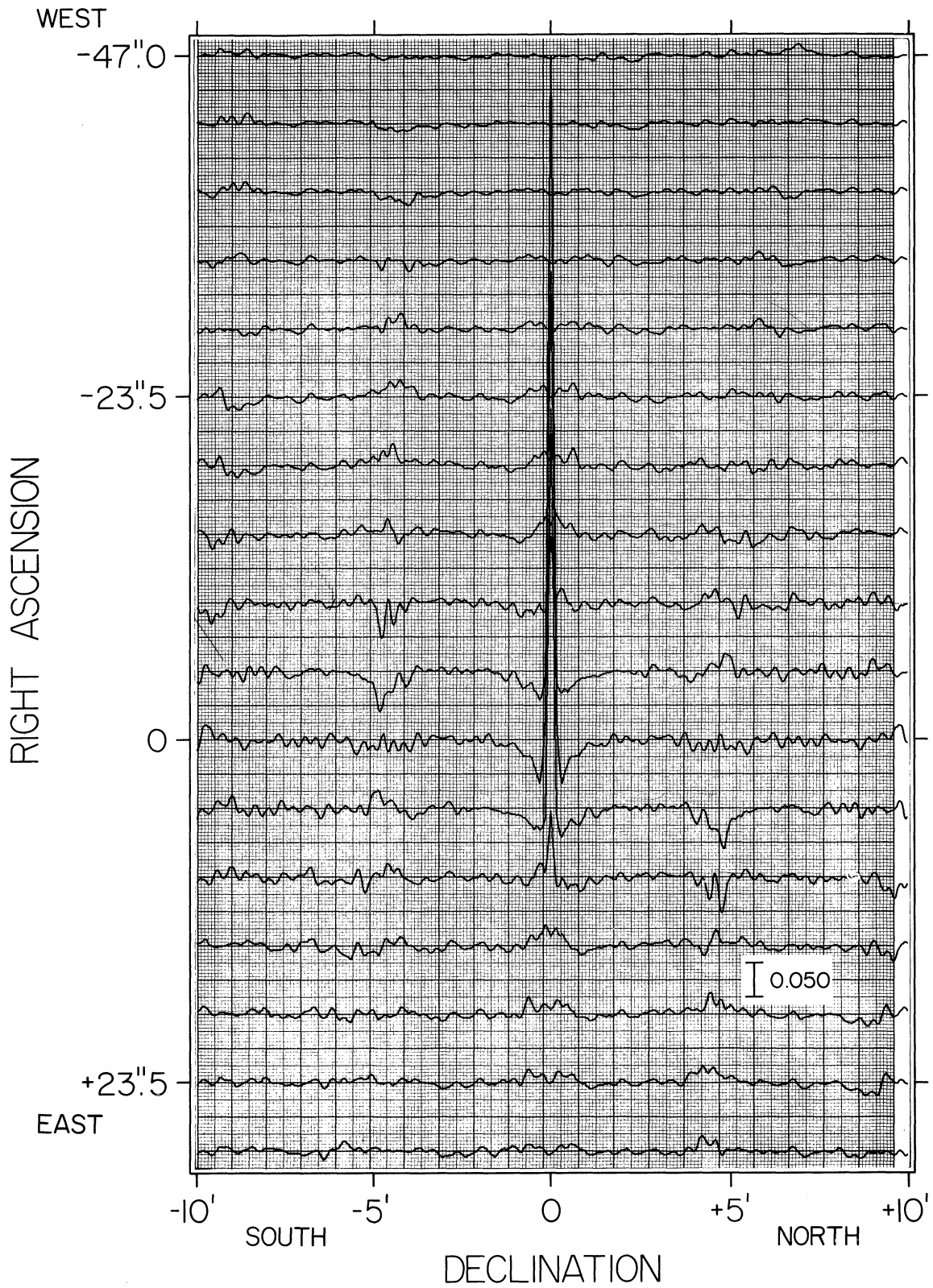


Figure 6 - 20. The power pattern of a 36 element wye for  $\delta=0^\circ$  and  $H=\pm 4$  hours.

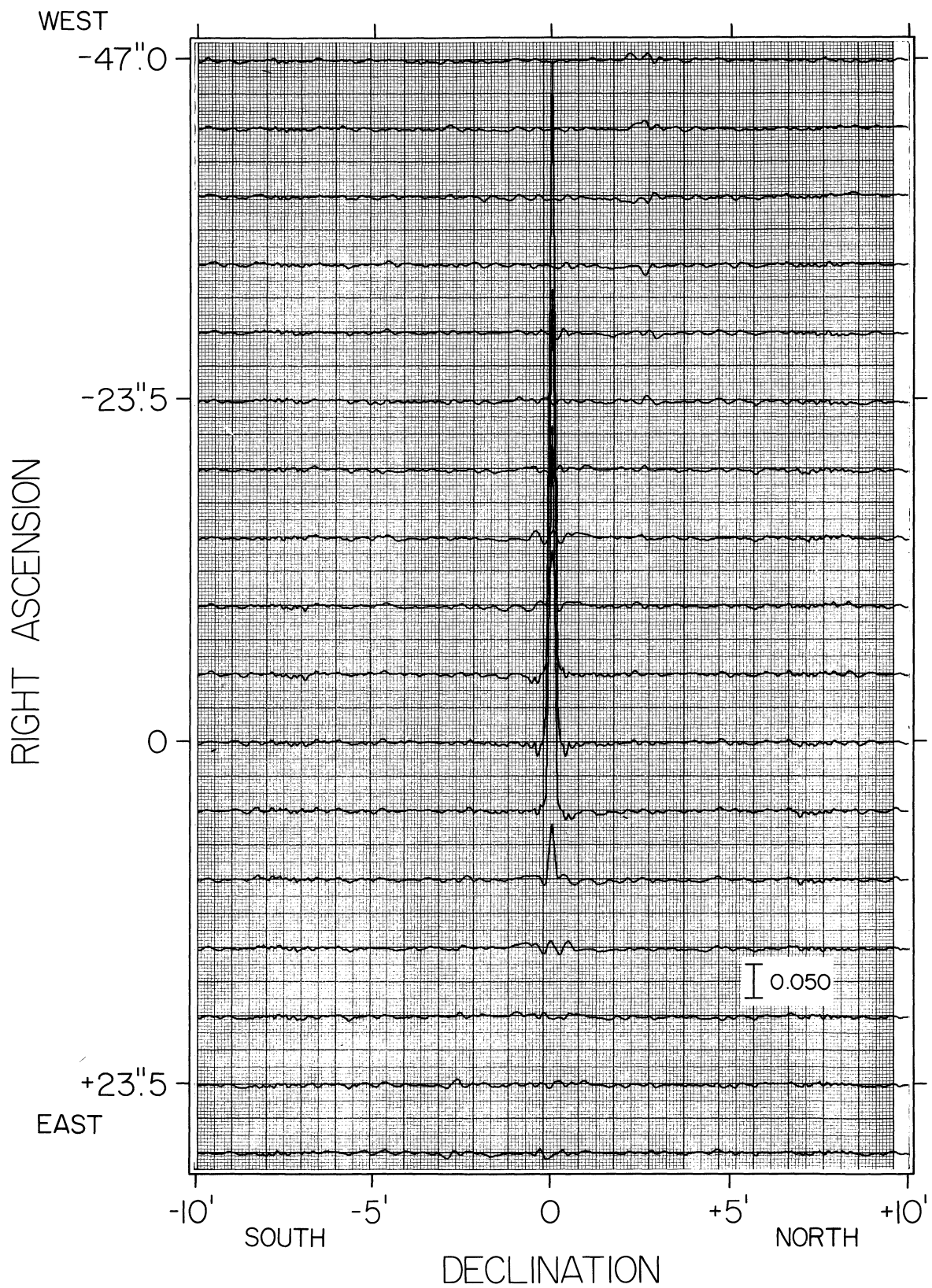


Figure 6 - 21. The power pattern of a 36 element wye for  $\delta = -15^\circ$  and  $H = \pm 4$  hours.

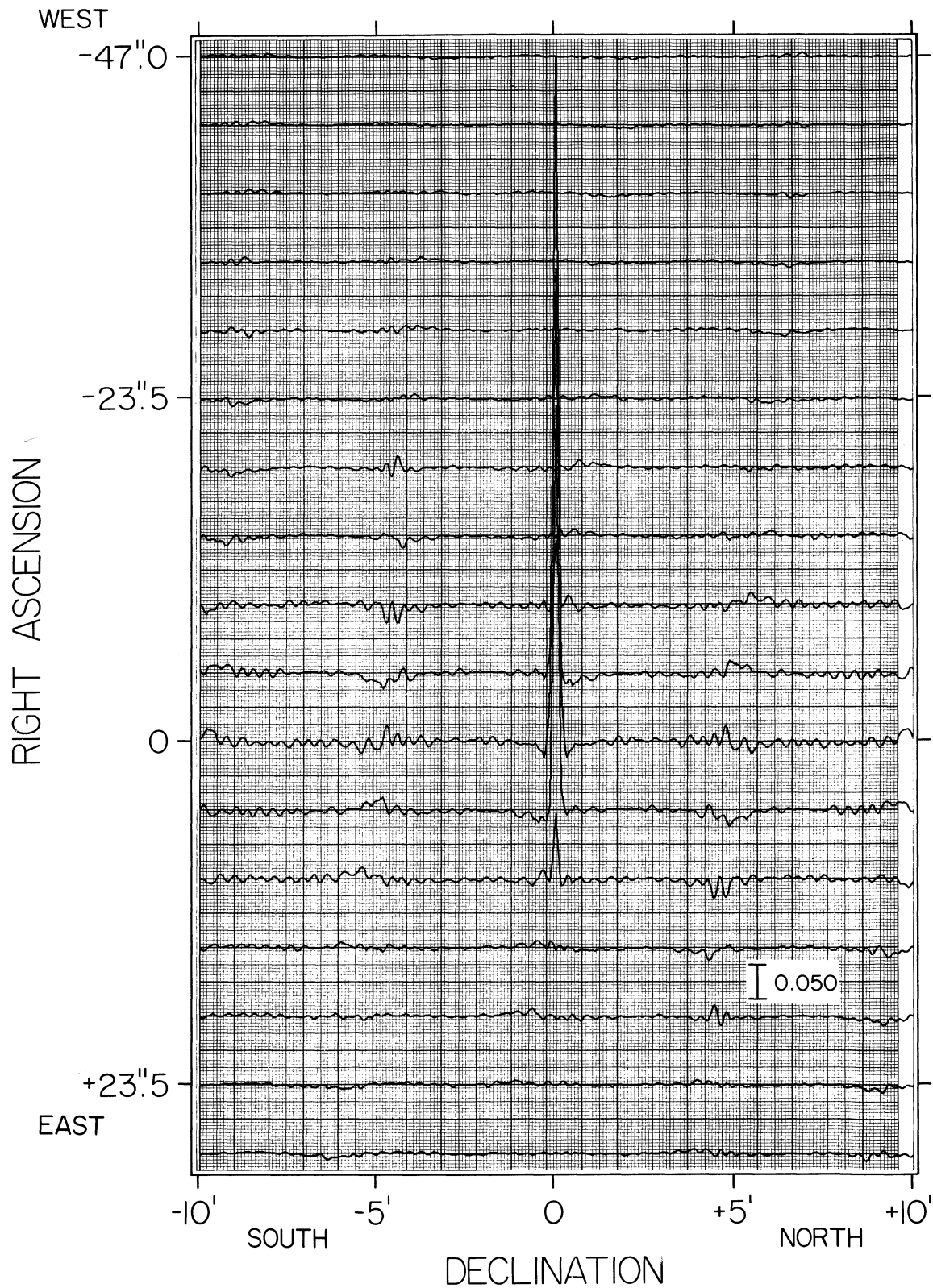


Figure 6 - 22. The power pattern of a 36 element ywe for  $\delta=0^\circ$  and  $H=\pm 5.3$  hours.

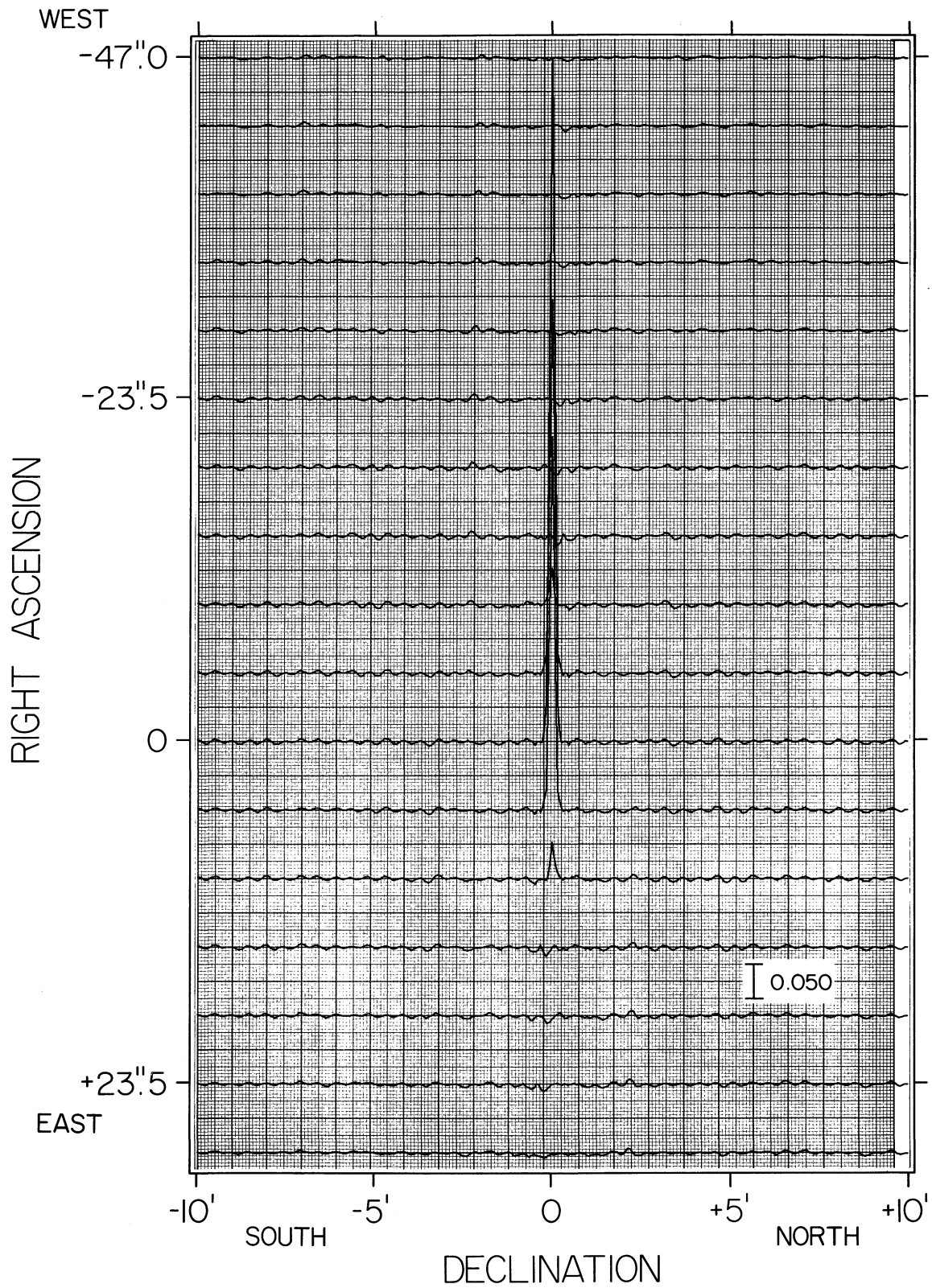


Figure 6 - 23. The power pattern of a 36 element wye for  $\delta = +30^\circ$  and  $H = \pm 6$  hours.

0".47 in right ascension and cover a range of 2' in declination. The side-lobe levels given in Table 6-7 are also applicable to resolutions other than 10", if the definitions of the zones are changed. For the 1" array, Zone 1 lies between 1".9 and 3".7, Zone 3 between 7".5 and 15", and Zone 5 between 30" and 60".

Table 6-8 gives the locations of the observing stations along each arm for the four basic configurations of the VLA. These locations are approximate only and are given mainly as a guide for the estimation of cable lengths, etc. There are 33 different stations on each arm, or a total of 99 for the whole array.

#### F. Appendix: The Application of the Theory of Random Arrays to the VLA

Since the VLA consists of a large number of elements interacting to produce a very complicated set of fringe visibility measurements by virtue of the earth's rotation, many of the attributes of its beam pattern behave as if the array consisted of a large number of elements randomly distributed in a plane. Thus, the theory of the random array can be used as a guide to the manner in which the beam pattern varies with various parameters, since these can now be written as analytic expressions. Three calculations will be presented below: the relation of the percentage holes to the side-lobes, the variation of the percentage of holes with number of elements and length of observation, and the effects of bandwidth on the far side-lobes.

##### 1. Percentage holes and side-lobes

The beam pattern of the array is given by the Fourier transform of the transfer function, which is taken to be non-zero only in a semi-circle of diameter  $N$

$$B = \left( \sum_{i=1}^{\frac{\pi}{8}N^2} W_i \cos 2\pi (xu_i + yv_i) \right) / \left( \sum_{i=1}^{\frac{\pi}{8}N^2} W_i \right) \quad (6-1)$$

where  $i$  indexes the points within this semi-circle. If there are  $n$  holes in the transfer function, then for these values of  $i$ , the weights

Table 6-7

## Side-Lobe Levels for the Wye Array

Number of Elements	Declination	Tracking Range (hours)	Half-Power Beam Width (seconds)	Side-Lobe Levels Within a Zone* (db)									
				Zone 1		Zone 2		Zone 3		Zone 4		Zone 5	
				Peak	Mean	Peak	Mean	Peak	Mean	Peak	Mean	Peak	Mean
39	+ 30°	± 4	10.1 x 10.3	<-18	-24.3	<-20	-25.1	<-16	-25.5	<-20	-27.6	<-18	-28.1
	0°	± 4	9.6 x 10.9	<-14	-21.0	<-16	-25.7	<-18	-27.8	<-14	-29.1	<-18	-31.4
	- 15°	± 4	10.8 x 12.3	<-16	-25.7	<-22	-29.4	<-20	-29.2	<-20	-30.5	<-22	-31.7
36	+ 30°	± 4	10.1 x 10.4	<-20	-23.6	<-18	-24.2	<-16	-25.0	<-18	-26.8	<-18	-27.6
	0°	± 4	9.4 x 11.3	<-12	-20.3	<-14	-24.6	<-18	-27.1	<-14	-28.7	<-16	-30.6
	- 15°	± 4	10.9 x 12.3	<-16	-24.2	<-20	-28.2	<-18	-27.8	<-18	-29.4	<-20	-30.5
	0°	± 5.3	9.8 x 11.4	<-16	-25.1	<-18	-28.2	<-20	-30.6	<-16	-31.8	<-18	-33.8
	+ 30°	± 6	10.2 x 10.5	<-20	-25.9	<-20	-27.4	<-20	-28.6	<-22	-30.3	<-22	-31.4

\* The zones are square annuli, lying at the following distances from the center of the main beam of the array: Zone 1, 19"-38"; Zone 2, 38"-75"; Zone 3, 75"-150"; Zone 4, 150"-300"; and Zone 5, 300"-600".

Table 6-8

## Observing Stations for VLA -- Wye Configuration

<u>Meters from Center</u>	<u>Resolutions in Seconds</u>			
	<u>27"</u>	<u>9"</u>	<u>3"</u>	<u>1"</u>
26	X			
52	X			
78	X	X		
156	X	X		
233	X	X	X	
311	X			
389	X			
467	X	X	X	
544	X			
622	X			
700	X	X	X	X
778	X			
933		X		
1,167		X		
1,400		X	X	X
1,633		X		
1,867		X		
2,100		X	X	X
2,333		X		
2,800			X	
3,500			X	
4,200			X	X
4,900			X	
5,600			X	
6,300			X	X
7,000			X	
8,400				X
10,500				X
12,600				X
14,700				X
16,800				X
18,900				X
21,000				X

---

$W_i = 0$ . The additional contributions to the beam produced by these holes, the "hole" side-lobes, are then given by

$$B' = \frac{\sum_{i=1}^n W_i' \cos 2\pi (xu_i + yv_i)}{\sum_{i=1}^n \frac{\pi N^2 - n}{8} W_i}$$

where  $W_i'$  is the weight which would be assigned if there were an observation at this point.

Consider, for the moment, the principle solution, in which all  $W_i = 1$ ; then it is clear that the maximum possible side-lobe is  $\frac{n}{\frac{\pi N^2 - n}{8}}$ . The mean squared side-lobe level is

$$\overline{B'^2} = u_o v_o \int_{-\frac{1}{2u_o}}^{\frac{1}{2u_o}} \int_{-\frac{1}{2v_o}}^{\frac{1}{2v_o}} \left[ \frac{\sum_{i=1}^n \cos 2\pi (xu_i + yv_i)}{\frac{\pi N^2 - n}{8}} \right]^2 dx dy$$

$$= \left( \frac{1}{\frac{\pi N^2 - n}{8}} \right)^2 \frac{n}{2}$$

which is essentially Parseval's theorem. It is also of interest to find the largest side-lobes far from the main beam. A quick estimate is made by replacing the cosine term of (6-1) by a square wave of unit absolute value, which changes sign at odd multiples of  $\frac{\pi}{2}$ . Then, assuming that the holes are randomly distributed, far from the origin -1 and 1 are about equally likely (at the origin, all the cosine terms are +1; they should become uncorrelated a few main beam diameters from the center), and the probability distribution of B approaches the binomial distribution.

$$\text{Prob} \left( \left( \frac{\pi N^2 - n}{8} \right) B' = m \right) = 2^{-n} \frac{n!}{\left( \frac{n+m}{2} \right)! \left( \frac{n-m}{2} \right)!}$$

$$\approx \sqrt{\frac{2}{\pi n}} \exp - \left( \frac{m^2}{2n} \right)$$

The probability that the side-lobe is less than  $x$  is

$$\text{Prob} ( |B'| < x ) = 2 \text{Erf} \left( \frac{\pi N^2}{8} - n \right) \frac{x}{\sqrt{n}}$$

The field of view contains about  $\frac{\pi N^2}{4}$  independent locations, so the strongest side-lobe in the field of view would have probability about  $\frac{2}{\pi N^2}$ . Thus, if  $x_0$  is the largest side-lobe far from the main beam,

$$x_0 \approx \frac{\sqrt{n}}{\frac{\pi N^2}{8} - n} \text{Erf}^{-1} \frac{1}{2} \left( 1 - \frac{2}{\pi N^2} \right)$$

If the holes are clustered, rather than being more or less randomly distributed, this theory can still be applied by increasing the grid size in the  $u-v$  plane. If the holes were highly clustered, the percentage of holes  $\frac{8n}{\pi N^2}$  is roughly independent of grid size, so that the side-lobe level, roughly proportional to  $\sqrt{\frac{n}{N^2}}/N$ , is correspondingly increased. The clustering is especially serious in the neighborhood of the origin, as this also tends to violate the assumption of randomness in the cosine terms.

## 2. An estimate of the percentage of holes

The track of a single interferometer in the transfer function plane is an ellipse with major axis  $\frac{D}{\lambda} \cos \delta = B_2$ , and minor axis  $B_2 \sin \delta$ . Near the equator, this ellipse collapses into a straight line. If  $\pm H$  is the tracking range, the circumference covered by this track is between  $2B_2H$  and about  $B_2H$ , depending on declination, the value of  $H$ , and the

orientation of the baseline. Let the mean length of the track be  $\frac{3}{2} B_2 H$ , except near the equator, where the track returns along itself, and the non-redundant track is thus about half as great. Now

$$B_2 = \frac{u}{\sin(H-h)}$$

so, making a very crude approximation,

$$\overline{B_2} \approx \frac{4}{3} \bar{u} \approx \frac{1}{3} N u_0$$

where  $u_0$  is the side of a unit cell in the  $u-v$  plane. Thus, the average length of track covered by a single correlator is about

$$L = \frac{1}{2} u_0 N H q$$

where  $q$  is unity, except within  $\frac{1}{N}$  radians of the celestial equator, where it is  $\frac{1}{2}$ .

There are, at any one time, about  $\frac{M^2}{6}$  correlators participating in the array, where  $M$  is the number of antennas. (There are  $\frac{M^2 + 3M}{3}$  independent correlators in a uniform Wye, of which about half are outside the circle of interest at any given time.) Thus, the total length of track covered is about

$$\frac{N M^2 H q u_0}{12}$$

If randomly distributed, these tracks will pass through about  $\frac{N M^2 H q}{3\pi}$  cells. The ratio of this number to the area of the semi-circle is about  $\frac{8M^2 H q}{3\pi^2 N}$ . Again assuming a sufficient degree of randomness, the percentage of holes is

$$P = \exp - \left( \frac{8M^2 H q}{3\pi^2 N} \right) .$$

For  $M = 36$ ,  $N = 240$ ,  $H = 4^h$ , this formula gives 22% holes, only slightly higher than the 14% actually found.

The largest side-lobes are, using the equations of Section 1,

$$x_o \approx \frac{1}{N} \sqrt{\frac{8}{\pi}} \frac{\sqrt{P}}{1-P} \operatorname{Erf}^{-1} \frac{1}{2} \left(1 - \frac{2}{\pi N^2}\right)$$

The largest side-lobe thus goes about as

$$x_o \approx \frac{2}{N} \exp - \left(\frac{4M^2 H q}{3\pi^2 N}\right)$$

for small  $N$  and remains constant at

$$\approx \frac{20}{M^2 q H}$$

for large  $N$ .

### 3. The effects of bandwidth

A change of frequency changes the scale of the  $u-v$  plane where the transfer function is plotted. If observations were made at several different frequencies, there would be for each correlator a sequence of tracks across the  $u-v$  plane, comprising the transfer function. If these are averaged together within the grid squares, the result, within the field of view of the inverse of the grid size, is similar to that obtained by using the individual tracks for the different frequencies and interpolating on a much smaller grid. Thus, if the grid size is about equal to the width of the tracks for a single correlator, for the different frequencies in the bandpass, the responses generated within that field of view from a source falling outside of it are about those computed for the case where the frequencies in the pass band are handled individually.

To modify the discussion of Section 2 for the finite bandwidth requires only that, in the case of a rectangular IF bandpass, from 0 to  $B$  Hz, the linear tracks of Section 2 be expanded to parallelograms of width

$$\frac{2B}{v_o} r \cos \theta$$

where  $\theta$  is the angle between the radius vector and the track and  $r$  is the distance from the origin. The average number of cells touched by a single track of this length and area is

$$\frac{4}{\pi} l \left( 1 + \frac{B}{v_0} r \right)$$

so, if the tracks are randomly distributed, they will pass through

$$\frac{N M^2 H q}{3\pi} \left( 1 + \frac{1}{3} N b \right)$$

cells, where

$$b = \frac{B}{v_0}$$

The percentage holes will be

$$P = \exp. - \frac{8M^2 H q}{3\pi^2 N} \left( 1 + \frac{1}{3} N b \right)$$

The maximum side-lobe levels for a 50 MHz bandwidth occur at  $N \approx 200$ , within the field of view of the investigations described above. This implies that the side-lobes introduced outside this field of view will be no worse than the ones within, which have been discussed previously. The maximum side-lobes predicted by the formula above are - 19 db, - 22 db, and - 24 db for 30, 36, and 42 antennas respectively, all for 8-hour observations, and a source far from the equator. With 10 MHz bandwidth, the largest side-lobes occur with  $N \approx 300$  and are about - 16 db, - 18 db, and - 20 db for 30, 36, and 42 antennas, respectively.

These analytic discussions, while not possessing sufficient accuracy to design the array in its entirety, roughly indicate the ways in which performance depends on the parameters of the array.

## REFERENCES

- Bracewell, R. N. 1958, Proc. Inst. Radio Engrs., 46, 97.
- Burns, R. 1964, Thesis, Carnegie Institute of Technology, p. 23.
- Leech, J. 1956, J. London Math. Soc., 31, 160.
- Silver, S. 1949, Microwave Antenna Theory and Design (McGraw-Hill, New York), p. 192.

Chapter 7

ARRAY SENSITIVITY AND REQUIRED ELEMENT SIZE

## Chapter 7

## ARRAY SENSITIVITY AND REQUIRED ELEMENT SIZE

A. Introduction

The factors limiting the sensitivity of an aperture synthesis array are the same as for any other kind of radio telescope: system noise temperature, operating bandwidth, effective integration time, and the effective collecting area of the aperture. In the present chapter, these parameters will be related to two quantities which describe the sensitivity of the system in a direct and useful way: the "minimum detectable flux density" and the "minimum detectable brightness temperature." These terms will be defined when they arise. Their mathematical formulation must take account of the nature of the instrument, of the fact that a single observation will continue for several hours as the array tracks the source, and particularly of the exceptional versatility of the array as planned.

Knowing these relations and the astronomical goals of the instrument, one can estimate the size required for the array elements. This is crucial, since it is the only basic array parameter which cannot be modified readily (and without prohibitive cost) once the system is built. It is necessary at the outset to make the wisest choice possible.

B. Assumptions

For the purpose of the present chapter, it is necessary to make a number of assumptions about the array and the way in which it will be operated. These assumptions underlie the entire discussion; some are obvious, and none is extreme or artificial:

1. Each observation will last an hour or more, with the array tracking the source.
2. Correlators will be present for every possible pair of antenna elements, and the output of each correlator will be recorded for the full duration of the observation. If there are  $M$  elements, the number of correlators is

$$v = \frac{1}{2} M(M-1). \quad (7-1)$$

3. The array configuration will be an equiangular Wye, with arms of equal length  $L$ . At any given instant, the points sampled on the transfer function plane will lie within an area resembling a six-pointed star.

4. The synthesized radiation pattern will be that of a uniformly-fed circular aperture. The part of the transfer function used for this purpose is the largest circle which can be inscribed in the six-pointed star just mentioned. If the operating wavelength is  $\lambda$  and the synthesized half-power beam width is  $\beta$  (in radians), this circle will have as its radius

$$L/\lambda = \frac{1.028}{\beta} \quad (7-2)$$

The effects of foreshortening due to source declination are ignored, but these become important only for those objects which transit at zenith distances greater than  $45^\circ$ .

Assumptions 3 and 4 have two consequences which will be of importance in determining the effective integration time of an observation. First, only the data which fall inside the circle of radius  $L/\lambda$  on the transfer function plane are used. At any time, a fraction  $P$  of the correlator outputs will fall within this area; then

$$P > \frac{\text{Area of inscribed circle}}{\text{Area of entire "star"}} = 3^{-3/2} \pi$$

so

$$P > 0.605 \quad (7-3)$$

The reason for the inequality is that many of the points within the circle are sampled simultaneously by two or more correlators, while there is no such redundancy in the sampling outside the circle. The amount by which the true value of  $P$  exceeds 0.605 depends on the hour angle and declination of the source at the instant in question; it also depends somewhat on the placement of the elements on the array arms. To be conservative, the discussion assumes that  $P = 0.6$ .

The second point, which follows from Assumption 4 above, is that the points within the circle are weighted in the Fourier inversion by

$$W(r) = \frac{1}{13} [8r(2+r) F(\phi, \kappa) + 4(2+r) (r^2 - 6r + 4) E(\phi, \kappa) - (1-r) \sqrt{9 + 12r(1-r)}] \quad (7-4)$$

where

$$r = \frac{\lambda}{L} \sqrt{u^2 + v^2}$$

$$\phi = \sin^{-1} \left( \frac{1-r}{2-r} \right)$$

$$\kappa = \frac{2-r}{2+r}$$

and  $F(\phi, \kappa)$  and  $E(\phi, \kappa)$  are elliptic integrals of the first and second kinds, respectively. The ratio of the direct mean and rms values of  $W(r)$ , taken over the circle,

$$E = \bar{W} / \sqrt{W^2},$$

is conceptually related to "aperture efficiency" for the array. For the weighting function (7-4),  $E = 0.781$ .

#### C. The Effective Integration Time

The effective integration time is a crucial factor in the array sensitivity. Since the noise components of the different correlator outputs are mutually uncorrelated, one can define the effective integration time as

$$\tau = vtPE^2 \quad (7-5)$$

where  $t$  is the duration of the observation. It is convenient to include  $P$  and  $E$  here, although it would be proper to regard them as factors reducing the effective area of the array rather than the integration time. This

makes no difference in the discussion of array sensitivity.

In view of the discussion given in Section B, one can take

$$PE^2 = 1/3$$

as a conservative value. Then, expressing  $\tau$  in seconds and replacing  $t$  by its equivalent in hours,  $H = t/3600$ , one has

$$\tau = 600 M(M - 1) H.$$

This will normally be very large. Thus, an 8-hour observation with a 36-element array would afford an effective integration time of  $6 \times 10^6$  seconds, or nearly three months.

#### D. The Minimum Detectable Flux Density

Consider first the case of a 2-element correlation interferometer. The rms noise on the correlator output, in antenna temperature units, can be shown to be

$$\Delta T = 2^{-1/2} T_R (Bt)^{-1/2} \quad (7-6)$$

where  $T_R$  is the system noise temperature,  $B$  is the IF bandwidth, and  $t$  is the integration time. If the minimum acceptable signal-to-noise ratio for source detection is  $q_n$ , then one can define the "minimum detectable flux density" for a point source as

$$S_m = \frac{2k}{\epsilon A} q_n \Delta T \quad (7-7)$$

where  $k$  is Boltzmann's constant, and  $\epsilon$  and  $A$  are respectively the aperture efficiency and geometrical area of a single interferometer element. If the elements are circular and have diameter  $d$ , then

$$S_m = \frac{2^{5/2} k}{\pi} \cdot \frac{q_n}{\epsilon} \cdot T_R (Bt)^{-1/2} d^{-2} \quad (7-8)$$

The expression for the minimum point-source flux density detectable by a correlator array is exactly analogous to (7-8), the sole difference being that the appropriate integration time is  $\tau$ , given by (7-5). Thus

$$S_m = \frac{2^{5/2} k}{\pi} \frac{q_n}{\epsilon} T_R (B\tau)^{-1/2} d^{-2} \quad (7-9)$$

for the array.

#### E. The Minimum Detectable Brightness Temperature

An extended brightness distribution can be specified conveniently by the values of brightness temperature on a rectangular grid of points, and this is the natural way to present the results of synthesis mapping. Each such value can be regarded as the average brightness temperature within a solid angle  $\Delta \Omega = \gamma^2$  centered on the point, where  $\gamma$  is the grid spacing in radians. If the flux density coming from  $\Delta \Omega$  is  $\Delta S$ , the corresponding average brightness temperature follows directly from the Rayleigh-Jeans law:

$$T_B = \frac{\lambda^2}{2k} \frac{\Delta S}{\Delta \Omega} \quad (7-10)$$

Assume that the field being mapped contains only a single, unresolved source at the position of one of the grid points. Unless the grid spacing  $\gamma$  is larger than about twice the synthesized beam width  $\beta$ , part of the energy of the source will appear in adjacent cells because of the finite width of the beam. Approximate the main lobe of the synthesized radiation pattern by the Gaussian function

$$f(x,y) = \exp \left\{ - \frac{4 \log_e 2}{\beta^2} (x^2 + y^2) \right\}$$

where  $x$  and  $y$  are orthogonal angular coordinates expressed in radians. The fraction of the flux density appearing in an area  $\Delta \Omega$  centered on the source is approximately

$$\begin{aligned}
 K &= \int_{\Delta\Omega} \int f(x,y) d\Omega \int_{\infty} f(x,y) d\Omega \\
 &= \left[ \operatorname{erf} \frac{\gamma}{\beta} \sqrt{\log_e 2} \right]^2 \\
 &= \left( \frac{\gamma}{\beta} \right)^2 G\left(\frac{\gamma}{\beta}\right)
 \end{aligned}$$

where

$$G\left(\frac{\gamma}{\beta}\right) = \frac{4 \log_e 2}{\pi} \left[ \sum_{n=0}^{\infty} \frac{(-\log_e 2)^n}{n! (2n+1)} \left(\frac{\gamma}{\beta}\right)^{2n} \right]^2$$

This function is not critically dependent on  $(\gamma/\beta)$  so long as  $\gamma < \beta$ , as would normally be true in practice. Assuming  $\gamma = \beta/2$ , a reasonable value, one has  $G(\gamma/\beta) = 0.78$ .

Now, letting

$$\Delta S = K S_m,$$

one has for the "minimum detectable brightness temperature,"

$$T_{B,m} = \frac{\gamma^2 G(\gamma/\beta)}{2k \beta^2} S_m$$

or

$$T_{B,m} = \frac{2^{3/2}}{\pi} \frac{q_n}{\epsilon} G(\gamma/\beta) \lambda^2 T_R (B_T)^{-1/2} d^{-2} \beta^{-2} \quad (7-11)$$

F. Some Simplification

It is reasonable to assume

$$q_n = 5,$$

$$\epsilon = 0.7,$$

$$\gamma/\beta = 0.5.$$

Then (7-9) and (7-11) can be written more compactly as

$$S_m = 1.78 \times 10^{-22} T_R (B\tau)^{-1/2} d^{-2} \quad (7-12)$$

$$T_{B,m} = 5.07 \lambda^2 T_R (B\tau)^{-1/2} d^{-2} \beta^{-2} \quad (7-13)$$

The units are ( $W m^{-2} Hz^{-1}$ ) for  $S_m$  and ( $^{\circ}K$ ) for  $T_{B,m}$ .

G. The Effective Area of the Array and Element Size

The effective area of a 2-element interferometer is the geometric mean of the effective areas of the individual elements. Since it is assumed that the elements are identical, the effective area is the product of the aperture efficiency  $\epsilon$  and the geometrical area  $A = (\pi/4) d^2$ . Using (7-6) and (7-7), one has

$$S_m = \frac{2^{1/2} k q_n T_R}{(\epsilon A) \sqrt{Bt}} \quad (7-14)$$

for a 2-element interferometer.

It is easy to find the analogous expression for the array. Using (7-1), (7-5), and (7-9), one obtains

$$S_m = \frac{2^{1/2} k q_n T_R}{a \sqrt{Bt}} \quad (7-15)$$

where the "effective area of the array" is

$$a = 2^{-5/2} \pi E \epsilon d^2 \sqrt{PM(M-1)} .$$

Taking  $\epsilon = 0.7$ ,  $E = 0.781$ , and  $P = 0.6$ , and noting that  $\sqrt{M(M-1)}$  is very closely approximated by  $(M - 1/2)$ , one finds

$$a = 0.235 d^2 (M - 1/2) \quad (7-16)$$

Assuming further that  $q_n = 5$  and  $\gamma/\beta = 0.5$ , one can write

$$S_m = \frac{9.76 \times 10^{-23} T_R}{a \sqrt{Bt}} \quad (7-17)$$

$$T_{B,m} = \frac{2.76 \lambda^2 T_R}{a \beta^2 \sqrt{Bt}} \quad (7-18)$$

Then the effective array area required to achieve specified values of  $S_m$  or  $T_{B,m}$  is

$$a = \begin{cases} \frac{9.76 \times 10^{-23} T_R}{S_m \sqrt{Bt}} & (7-19a) \\ \frac{2.76 \lambda^2 T_R}{T_{B,m} \beta^2 \sqrt{Bt}} & (7-19b) \end{cases}$$

Now consider the element diameter required to meet specific astronomical performance goals, assuming that  $T_R = 100^\circ\text{K}$  and that each observation will last 8 hours ( $2.88 \times 10^4$  seconds). For convenience, it is desirable to express  $\beta$  in seconds-of-arc rather than in radians:

$$\beta_s = 2.063 \times 10^5 \beta .$$

Then

$$a = \begin{cases} \frac{5.75 \times 10^{-23}}{S_m \sqrt{B}} & (7-20a) \\ \frac{6.92 \times 10^{10} \lambda^2}{T_{B,m} \beta_s^2 \sqrt{B}} & (7-20b) \end{cases}$$

Experience with the present NRAO interferometer has shown that adequate calibration of the array, with the aid of unresolved sources having intensities of a few flux units, requires that the elements be at least 10 m in diameter. This, then, is the lower limit to the element diameter.

In the following, the value of  $a$  required by each of three examples is found. The value of  $d$  corresponding to  $M = 36$  elements is given also, since this is about the number of elements required to achieve adequate coverage of the transfer function plane in a single 8-hour observation.

The Whitford Committee Report implies that the array should be able to detect sources with flux densities as low as  $2 \times 10^{-28} \text{ W m}^{-2} \text{ Hz}^{-1}$ . Assuming an IF bandwidth of 50 MHz, this requires

$$a = 40.6 \text{ m}^2,$$

$$d = 2.2 \text{ m} \quad (\text{for } M = 36).$$

Since this is much less than the 10 m required for calibration, the array must in fact be far more sensitive than the Whitford Committee calls for.

One can assess the effective array area needed for mapping at 11 cm wavelength (with a bandwidth of 50 MHz) by reference to Fig. 1, which shows  $a$  as a function  $T_{B,m}$  for synthesized beam widths of 1", 3", and 10". The horizontal lines correspond to element diameters of 10 m to 30 m, at intervals of 5 m, for a 36-element array.

Perhaps the most severe foreseeable demand that will be placed on the continuum sensitivity of the array is the detailed polarization mapping of radio galaxies. At 11 cm wavelength, most of these objects have brightness

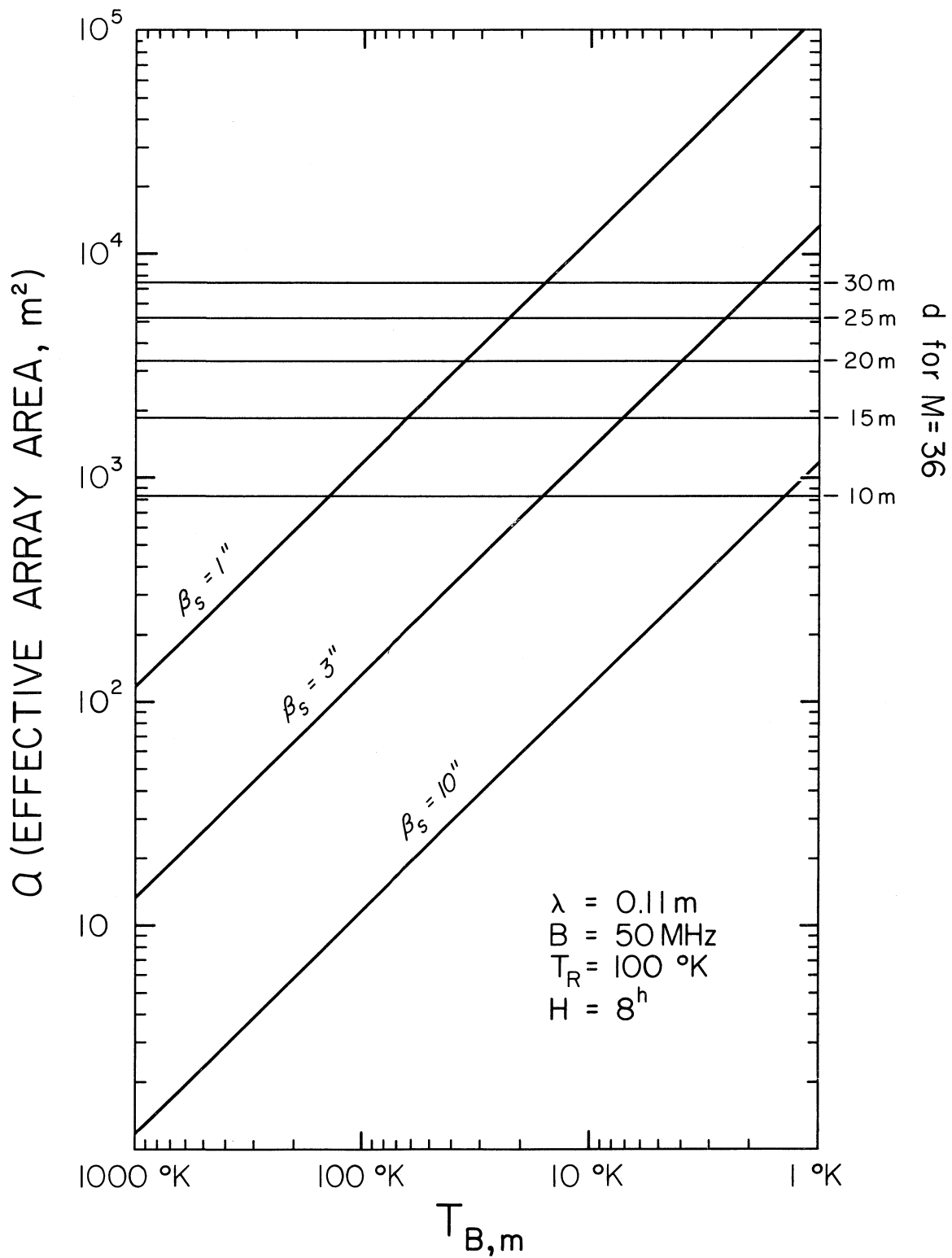


Figure 7 - 1

temperatures in range of a few hundred to a few thousand degrees, although some approach a million degrees. Therefore, mapping of polarization down to one or two percent will ordinarily require  $T_{B,m}$  to be a few tens of degrees or less. Furthermore, it is likely that the polarization will change rapidly as a function of position on the source, so one must expect to use as narrow a beam as possible. A reasonable minimum goal is the ability to map the polarization of a source with a brightness temperature of  $1000^\circ\text{K}$  at the two percent level. This calls for  $T_{B,m} = 20^\circ\text{K}$ ; then  $\mathcal{A} = 5800 \text{ m}^2$  for  $\beta = 1''$ , corresponding to  $d = 26 \text{ m}$  if  $M = 36$ .

Another field demanding high sensitivity is spectral line studies. Here the brightness temperatures generally are low, and one is also forced to use much narrower bandwidths than in continuum work. On the other hand, most of the important foreseeable line problems do not require nearly as narrow a beamwidth as is needed for continuum observations. Fig. 2, which is analogous to Fig. 1, shows  $\mathcal{A}$  as a function of  $T_{B,m}$  for synthesized beam widths of  $10''$ ,  $30''$ , and  $60''$  in the 21-cm hydrogen line. The solid and dashed lines correspond to IF bandwidths of 100 kHz and 10 kHz, respectively. It is assumed that the array will be operated as a single-sideband system for line work. As in Fig. 1, the horizontal lines show element diameters, assuming  $M = 36$ .

Many of the spectral line problems that can be attacked with the array have been discussed elsewhere in this proposal. Most call for very high sensitivity. The high-resolution mapping of the 21-cm hydrogen radiation of spiral galaxies is representative of these problems. One can estimate, on the basis of what is known at present about the HI emission of spiral galaxies, that an instrument with  $T_{B,m} = 7^\circ\text{K}$  and 100 kHz bandwidth would be adequate for mapping the large-scale HI distribution of such objects. To do so with a synthesized beam width of  $17''$  (corresponding to the 2.3 km arm length configuration) would require  $\mathcal{A} = 5000 \text{ m}^2$  or  $d = 25 \text{ m}$  for  $M = 36$ . The synthesized beam width of  $17''$  corresponds to 1 kpc at the distance of the Virgo Cluster ( $\sim 12.5 \text{ Mpc}$ ). For comparison, it should be noted that the  $10'$  beam of the 300-foot antenna at  $\lambda 21.4 \text{ cm}$  corresponds to 2 kpc at the distance of the Andromeda galaxy. Further, a typical spiral arm has a width (in the plane of the galaxy) of about 500 kpc, the arms ordinarily being separated by a somewhat greater

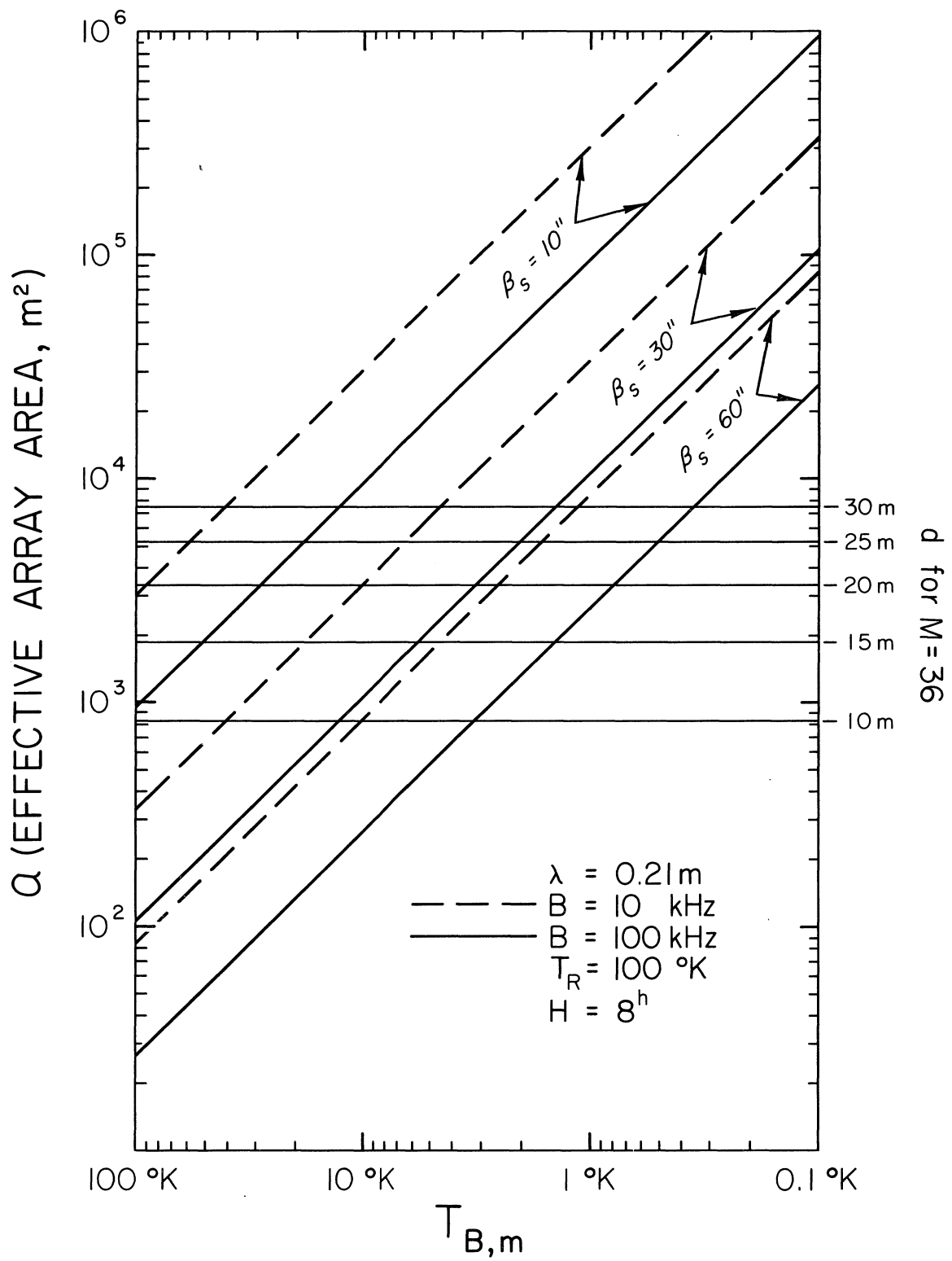


Figure 7 - 2

distance. Thus very detailed mapping of the HI distributions of spirals within 5 Mpc of the sun should be possible.

It is clear from these examples that element diameters in the vicinity of 25 m are needed if the array is to perform efficiently the tasks considered above. It is for problems of this nature that the proposed array is unique. They are beyond the reach of any other array now being built or planned. And it is such detailed studies which should lead to major advances in our understanding of the physical and dynamic processes occurring in galaxies. Similar considerations apply to many areas of galactic radio astronomy as well.

Assuming now that the array consists of 36 elements, each 25 m in diameter, one has  $a = 5200 \text{ m}^2$ . Then, from (7-20a), one has for  $B = 50 \text{ MHz}$ ,

$$S_m = 1.7 \times 10^{-30} \text{ W m}^{-2} \text{ Hz}^{-1} .$$

This is so low that one must consider whether the array may be seriously confusion limited. If so, the estimate of the sensitivity of the system is overly optimistic. A rough assessment can be made in the following way. Following von Hoerner (1961) in requiring 75 beam areas per source in order to be reasonably safe from serious errors due to confusion, one is limited to

$$N_R = (75 \alpha)^{-1}$$

resolvable sources per steradian, where  $\alpha$  is the effective solid angle of the array beam:

$$\alpha = \frac{\pi}{4} \beta^2 = 1.6 \times 10^{-11} \beta_s^2$$

Then

$$N_R = 8.3 \times 10^8 \beta_s^{-2}$$

Now, following Von Hoerner's extrapolation of the 3C catalogue, the number of sources per steradian with flux density  $\geq S$  is

$$N_V = 15 (1.2 \times 10^{-25})^{-n} \lambda^{\alpha n} S^n$$

where  $\alpha$  is the mean spectral index of the sources and  $n$  is the slope of the  $(\log N, \log S)$  relation. Adopting  $\alpha = -0.8$  and  $n = -1.8$ , and solving for  $S$ , one finds

$$S = 5.4 \times 10^{-25} \lambda^{0.8} N_V^{-0.555}$$

Then  $N_V \approx N_R$  when

$$S = 6 \times 10^{-30} \lambda^{0.8} \beta_S^{1.11}$$

For  $\lambda = 0.11$  m, this gives

$$S = 10^{-30} \beta_S^{1.11}$$

This indicates that the array will be operating near the confusion limit when  $\beta_S = 1''$ , and that it will be confusion limited when  $\beta_S = 3''$ . This conclusion is likely to be unduly pessimistic, since one is extrapolating very far from the 3C, both in flux density and in wavelength. It assumes that the  $(\log N, \log S)$  relation remains linear down to  $S = 10^{-30} \text{ W m}^{-2} \text{ Hz}^{-1}$ ; if it in fact "breaks" at a higher flux level, the confusion problem will be eased. It is apparent, however, that confusion could be a fairly serious restriction. This problem is discussed in greater detail in Section D of Chapter 2. It should be noted that these considerations apply only to continuum work. In line studies, the confusion noise cancels out.

#### REFERENCE

von Hoerner, S. 1961, Publ. NRAO, 1, 19.

Chapter 8

THE ARRAY SITE

## Chapter 8

## THE ARRAY SITE

A. Introduction

Many factors bear on the selection of a suitable place to build the array. Some of these are absolute, since they directly affect the astronomical capabilities of the instrument; examples are the most northerly acceptable latitude and the physical extent demanded by the angular resolution requirements. Others are relative, depending on qualitative desiderata which sometimes conflict. Thus one would like the installation to be readily accessible to urban amenities, yet it must be well removed from sources of man-made interference.

The present chapter sets forth the criteria which have guided the search for acceptable sites; then it considers the results of the search. It will be shown that there are not many attractive locations. The discussion is in general terms, since the detailed evaluation of the possible sites is still in progress; it would be premature to treat them individually at this time. It is clear, however, that quite good places for the array exist; the remaining problem is to make the wisest choice among them.

B. The Primary Criteria

These are the essential requirements which must be satisfied by any site that can be considered seriously. They are the constraints governing the choice of areas to be evaluated later in the light of a broader range of factors. They fall naturally into three categories.

1. Geographic

This is the definition of the boundaries within which sites were sought. It was specified to be United States territory south of latitude  $40^{\circ}\text{N}$  and west of longitude  $100^{\circ}\text{W}$ . The latitude limit is set by the need for the array to have as large a useful declination range as possible. There are two reasons for the longitude limit. First, the relatively dense population and heavy cultivation to the east of this line are not consistent with a quiet radio environment. Second, the much drier climate and generally higher ground elevations to the west should minimize the adverse influence of the atmosphere on the attainable angular resolution.

## 2. Topographic

It must be possible to place the array on reasonably level solid ground while maintaining the desired configuration of an equiangular Wye with arms 15 miles long. It would also be well to have a site located where mountains could provide some shielding from radio interference. Further, the small-scale ground relief along the array arms should be gentle, since it must be possible to move the array elements easily. The gradients along the arms should not exceed two percent.

## 3. Cultural

The site must not already be heavily preempted by human use; otherwise its acquisition might be complicated and prohibitively expensive, and there would probably be excessive man-made interference in the vicinity. Moreover, the array should not be built in an area which is likely to be "developed" in the foreseeable future. This means that the natural resources near each site must be considered.

These are the guidelines. The first tells where to look; the second what to look for; the third what to avoid.

The region defined by the geographic requirement covers about 700,000 square miles. It contains nearly one-fourth of the conterminous United States.

The topographic requirements severely limit the number of possible sites. Few areas are flat enough over sufficiently great distances, and some of these fail to meet the cultural requirement.

## C. The Secondary Criteria

These are the basis for assessing the relative merits of the sites satisfying the primary criteria. They include the following.

### 1. Elevation

The array should be as high above sea level as possible. There are two reasons for this. First, the summers are hot throughout the Southwest, and the heat is particularly intense at the lower elevations. In this region, it is generally true that the climate of a locality depends more on elevation than latitude. The mean daily maximum temperatures for July typically range from 110°F near sea level down to 85°F at 7500 ft. High temperatures are to be avoided if possible, since they can be

troublesome for both the instruments and the people who operate them. The second reason for desiring a high site is perhaps more important. The attainable angular resolution of the array will be limited ultimately by the short-term variations in the relative optical path lengths through the atmosphere for the different elements of the array. The primary cause for these variations is the nonuniform distribution of water vapor and droplets. In the absence of visible clouds, this effect is not likely to be important for an array operating at centimeter wavelengths (Kaidanovskii and Smirnova, 1965). On the other hand, experience with radio interferometric tracking systems at Cape Kennedy shows that the refractive anomalies associated with temperature inversions and clouds with a well-developed convective cell structure (chiefly cumulus) can cause serious errors (Vickers et al., 1965). The most troublesome effects arise in the lower troposphere, below 5000 ft. They are particularly severe when the absolute humidity and the refractive index are high ( $\geq 19$  gm/m<sup>3</sup> and  $\geq 370$  N-units, respectively) at ground level. It is not clear how far one is justified in applying these results, which refer to the Florida Coast, to arid inland areas. Very little information of the kind needed to assess the problem in the Southwest is available. One can only assume that the frequency of occurrence of serious atmospheric effects is directly related to the amount of air above a given site, and therefore that the higher sites will be less often affected.

## 2. Proximity to urban areas

This involves two considerations. First, there should be a town or small city close enough to the site that the resident staff could find suitable accommodation. This requires the availability of adequate educational, shopping, medical, and entertainment facilities. The distance from the site should not be so great that daily commuting by automobile would be burdensome. Secondly, the site should be readily accessible to a city large enough to have regularly scheduled air service. Preferably the driving time to the site should not be more than two hours. At the same time, the distance should be great enough that radio interference from the city would not be troublesome.

## 3. Utilities and access

Adequate roads and power should pass within a reasonable distance of the array. Otherwise, it might be necessary to go to considerable

expense to provide access roads and electric power. As it happens, the existing road and power distribution systems in the Southwest are fairly well developed, and they are quite accessible to all of the good potential array sites.

#### 4. Drainage

Although the Southwest is arid, rain tends to be heavy when it occurs. As a result, many of the potential array sites would require extensive protection against runoff damage. Others are on permeable soil and runoff would not be a problem. The culverts and dikes needed to protect 45 miles of array arms would be expensive, and sites requiring them should be avoided if possible.

#### 5. Land ownership

It is desirable that as much of the array as possible be placed on public land. This would facilitate acquisition, and it would be far less expensive than purchase or lease from private owners.

### D. Site Search and Evaluation

The first step in the site search was to examine the 1:250,000 U.S.G.S. topographic maps for the entire area defined by the geographic requirement, in order to locate the places which might meet the topographic requirements. The contour interval on most of these maps is 200 ft, which is coarse enough to conceal a great deal of terrain relief. Large-scale maps with closer contour intervals are not available at present for most of the Southwest. Therefore, the map search was simply a reconnaissance which revealed the places deserving closer scrutiny.

In all, 29 potential sites satisfying the primary criteria were found. Further examination, in many cases by personal inspection by members of the Design Group, eliminated more than half of these from further consideration. The reasons for the rejections are instructive.

#### 1. Orientation

The nature of the topography surrounding two of the sites would not permit the array to be built with the desired orientation (one arm  $4^\circ$  to  $8^\circ$  from a north-south line).

#### 2. Roughness

The small-scale ground relief is excessively rough on six of the sites.

### 3. Existing activity

Six sites lie wholly or partly in missile test ranges or Air Force bombing and gunnery ranges. There are also two which are in the midst of oil fields. Such activities make for an imperfectly tranquil environment.

These considerations removed 16 of the potential sites. The remaining 13 can be divided into two groups by latitude: five are between 38°N and 40°N, while the other eight are all south of 35°N.

Since it is desirable to build the array as far south as possible, the five sites in the northern group were reserved for study only if none of the southern group proved suitable.

Four of the eight sites in the southern group are within 2000 ft of sea level, while the other four are at elevations ranging from 2800 to 7000 ft. These latter four were examined closely by members of the Design Group, both from the air and on the ground. It was evident that all of these sites meet the minimum requirements. Two of them, however, would have one arm crossing both a main railway line and a four-lane highway; furthermore, these sites are appreciably farther from large cities than the other two. Therefore, it is upon the other two sites that the main interest is centered. One is designated Y-15, the other Y-23. Each has been given a thorough preliminary engineering study. The results will be discussed in Chapter 12.

#### REFERENCES

- Kaidanovskii, N. L. and Smirnova, N. A. 1965, Radiotekhnika i Elektronika, 10, 1574.
- Vickers, W. W., Fain, G. G., Meyer, J. H., and Griffith, R. 1965, "Meteorological Effects on Range Rate Errors of Radio Interferometer Tracking Systems," AFCRL Report AFCRL-65-819.

Chapter 9

MANAGEMENT AND OPERATION

## Chapter 9

## MANAGEMENT AND OPERATION

A. Project Management

The NRAO will act as prime contractor for the design and construction of the VLA. Detailed design, construction of components and subsystems, and installation and checkout will be done partly in-house and partly through subcontracts with industrial firms. In either case, scientific and technical supervision will be provided by the same group of NRAO scientists and consultants who have been responsible for the basic design, and administrative supervision will be provided by NRAO scientists and administrators.

The VLA management staff, under the project manager, will be responsible for program definition, schedules and budgets, specifications, contracting and procurement, monitoring of in-house and contract design work, and supervision of construction, installation, and checkout. The estimated man-years of effort required for these functions are shown in Table 9-1. The estimates are based on the time schedule of Figure 10-1 and assume that construction will be authorized in FY 1969.

Table 9-1

Fiscal Year	68	69	70	71
Man-Years, project management	12	20	30	30
Project management cost (\$1,000)	210	350	525	525

The last row of the table is based on an assumed average operating cost (salary and overhead) of \$17,500 per man-year (present NRAO operating cost is about \$16,500 per man-year).

Approximately one-half the management will be by regular NRAO staff members whose time cannot be specifically charged to the VLA; many of the senior scientific, business, and administrative staff will spend one-fourth to one-third time on the project, for example.

Thus about one-half the costs shown in Table 9-1 should be charged directly to the VLA project management. During FY 1965-67 NRAO operating costs, in the form of staff design and administrative effort, attributable but not charged directly to the VLA, are estimated to have been \$150,000 to \$200,000 per year.

No project management costs are shown beyond FY 1971. As construction phases out and operation phases in during FY 1972 and following, project management is included in the operating costs discussed in the next section.

B. Operation

The VLA will be a national facility available to any qualified scientist solely on the basis of the scientific merit of the proposed program. It will be operated by the NRAO as one of its several observing facilities, under the same policies as now apply to the telescopes at Green Bank. The NRAO, in turn, is operated by Associated Universities, Inc., under contract with the National Science Foundation. The AUI policies established for the NRAO require that not less than 70% of the observing time of NRAO-operated instruments be allocated to scientists not on the NRAO staff, without regard to their institutional affiliation.

The VLA will be operated by a resident staff of specially trained technicians. The complexity of the instrument requires that its operation be highly automated. A scientist planning to carry out a program must specify the particular array, geometric and electronic configuration, and types of calibrations, initial data processing and outputs best suited to his needs, along with his observing program. It will not be necessary for him to be at the site during the observations. Preliminary, real-time evaluation of the observations can be provided by periodically presenting the data in the form of contour maps and transmitting the maps by telephone facsimile directly to inexpensive terminal equipment in the scientist's home office or by digital telephone transmission of selected data to the scientist's institutional computer center. The full observational and ancillary monitor and identification data will be collected on magnetic tape and periodically sent to the scientist or to the NRAO computing center in Charlottesville if the scientist wishes to use that facility, for further processing and analysis.

The NRAO must make available to institutional libraries and individual scientists an extensive collection of transfer functions and beam patterns for the various available array configurations, together with complete documentation of system parameters, observing procedures, calibrations, data processing and analysis programs, etc.

A small number of dormitory rooms will be available for scientists who do wish to be present at the site. Housekeeping facilities will not be as extensive as they are at Green Bank, however, partly because of the nature of VLA operations and partly because the site is expected to be within reasonable commuting distance of a town with adequate amenities.

Most of the administration and business management, equipment development, and scientific work associated with operation of the VLA will be conducted from the Charlottesville and Green Bank offices of the NRAO, in consolidation with the operation of other NRAO facilities. The resident VLA staff will consist only of the technical and administrative personnel required for actual operation and maintenance of the instrument.

The resident staff requirements are shown in Table 9-2. The resident director will be a radio astronomer, and the site superintendent a mechanical or civil engineer. The scientific group is responsible for the calibration, testing, and evaluation of the instrument and liaison between observers, operators, and maintenance personnel. Although some of this work will be done by non-resident scientists, a small resident staff is needed to provide continuity and to make the necessary on-the-spot decisions that directly affect the scientific performance of the instrument.

The operations group is responsible for routine operation of the instrument. Operation will be on a three-shift/seven-day week basis with one operator and one data clerk on duty each shift. Normally, these will be the only persons on duty during the night shifts, with technicians available on call.

The maintenance group is responsible for all plant, telescope, and electronic maintenance. Because of the large number of duplicate components in the VLA, the emphasis must be on preventive maintenance,

computer diagnosis of malfunctions, and plug-in replacements of faulty components. Enough technicians and mechanics are included in the staff to handle the routine preventive and emergency maintenance, and repair of the standard plug-in replacement components, to keep the instrument operating reliably. Experience may later indicate that periodic shut-downs for intensive maintenance is necessary, especially for mechanical components.

The total resident staff is estimated at 53 persons. Again adopting an operating cost-per-man of \$17,500, the total operating cost for the VLA site is estimated to be \$930,000 per year. This includes salaries and personnel benefits, travel, and all materials, supplies and services except electronic and mechanical replacement components. These are estimated at \$200,000 per year.

Table 9-2

## VLA Resident Staff

<u>Administrative Group (6)</u>	<u>Maintenance Group (28)</u>
Resident Director	Engineers (5)
Business Manager	Technicians (10)
Site Superintendent	Mechanics (7)
Payroll Clerk	Machinist
Bookkeeper	Electrician
Secretary	Stock Clerk
	Secretary
<u>Scientific Group (4)</u>	Laborers (2)
Scientists (2)	
Engineer	<u>Housekeeping Group (5)</u>
Programmer	Cooks (2)
	Maid
<u>Operations Group (10)</u>	Janitor
Operators (5)	Driver
Data Clerks (5)	

---

VLA operating costs are also incurred at Charlottesville-Green Bank, in addition to the on-site costs. The direct VLA costs are estimated to

be 14 scientific and technical man-years/year and 6 administrative man-years/year, for a total of \$350,000 per year in 1972.

The total annual operating budget for the VLA, exclusive of capital improvements, is thus estimated to be \$1,480,000.

The project management staff will form the nucleus of the operating staff. Recruitment of additional on-site operating personnel should begin in FY 1971 so that they may assist in and gain experience from the installation and checkout of the system.

Table 9-3 summarizes the above cost estimates, by fiscal year. Also shown in Table 9-3 is \$200,000 per year for general capital equipment. This includes general maintenance equipment, laboratory and office furnishings, and electronic test equipment.

Table 9-3

Operating Costs Summary (thousands)

	<u>1968</u>	<u>1969</u>	<u>1970</u>	<u>1971</u>	<u>1972</u>
Project management and operations	\$105	\$175	\$262	\$700	\$1,480
General equipment	—	—	<u>200</u>	<u>200</u>	<u>200</u>
Total	\$105	\$175	\$462	\$900	\$1,680

The costs summarized in Table 9-3 are needed in addition to the design and construction costs given in Chapter 10.

Chapter 10  
COST ANALYSIS

## Chapter 10

## COST ESTIMATES AND TIME SCHEDULE

Cost estimates for the various elements of the VLA are developed in Chapters 11 through 21. They are summarized in Table 10-1. The estimates in this table are for the proposed basic array, consisting of the following components:

(1) Antenna system: Thirty-six 25 m diameter antennas, including drives and servo system, Cassegrain secondary reflector, equipment enclosures, cable trays, encoders and all electrical components except radiometers and feeds. Three transport systems are also included.

(2) Electronic system: All electronics for single-channel operation at  $\lambda$  11 cm. Sufficient cabling and IF transmission is provided for two simultaneous channels. Feeds for dual left and right-hand circular polarization are included. Feeds, front ends, and correlators for additional channels are not included. Control consoles for operation and maintenance are included.

(3) Computer system: Data processor, monitor computer, multiplexors, and communication equipment.

(4) Site: Buildings, roads, airstrip, utilities, telescope foundations for 99 observing stations (four configurations), cable trenches and equipment huts, and the railroad track system for a Wye with 21 km arms.

The cost estimates in Table 10-1 include design, prototypes as needed, fabrication and construction, installation, engineering and administration, and all other costs for procurement of a complete system. The estimates are in 1966 dollars and do not include any contingency or price escalation. Costs of both technical components and conventional construction are dependent to some degree upon regional and local conditions such as labor supply and prevailing wages, distance from suppliers, transportation facilities, and extent of local industry. The cost of the railroad system is heavily dependent on the terrain and drainage of the site. For these reasons, the estimates in Table 10-1 are for a particular site -- Y15. The estimate for the other site which was developed -- Y23 -- is approximately \$2 million greater.

Table 10-1  
Cost Estimates

	<u>Cost (millions)</u>
<u>Antenna System</u>	
Mechanical	\$ 14.494
Electrical	2.358
Transports	<u>.207</u>
Subtotal	17.059
<u>Electronic System</u>	
LO	1.132
Front ends	.878
IF and delay	2.493
Correlators	.256
System monitor	.328
System integration	<u>.500</u>
Subtotal	5.587
<u>Computer System</u>	
Data processor	.854
Monitor computer	1.286
Communications	1.269
Programming	<u>.300</u>
Subtotal	3.709
<u>Site</u>	
Buildings	.977
Wye	6.733
Utilities and facilities	1.916
Site acquisition	<u>.100</u>
Subtotal	9.726
Total	\$ 36.081

---

Table 10-2 shows the cost of the array broken down into (1) material, labor, and technical components; (2) engineering and design; (3) overhead, general and administrative expenses, and profits, of suppliers.

Table 10-2

## VLA Cost

<u>Item</u>	<u>Cost (millions)</u>
Material, components, and labor	\$ 30.1
Design and engineering	2.7
Supplier overhead, G&A, profit	<u>3.3</u>
Total	\$ 36.1

---

All estimates are believed to be reliable to within  $\pm 10\%$ . A 15% contingency should be provided, however, to allow for the uncertainties of the estimates, incompleteness of the detailed design, and the vagaries of the market at the time of procurement. In addition, price escalation during construction should be anticipated. It is estimated at an average of 3-1/2% per year, based on data from Engineering News Record.

The basic array priced in Table 10-1 provides for operation at one wavelength, 11 cm, with measurement of any one of the four polarization components. The capability of the array can be greatly extended, at relatively low cost, by providing the equipment necessary for simultaneous dual frequency or four polarization components operation. The additional correlators, IF equipment and delay lines needed for two-channel operation -- either as a dual frequency system or to simultaneously measure all polarization components -- is estimated to cost \$1,165,000. Front ends and feeds for 5.5 cm wavelength cost \$760,000. Additional 11 cm front ends for simultaneous measurement of all polarization components cost \$600,000. These cost estimates are summarized in Table 10-3. It is recommended that this equipment be included as part of the initial system.

Table 10-3

## Continuum Research Equipment

<u>Item</u>	<u>Cost (thousands)</u>
Two-channel system	\$ 1,165
5.5 cm feeds and front ends	760
11 cm front ends for polarization	<u>600</u>
Total	\$ 2,525

Equipment for spectral line work is estimated at \$3,317,000. It is recommended that this equipment also be included with the initial system.

Procurement of this additional equipment -- for two-channel continuum operation and for spectral line work -- could be postponed to a later date without serious harm to the primary function of the VLA. However, the additional equipment so extends the power of the VLA that it will be desirable to add it at some time. The acquisition and incorporation of the additional equipment into the VLA can be accomplished most economically and efficiently during the initial construction. It should, therefore, be included as part of the initial program if at all possible.

Table 10-4

## Total Funds

<u>Item</u>	<u>Cost (millions)</u>
VLA	\$ 36.1
Contingency	5.4
Escalation	4.6
Research equipment -- 5.5 cm and 11 cm	2.5
Research equipment -- spectral line	<u>3.3</u>
Total	\$ 51.9

The total cost of the VLA, plus contingency, escalation, and additional research equipment, is summarized in Table 10-4. The NRAO requests

that construction funds be authorized in Fiscal Year 1969.

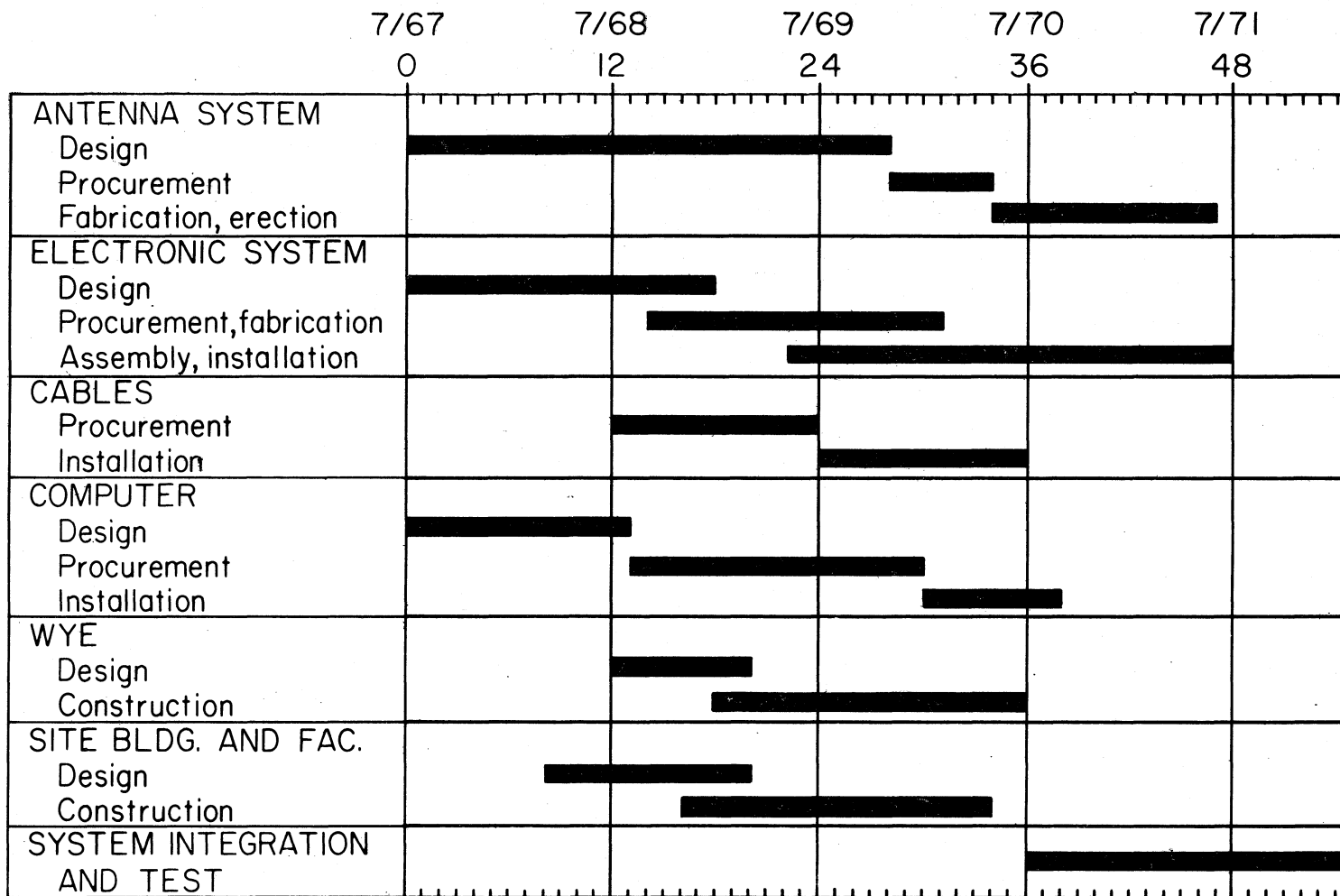
Table 10-5  
Commitment Schedule

<u>Fiscal Year</u>	<u>Commitments (millions)</u>
1967-1968	\$ 2
1969	16
1970	20
1971	9

---

The estimated time schedule for design and construction of the VLA is shown in Figure 10-1. It is based on the advice of industrial consultants and experience with similar jobs at the NRAO. As seen from the schedule, total time for completion is estimated to be about four years, from July 1, 1967.

An estimated commitment schedule, based on the above cost and time estimates, is shown in Table 10-5. The schedule assumes that design work will continue through FY 1967 and FY 1968 and that construction funds will be available in FY 1969.



NOTE: On-site work begins in twelfth month.

Figure 10 - 1. Design and construction schedule.